

**FUNDAMENTAL STUDIES OF IN-SITU POLYMERIZATION  
OF NYLON-6 NANOCOMPOSITE**

Presented to the Graduate Council  
of Texas State University-San Marcos  
in Partial Fulfillment  
of the Requirement

for the Degree

Master of SCIENCE

by

Shagufta Shabbir, B.Sc.

San Marcos, Texas  
August 2004

## ACKNOWLEDGEMENT

I would like to express my sincere appreciation and respect to Dr. Gary Beall, Assistant Professor of Chemistry, for his patience, dauntless creative spirit and knowledgeable supervision throughout my research. I would also like to thank Dr. Micheal Blanda, Professor of Chemistry, and Dr. Chad Booth, Assistant Professor of Chemistry at Texas State University, for taking the time for reviewing this writing.

Many thanks to all the staff, graduate and undergraduate students of the Polymer Research Group for their friendly assistance. Special thanks to Stewart Harris, Elizabeth Peterson, Jeremy Bartels and Casey Smith for assisting with the operation of instruments and for their guidance with the experimentation.

I would also like to thank the Department of Physics at Texas State University-San Marcos for allowing me the use of X-Ray Diffraction Instrument.

Last but not the least, I would like to thank my husband Hasnain Shabbir for his support.

This manuscript was submitted on July 25, 2004.

## TABLE OF CONTENT

ACKNOWLEDGEMENT .....	iii
LIST OF FIGURES .....	vi
LIST OF TABLES.....	viii
ABSTRACT .....	ix
CHAPTER 1 .....	1
1.0 INTRODUCTION.....	1
1.1 Background.....	1
1.1.1 Structure of Montmorillonite.....	5
1.1.2 Cation-Exchange Characteristic .....	6
1.1.3 Compatibilizing Agents.....	8
1.1.3.1 Amino Acids.....	8
1.1.3.2 Alkyl Ammonium Ions.....	9
1.1.3.3 Silanes Coupling Agents .....	10
1.1.4 Nylon 6 Nanocomposite .....	10
1.1.5 Preparation of Nylon 6 Nanocomposite .....	11
1.1.5.1 Melt Compounding.....	12
1.1.5.2 In-Situ Polymerization.....	17
1.1.6 Characterization of Nanocomposite .....	18
1.1.6.1 Mechanical Properties .....	19
1.1.6.2 Barrier Properties (O <sub>2</sub> and H <sub>2</sub> O).....	19
1.1.6.3 Thermal Properties .....	20
1.2 Goals of This Research Work.....	21
CHAPTER 2 .....	23
2.0 RESEARCH OUTLINE.....	23
2.1 Case 1: To Optimize the Molecular Weight of the Polymer .....	23
2.2 Case 2: Surface & Edge Treatment .....	24
2.3 Case 3: Building a House of Cards.....	25
2.4 Case 4: Edge Treated Nanocomposite.....	26
2.5 Case 5: Nylon-6 Nanocomposite Using Laponite .....	27
2.5.1 Laponite Clay Structure and Dimension .....	28
2.5.2 Polymerization Using Laponite .....	28
CHAPTER 3 .....	29
3.0 EXPERIMENTATION .....	29
3.1 Materials .....	29
3.2 Treatment of Clay with Initiator.....	30
3.3 In-situ Polymerization .....	33
3.4 Characterization of the Clay Nanocomposite.....	33
3.4.1 Thermogravimetric Analysis (TGA) .....	34

3.4.1.1	Derivative Thermogravimetry (DTG) .....	34
3.4.2	Modulated Temperature Differential Scanning Calorimetry (mt-DSC)	35
3.4.3	Dynamic Mechanical Analysis (DMA).....	36
3.4.4	Notched Izod Impact Testing .....	37
3.4.6	Wide Angle X-ray Diffraction (WAXD).....	38
CHAPTER 4	.....	39
4.0	RESULTS & DISCUSSION .....	39
4.1	Thermal Properties .....	39
4.2	Dynamic Mechanical Behavior of Nylon 6 Nanocomposite.....	48
4.3	Mechanical Properties of Nylon 6 Nanocomposite .....	53
4.4	Wide Angle X-ray Diffraction.....	55
CHAPTER 5	.....	57
5.0	CONCLUSIONS .....	57
5.1	Optimizing Molecular Weight of the Nanocomposite .....	57
5.2	Effect of the Edge Treatment on Nanocomposite .....	58
5.3	Edge Treated Nanocomposite.....	59
5.4	Effect of Particle Size on the Nanocomposite .....	59
APPENDICES	.....	61
APPENDIX A	– DSC GRAPHS OF NYLON 6 NANOCOMPOSITES .....	62
APPENDIX B	– TGA OF NYLON 6 NANOCOMPOSITES .....	73
APPENDIX C	– DMA OF NYLON 6 NANOCOMPOSITES .....	84
APPENDIX D	– X-RAYS OF NYLON 6 NANOCOMPOSITES .....	115
REFERENCES	.....	126

## LIST OF FIGURES

Figure 1: Polymer-clay interaction [4]. .....	3
Figure 2: Clay making machine [1].....	4
Figure 3: Electron microscope picture of montmorillonite clay plate.....	5
Figure 4: Structure of Montmorillonite [8].....	6
Figure 5: 53milliequivalent Cation Exchange Capability .....	7
Figure 6: 108 milliequivalent Cation Exchange Capability .....	7
Figure 7: Clay surface treated with amino acid [1] .....	8
Figure 8: The cation exchange process between alkylammonium ions and cation initially intercalated between the clay layers [9] .....	9
Figure 9: Interaction of silane with the organic and inorganic material.....	10
Figure 10: Flowchart of the melt intercalation process [9] .....	12
Figure 11: Nylon 6 nanocomposite formed through in situ polymerization with montmorillonite [1].....	15
Figure 12: Flowchart presenting different steps of in-situ polymerization [1].....	17
Figure 13: TEM of a well-exfoliated nanocomposite.....	18
Figure 14: Three-dimensional structure of nylon 6 nanocomposite [30]. .....	20
Figure 15: 6-Aminocaproic acid is used which improves intercalation and Optimizing the number of acid initiators to get a 25000 mol. wt. Polymer .....	23
Figure 16: Dimensions of the nanocomposite. ....	23
Figure 17: Edge interaction with silane coupling agent .....	24
Figure 18: Dimensions for the surface and edge treated nanocomposite .....	24
Figure 19: Interconnection of the edges with the carboxyl terminated surface to give a house of cards .....	25
Figure 20: Clay treated with alkyl ammonium ion and the edges treated with silane coupling agent.....	26
Figure 21: Idealistic structural formula of laponite [30] .....	27
Figure 22: Single laponite plate crystal [30] .....	27
Figure 23: Kitchen Aid Mixer .....	30

Figure 24: Hobert Commercial Auger Extruder (model 4822) .....	30
Figure 25: Extruded material .....	31
Figure 26: Coffee grinder and 75 $\mu$ m mesh.....	31
Figure 27: Clay sieving machine .....	31
Figure 28: Bulk Polymerization Process .....	33
Figure 29: TGA Q50.....	34
Figure 30: Modulated DSC 2920.....	35
Figure 31: Carver Model C Platen Press .....	36
Figure 32: DMA Q800 .....	37
Figure 33: Specimen loaded on DMA Q800 .....	37
Figure 34: Impact testing machine .....	37
Figure 35: Schematic of hydrogen bonding within the $\alpha$ and $\gamma$ crystalline forms of nylon 6 as seen from end and side view of each crystal. Closed and open circles represent chain axes projecting out of and into the page respectively. Hydrogen bonds between polyamide chains are represented by dashed lines [36] .....	41
Figure 36: DSC of Surface Toyota Nanocomposite .....	42
Figure 37: TGA curves of Nylon 6 and all the Different Nylon 6 Nanocomposite .....	45
Figure 38: TGA curve and the 1st derivative curve of laponite edge treated nanocomposite .....	46
Figure 39: TGA and 1 <sup>st</sup> derivative curve of Surface Toyota and Edge nanocomposite...46	
Figure 40: Bar Diagram of Dynamic mechanical behavior of nanocomposites.....	51
Figure 41: Storage modulus plots of nylon 6 and nylon 6 nanocomposites.....	52
Figure 42: Tan $\delta$ plots of nylon 6 and selected nylon 6 nanocomposites.....	52
Figure 43: Impact test data graph .....	54
Figure 44: Schematic illustration of the nanocomposite formation process .....	55

## LIST OF TABLES

Table 1 – Materials Used in the Study .....	29
Table 2 – Description of samples .....	32
Table 3 – Differential scanning calorimetry data of nanocomposites .....	39
Table 4 – Thermal Gravimetric analysis data of nanocomposites.....	44
Table 5 – Dynamic Mechanical data of nanocomposite.....	50
Table 6 – Impact test data.....	53
Table 7 – Wide Angle X-ray Diffraction data.....	56

# **ABSTRACT**

## **FUNDAMENTAL STUDIES OF IN-SITU POLYMERIZATION OF NYLON-6 NANOCOMPOSITE**

By

Shagufta Shabbir, B.Sc.

Texas State University-San Marcos

August 2004

**SUPERVISING PROFESSOR: DR. GARY BEALL**

Nanocomposites were originally studied as early as the 1960's. In more recent times nylon 6-montmorillonite clay nanocomposite have their origin in the pioneering research conducted at Toyota Central Research Laboratories where these two divergent organic and minerals were successfully integrated. To understand the fundamental behavior of these nanocomposites, several different types of nylon 6 nanocomposites were prepared via in-situ polymerization in our lab. The mechanical and physical properties were determined and compared to the material made previously.

This research project focuses on formation of nanocomposite by in-situ polymerization and understanding the resulting properties of the composite. Nylon 6 nanocomposites were made using montmorillonite and laponite, to study the effect of different particle size on the nanocomposite. Another aspect which is looked at is optimizing the molecular weight of the nanocomposite. Nylon 6 montmorillonite

nanocomposite made by Toyota (CRL) showed a low molecular weight. Thus, in this research the number of initiators used in the polymerization process is reduced to give high molecular weight nanocomposite. Silane edge treated nanocomposite are also studied, the silane-coupling agents interacts with hydroxyl groups present on the edges of the clay plates it is functionalized so that it participates in the polymerization process.

Two different general types of nanocomposite using silane were made, one in which the surface is treated with the aminocaproic acid which initiates polymerization on the surface of the clay plates, thus resulting in a nanocomposite which has polymer growing from the surface as well as from the edges of the clay plate and another in which the surface is not treated with the initiator and the polymer grows from the edges of the clay plate.

From the comparative results the conclusions that were drawn were that the edge and the surface treated nanocomposite showed a dramatic improvement in the impact property as compared to the surface treated nanocomposite. The edge treatment of the organoclay showed a well-exfoliated structure as compared to other melt-compounded nanocomposites. Optimizing the molecular weight and the use of laponite instead of montmorillonite did not show any significant improvement in the nanocomposite characteristic.

# CHAPTER 1

## 1.0 INTRODUCTION

### 1.1 Background

The term “**nanocomposite**” refers to a two-phase material where one phase is dispersed in the second one on a nanometer ( $10^{-9}$ m) level. This term is commonly used in two distinct areas of material science: ceramics and polymers. However we will only consider nanocomposites based on polymers. Nanocomposite technology has been described as the next great frontier of material science [1]. Nanocomposites are commonly based on polymers matrices reinforced by nanofillers such as smectic clay [2]. The smectic clay in particular is unique in the fact that they exist in nature in turbostratic units (a type of crystalline structure where there is no crystallographic relationship between plates) that are hydrophilic and can be broken down into one-nanometer thick platelets. They find many and diverse industrial applications, including use as water-based thickeners, cation exchangers, oil-well drilling fluids, cat-litter, cosmetics, paper coatings, additives, landfill liners, foundation leak barriers and adsorbents for wine clarification, vegetable oil refining, water purification and the efficient application of agricultural chemicals.

The origin of modern polymers can be traced to the pioneering work by Wallace H. Carothers at DuPont, where his crowning achievement was the synthesis of nylon as a superior replacement for silk. As new polymers were rapidly introduced in the 1950s and 1960s, plastics earned an undeserved reputation as being a cheap substitute for wood or metal. This point of view has largely faded owing to the enormous and varied use of plastics in all kinds of products that we encounter in our daily lives. This can best be seen in food packaging industry and the automobile industry. However plastics have certain limitations in both the food packaging and the automobile industries. In the packaging industry, for instance certain foods (e.g. tomato products and beer) are sensitive to oxygen and cannot be stored in plastic containers owing to the oxygen permeability of the plastic. In the auto industry, low stiffness and tensile strength and the tendency to warp or creep under heat load have limited the use of plastics in automotive applications. If need is indeed the mother of invention, then nanocomposites are a great example of the fulfilling of a need.

Polymer-clay interactions have been actively studied during the sixties and the early seventies [3] but it is only relatively recently that the researchers at Toyota produced a commercial nanostructure from polymer and organophilic clay. Their new material based on polyamide 6 (nylon-6) and organophilic montmorillonite showed dramatic improvement of mechanical properties barrier properties and thermal resistance as compared with the pristine matrix and this is at low clay content (4wt%).

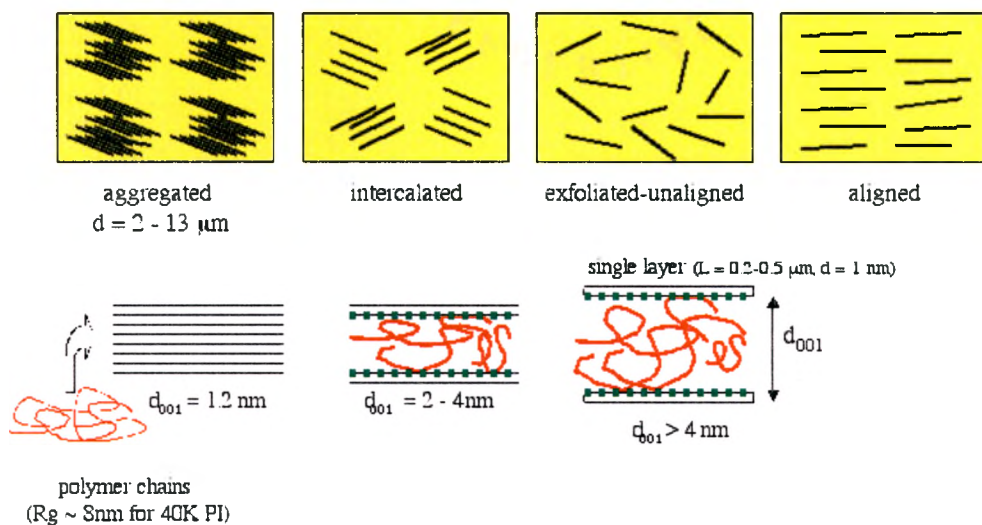


Figure 1: Polymer-clay interaction [4].

According to the early work of Giannelis [5] on clay polymer interaction in general two types of hybrid structures can be obtained upon polymer-clay nanocomposites preparation, intercalated in which a single or several layers, extended polymer chain is intercalated between the silicate layers, resulting in a well-ordered multilayer with alternating polymer/inorganic host layers and a repeat distance of a few nanometers, and disordered or exfoliated in which the silicate layers (1 nm thick) are dispersed in a continuous polymer matrix an intercalated system will generally exhibit a strong X-ray diffraction pattern. The best performance is commonly observed for the exfoliated nanocomposites the two situations can however, coexist in the same material. In any case, to make a successful nanocomposite it is very important to be able to disperse the inorganic material throughout the polymer. If a uniform dispersion is not

achieved, agglomerates of inorganic material are found within the host polymer matrix, thus limiting improvement [5, 6].

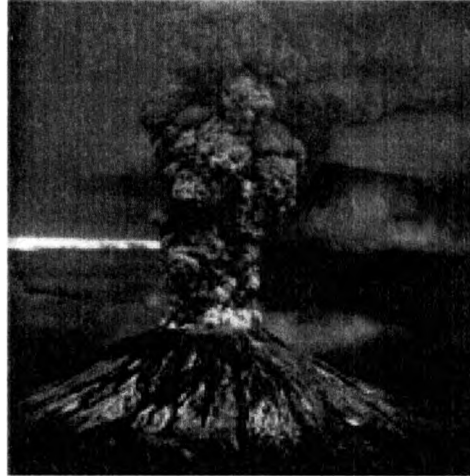


Figure 2: Clay making machine [1]

To understand the concept of polymer clay interaction we have to take a good look at the layered silicate structure to get an understanding of the types of interactions possible. In particular the smectite groups of clay minerals such as montmorillonite, saponite and hectorite have mainly been used because they have excellent intercalation abilities. Montmorillonite is a common clay mineral with numerous worldwide localities. It has in most cases been formed by the in-situ alteration of volcanic ash. Another less common origin is the hydrothermal alteration of volcanic rocks [7]. They are extremely fine-grained and thin-layered, more than any of the other clay minerals, is shaped like a sheet of paper. Figure 3 displays a montmorillonite clay plate. It looks like a crumpled tissue paper due to high vacuum needed for the electron microscope.

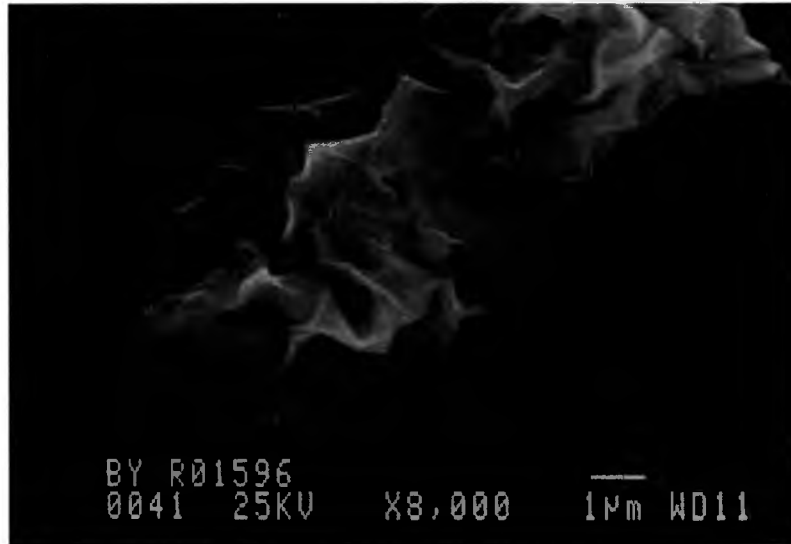


Figure 3: Electron microscope picture of montmorillonite clay plate

### 1.1.1 Structure of Montmorillonite

The model structure of montmorillonite consists of two fused silica tetrahedral sheets sandwiching an edge-shared octahedral sheet of either aluminum or magnesium hydroxide. [8] (Figure 4) Isomorphous substitution of  $\text{Al}^{+3}$  for  $\text{Si}^{+4}$  in the tetrahedral lattice and of  $\text{Mg}^{+2}$  for  $\text{Al}^{+3}$  in the octahedral sheet causes an excess of negative charges within the montmorillonite layers. These negative charges are counterbalanced by cations such as  $\text{Ca}^{+2}$  and  $\text{Na}^{+1}$  situated between the layers due to the high hydrophilicity of the atoms on the surface of the clay water molecules are usually also present between the layers.

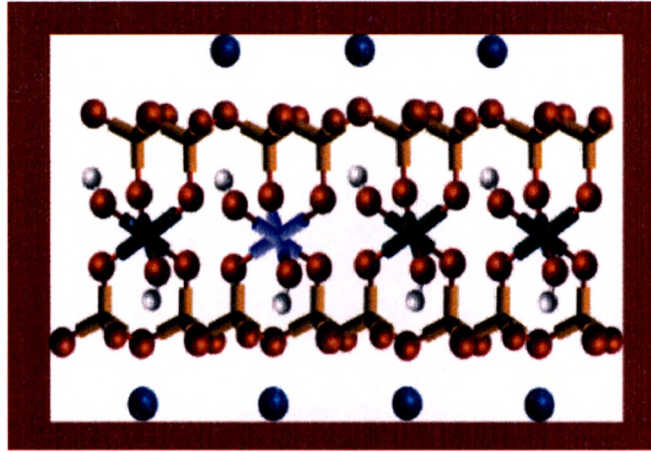


Figure 4: Structure of Montmorillonite [8]

Stacking of the layers leads to regular Van der Waals gaps called interlayers or galleries [9]. The edges of the clay plates consist of hydroxyl groups, where the regular lattice is terminated.

### 1.1.2 Cation-Exchange Characteristic

A characteristic feature of smectites such as montmorillonite is their ability to absorb certain cations and to retain them in an exchangeable state. It means that these intercalated cations can be exchanged by treatment of other cations in a water solution. For given clay, the maximum amount of cations that can be taken up is constant and is known as the cation exchange capacity. Generally montmorillonite have cation exchange capacity of 95 milliequivalent per 100g. Montmorillonite is a fine sheet-like particle with a dimension of about 0.1  $\mu\text{m}$  in length and 0.1  $\mu\text{m}$  width and 10  $\text{\AA}$  in thickness, which shows that it has a large surface area and a large aspect ratio compared to its thickness.

Summarizing the above facts we know that montmorillonite is a kind of clay consisting of stacked silicate layers with basal spacing of around 1nm. The silicate layers is separated from its neighbors by Van der Waals gap called gallery, which is occupied by hydrated alkaline or alkaline-earth metal cations. As will be further discussed below by replacing the metal cations with onium ions such as alkyl ammonium cation through ion exchange reaction, the hydrophilic montmorillonite is rendered hydrophobic or organophilic. This makes it possible for the polymers with varying polarity to intercalate in forming polymer-layered silicate nanocomposite. The surfaces of the clay plates are not completely covered with cations as illustrated in [Figure 5 and 6](#) below.

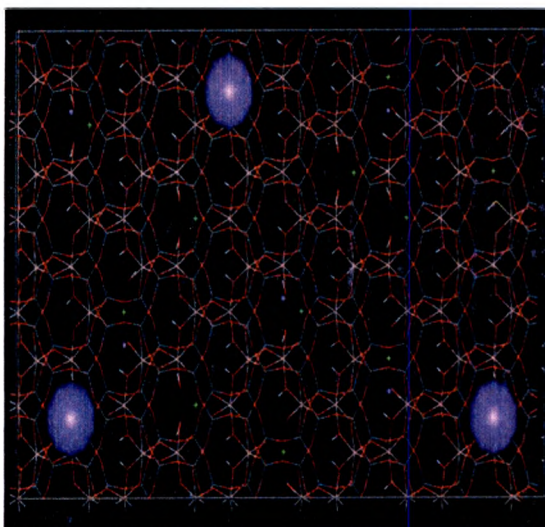


Figure 5: 53 milliequivalent Cation Exchange Capability

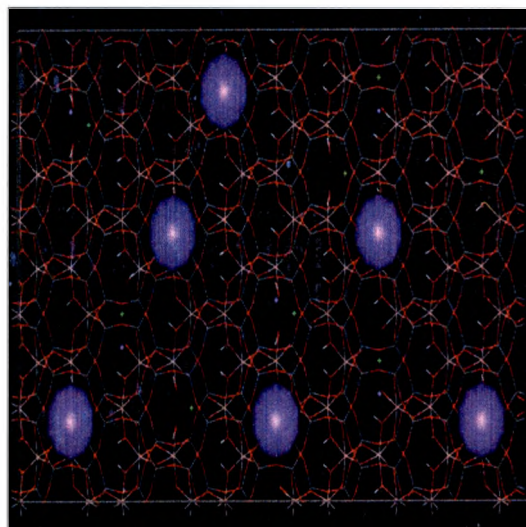


Figure 6: 108 milliequivalent Cation Exchange Capability

Therefore there is a lot of surface available for interaction with the organic modifier and the polymer. The edges of the clay plates consists of hydroxyl group, which hinders the intercalation of the polymer in between the clay plates because the polar hydroxyl groups do not interact well with the non-polar polymer chain thus raising the activation barrier for intercalation process. This unfavorable interaction can be overcome

by using silane-coupling agents. Overall the process of intercalation of the polymer is entropically and enthalpically favorable. Entropically driven by displacement smaller molecules from in between the clay plates and enthalpically driven by the polar interaction of the polymer with the clay plates.

### 1.1.3 Compatibilizing Agents

Dispersing clay in a polymer is like trying to mix oil with water. It is a known fact that oil does not disperse well in water except when we use a detergent, which makes the oil compatible for water. Just like that a surfactant is used in the case of clay and polymer, which act as a compatibilizing agent. It is a molecule constituted of one hydrophilic function which likes polar media like clay and an organophilic function (which likes organic molecules like polymer) this allows us to disperse clay in polymer matrix.

#### 1.1.3.1 Amino Acids

The first compatibilizing agents used in the synthesis of nanocomposite (polyamide 6-clay hybrids) were amino acids [10]

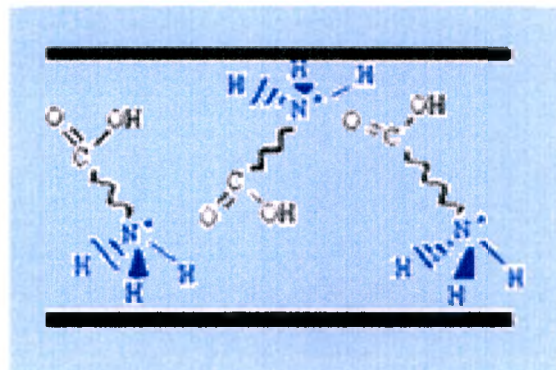


Figure 7: Clay surface treated with amino acid [1]

Amino acids are molecules, which consist of a basic amino group ( $-NH_2$ ) and an acidic carboxyl group ( $-COOH$ ). In an acidic medium, a proton is transferred to the  $-NH_2$  group and then a cation ion exchange is then possible between the  $-NH_3^+$  function formed and a cation intercalated between the clay layers so that the clay becomes organophilic. Amino acids were successfully used in the synthesis of polyamide 6-clay hybrid because their acid function has the ability to polymerize with  $\epsilon$ -caprolactam intercalated in between the layers. Thus this intercalation delaminates the clay in the polymer matrix and a nanocomposite is formed.

### 1.1.3.2 Alkyl Ammonium Ions

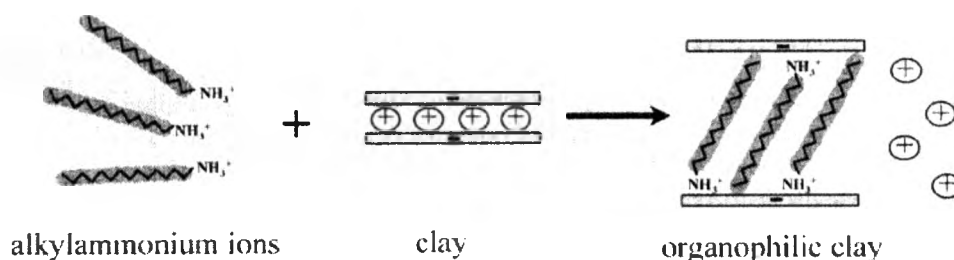


Figure 8: The cation exchange process between alkylammonium ions and cation initially intercalated between the clay layers [9]

Alkyl ammonium ions can be intercalated easily between the clay layers and offer a good alternative to amino acids for the synthesis of nanocomposites based on other polymer systems than polyamide 6. The most widely used alkyl ammonium ions are based on primary alkyl amines put in acidic medium to protonate the amine function. Figure-8 alkyl ammonium ion intercalate in between the clay plates and the spacing

between the plates increases by about 10 Å. Alkyl ammonium ions lowers the surface energy of the clay so that organic species with different polarities can get intercalated between the clay layers.

### ***1.1.3.3 Silanes Coupling Agents***

A general explanation of the clay edges earlier sets the stage for this discussion. Silane coupling agents interact with “receptive” inorganic edges forming tenacious covalent bonds at the interface. These receptive inorganic surfaces are characterized by the hydroxyl group (OH) attached principally to silicon and aluminum and are particularly favorable for bonding with silanes. In the clay, hydroxyl groups are present on the edges of the clay. The silane-coupling agent has organofunctional groups, which can interact with the organic polymer or in the case of in-situ polymerization, can participate in the reaction.

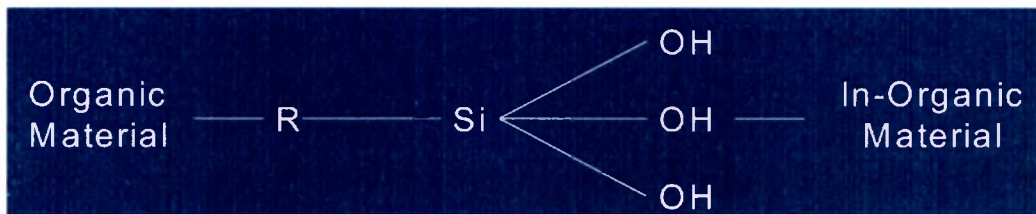


Figure 9: Interaction of silane with the organic and inorganic material

### **1.1.4 Nylon 6 Nanocomposite**

Nylon-6 (polycaprolactam) has good mechanical properties and is a commonly used engineering polymer. It has been successfully reinforced by glass fiber or other inorganic material. In these reinforced composites, the polymer and additives are not homogeneously dispersed at the microscopic level [10]. Toyota researchers decided to disperse layered silicate in the polymer to achieve microscopic distribution on the

nanoscale level. Since then, numerous researchers have demonstrated that only a few percent of layered silicate can lead to a wide array of property enhancement [11, 12]

The timing belt covers of automotive engines are usually made of glass fiber reinforced nylon. Nylon 6 nanocomposite, as will be discussed below, shows high modulus and a high distortion temperature. An attempt was made to make the timing belt covers of nylon 6 nanocomposite by injection molding. The timing belt covers, which showed good rigidity and excellent thermal stability, were used in Toyota's automotive engine parts. Also, for timing belt covers, the weight saving reached was up to 25% owing to the low content of inorganic compared with glass fiber reinforced nylon. This was the first example of industrialization use of a polymer-clay nanocomposite.

Nylon 6 films are usually used for food packaging film because it has a high gas barrier property because of the nanometer level dispersion of the silicate layers. The gas permeability decreases by 50% with clay addition of 4.8 vol%.

#### **1.1.5 Preparation of Nylon 6 Nanocomposite**

At present there are four principal methods for producing exfoliated nanocomposites:

1. In situ polymerization [11, 12, 13, 14]
2. Emulsion polymerization [15, 16]
3. Sol-gel templating [17, 18]
4. Melt compounding. [19, 20, 21]

### 1.1.5.1 Melt Compounding

Viaa *et al* first reported the melt intercalation process in 1993 [22]. It is most environmentally friendly because no solvent is required and is broadly applicable to a range of commodity polymer, from the essentially nonpolar polystyrene, to weakly polar poly (ethylene terephthalate) and to strongly polar nylon. Nanocomposites can therefore be processed using currently available techniques, such as extrusion, lowering the barriers to large-scale commercialization. The strategy consists in blending a molten thermoplastic with an organoclay in order to optimize the polymer–clay interactions (Figure 10). The mixture is then annealed at a temperature above the glass transition temperature of the polymer and forms a nanocomposite.

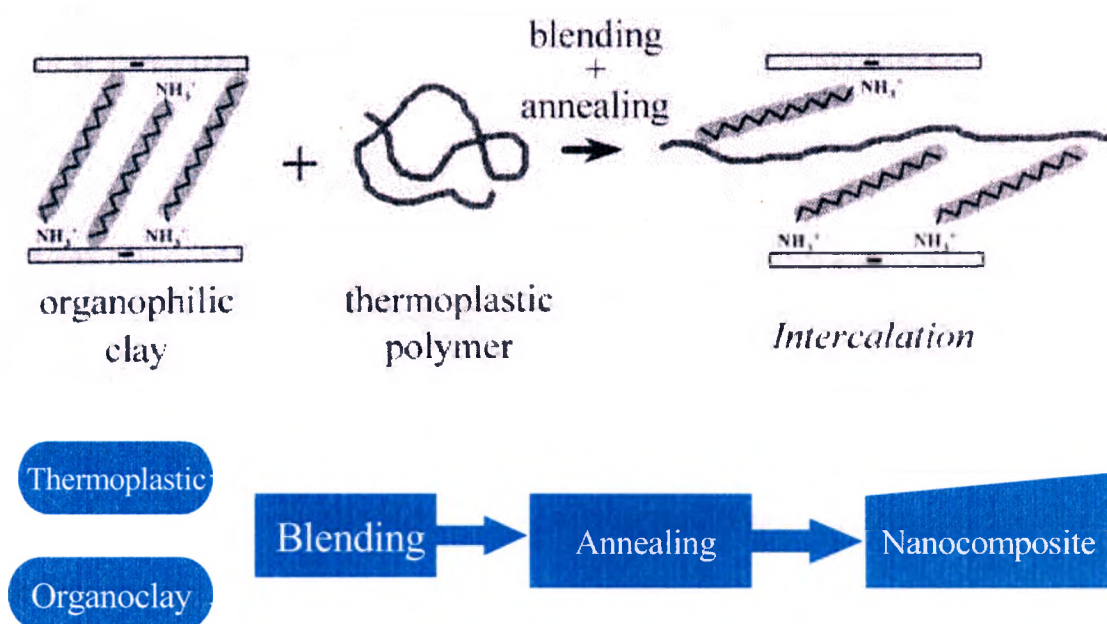


Figure 10: Flowchart of the melt intercalation process [9]

The polymer chain experiences a dramatic loss of conformational entropy during the intercalation. The proposed driving force for this mechanism is an important enthalpic contribution of the polymer/organoclay interaction during blending and annealing steps. The melt intercalation process has become increasingly popular because of its great potential for application in industry.

Recently, a better understanding of the formation and properties of these nanocomposites has been obtained using melt intercalation of polymers into layered silicates above the softening temperature of the polymer. Depending upon the interaction between the layered silicate (which is typically organically modified by replacing the charge balancing interlayer cations with alkyl ammonium ions in order to render the silicate layers organophilic) and the polymeric species, different micro structured nanocomposites ranging from immiscible to intercalated to delaminated are possible. In intercalated nanocomposite, a single extended polymer chain is inserted between the silicate layers, resulting in a well-ordered multilayer with a repeated distance of a few nanometers while in delaminated hybrids, the silicate layer (1nm thick) are exfoliated and dispersed in continuous polymer matrix. Recent report about automotive application have emphasized that melt processing plays a pivotal role in the development of commercially viable material [23].

#### ***1.1.5.1.1 Optimizing the Process of Melt Compounding For Nylon 6 Nanocomposite***

To get an exfoliated nylon-6 nanocomposite by melt compounding, you need:

1. Medium Shear Twin Screw Extruder [24]
2. High Molecular Weight Polymer [25, 26]
3. Compatibility Of The Organoclay With The Polymer [27]

Recent work [24, 25, 26, 27] has focused on the effects of processing conditions, polymer structure and rheology and the structure of the organic modifier of the clay on the formation of polymer nanocomposite via melt processing. For nylon-6 the extruder must be optimized with regard to both shear intensity and residence time to achieve high level of clay platelet exfoliation [24]. The results of this work have shown that there are two possible clay delamination pathways.

In **Pathway 1** stack of platelets are decreased in height by sliding platelets apart from each other a pathway that requires shear intensity. **Pathway 2** shows polymer chains entering the clay galleries pushing the end of the platelets apart. This pathway does not require high shear intensity but involves diffusion of polymer into the clay galleries (driven by either physical or chemical affinity of the polymer for the organoclay surface) and is thus, facilitated by residence time in the extruder. As more polymer chains enters and goes further in between clay platelets, especially near the edge of the clay galleries, the platelets appear to peel apart. It is important to note that the top platelet in the stack maybe able to curl away as polymer enters from the edge since the platelets are able to bend.

The non-intermeshing twin-screw extruder (medium shear) used gave the best delamination and dispersion. It is believed that excellent delamination and dispersion can be achieved with both co-rotating and counter-rotating intermeshing types of extruders when a fully optimized screw configuration is used. It is recognized that the extruder process conditions are important variable that must be optimized to affect a high degree of delamination and dispersion.

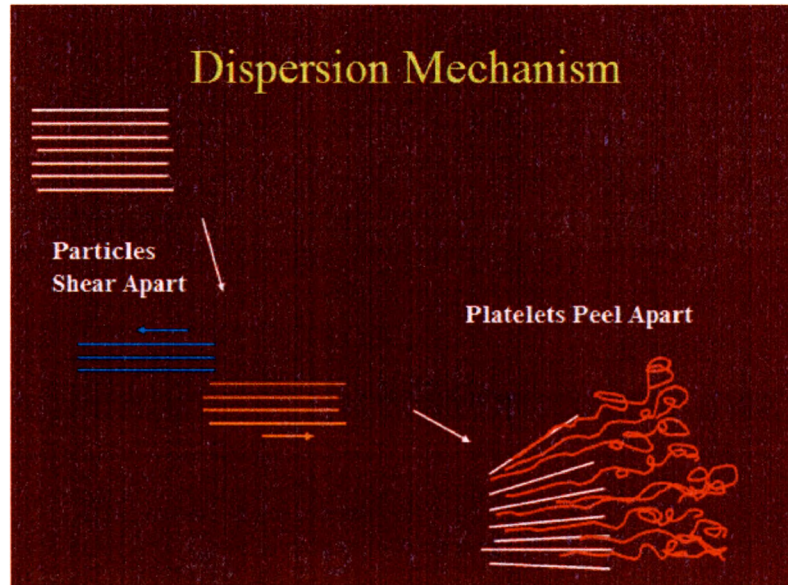


Figure 11: Nylon 6 nanocomposite formed through in situ polymerization with montmorillonite [1]

Another study has shown that the use of high molecular weight nylon 6 leads to much better exfoliation owing to the high shear stresses in the extruder that result from its high melt viscosity [25, 26]. The high melt viscosity exerts a greater stress on the tactoids and that the stress shears the taller stacks into shorter ones. The final step in exfoliation involves peeling the platelets of the stacks one by one; and this takes time and requires the matrix polymer to have sufficient affinity for the clay surface to cause spontaneous wetting. The higher shear stress is believed to be the major contributor to exceptional exfoliation of clay platelets in the higher molecular weight matrix.

The relationship between the structure of the organic cation on the organoclay and the morphology and properties of nylon-6 nanocomposite formed by melt processing was

also studied [27]. Three distinct surfactant structural effects have been identified that lead to greater extent of exfoliation, higher stiffness, and increased yield strengths for nanocomposites based on the high molecular weight polyamide.

1. One long alkyl tail on the ammonium ion rather than two
2. Methyl groups on the amine rather than 2-hydroxy-ethyl groups
3. An equivalent amount of amine surfactant on the clay as opposed to an excess amount.

It is proposed that these effects stem from the amount of exposed silicate surface.

Alkyl ammonium ions that cover a larger percentage of the silicate surface, shield desirable polar polyamide-polar clay interactions and ultimately lead to less platelet exfoliation. This proposal, however, does not imply that unmodified clay, i.e. sodium montmorillonite would be optimum. Organic modification of the clay is required to overcome the cohesive forces between neighboring platelets so that polymer intercalation and platelet exfoliation can occur during melt processing. It should also be emphasized that the effects observed in this work may be specific to nylon 6 matrix; thus, the nature of polymer-organoclay thermodynamic interaction may be different structure-property effects. From these studies, it is clear that with proper selection of nylon 6, organoclay modifier, and processing procedure can lead to attractive nanocomposites by melt processing.

### 1.1.5.2 *In-Situ Polymerization*

An important class of polymer layered silicate nanocomposites is prepared by *in situ* polymerization of certain monomers with the initiating species tethered to the silicate surface.

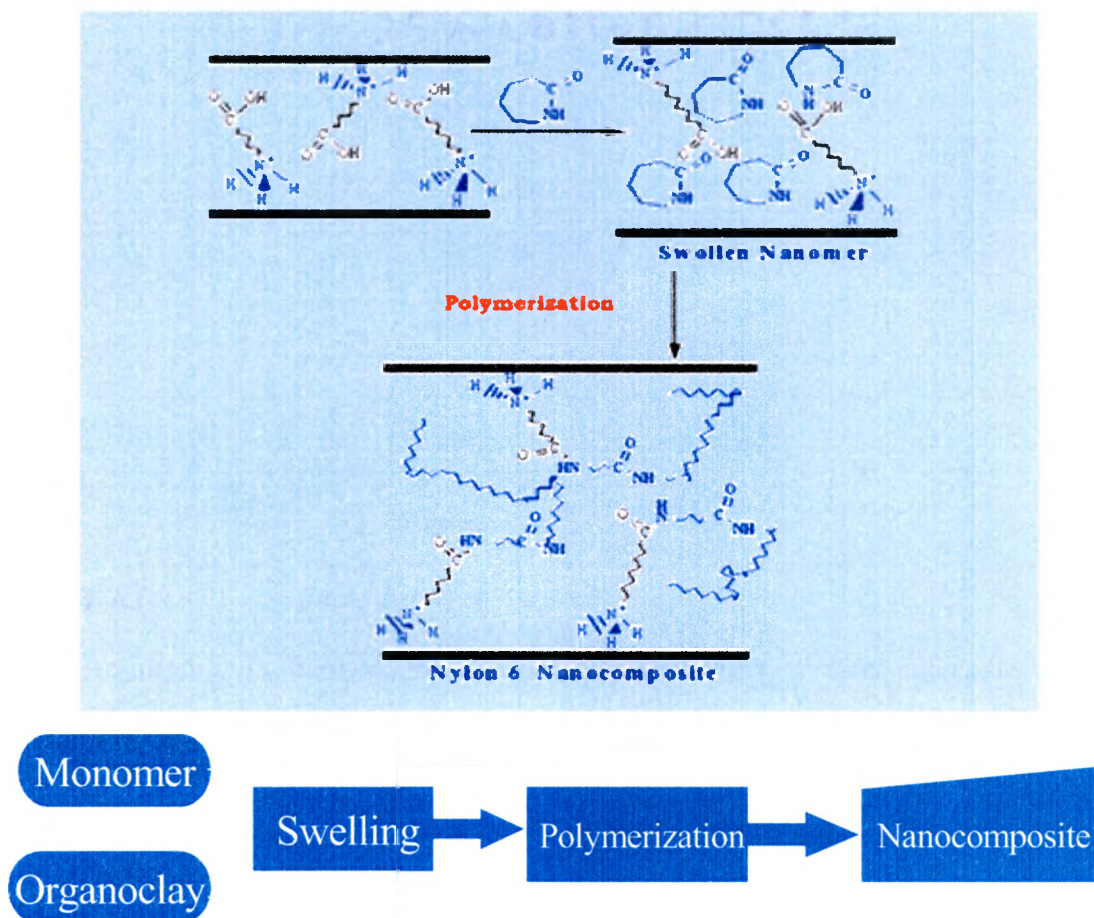


Figure 12: Flowchart presenting different steps of in-situ polymerization [1]

This technique first demonstrated by Fujiwara and Sakamoto [28] and later optimized by Toyota researchers [10]. The preparations of the end-tethered poly ( $\epsilon$ -

caprolactam) montmorillonite nanocomposites have been described in a previous publication. The end tethered composites were prepared by first converting the silicate surface from a hydrophilic to an organophilic surface by an ion exchange of the metal cation by 12-aminolauric acid. First the organoclay is swollen in the monomer ( $\epsilon$ -caprolactam) the polymerization of  $\epsilon$ -caprolactam is then initiated by the carbonyl group of the aminolauric acid and the polymerization proceed via ring opening of the  $\epsilon$ -caprolactam. The polymer is bounded to the silicate layer by the protonated amine terminus.

#### 1.1.6 Characterization of Nanocomposite

Characterization of the nylon 6 nanocomposite by X-ray diffraction has shown the absences of any stacking of the silicate which is indicated by the absence of the basal diffracted peak, suggesting that the host layers are well dispersed. TEM confirmed almost complete exfoliation of the nanocomposite, which is illustrated below.

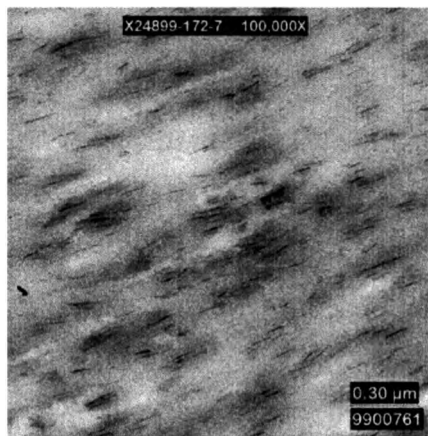


Figure 13: TEM of a well-exfoliated nanocomposite

### **1.1.6.1 Mechanical Properties**

The nano-effect is quite evident judging from mechanical properties. As for mechanical properties 91% increase in the flexural and tensile modules and a 134 % increase in the heat distortion temperature with 5% clay. The impact strength of the nanocomposite was compromised as compared to pure nylon-6 but the addition of hexamethylenediamine to the nanocomposite regained the impact strength of the polymer [29]. This can be explained by the fact that hexamethylenediamine reacted with the carboxylic end group and converted the end group of the polymer to an amine or it may connect the two carboxyl terminated polymer chains. Therefore overall there was no negative effect on the notched Izod impact strength from nanocomposite formation.

### **1.1.6.2 Barrier Properties ( $O_2$ and $H_2O$ )**

The nanocomposite has excellent barrier properties against oxygen, nitrogen, carbon dioxide, water vapor, gasoline, etc. Gas barrier properties for oxygen and water vapor show an excellent barrier performance as compared to pure nylon 6. This effect has been explained by tortuous path principle. Dispersed platelets of the silicate sheet block the shortest path of gas molecules and force them to take a roundabout way. As a result the permeation pathway is elongated. Nylon 6 nanocomposites have wide applications in food packaging ranging from a single layer and multi layers to film to rigid plastic containers.

In addition the water uptake for the nanocomposites is dramatically decreased. For example, the nanocomposite with 4 wt% clay uptakes around 40% less water after 800 hours immersion than does neat resin. Reduced water uptake allows nanocomposite to

maintain better structural integrity as compared with the neat resin under prolonged water exposure conditions.

### ***1.1.6.3 Thermal Properties***

The molded specimens were found to be anisotropic. The coefficient of thermal expansion of nylon 6 nanocomposite in the flow direction was lower than half of that in the perpendicular direction whereas nylon 6 was isotropic. This proves that sheets of silicate were parallel to the flow direction of the mold, the polymer chains also oriented in the same direction. It seems that anisotropy of thermal expansion resulted from the orientation of silicate and polymer chains.

Toyota researchers also observed the three dimensional clay dispersion at the intersection of the nylon 6 nanocomposite to form a novel “nano wall” structure which is shown below [30]

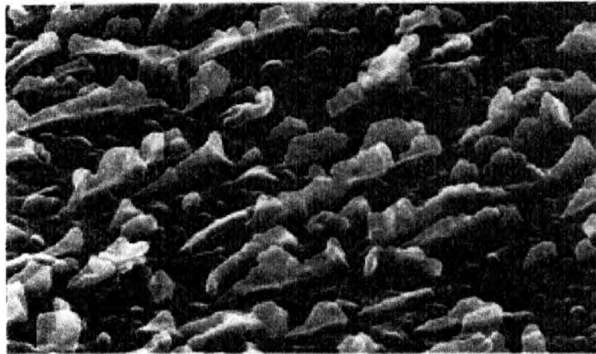


Figure 14: Three-dimensional structure of nylon 6 nanocomposite [30].

Excellent properties in nylon 6 nanocomposite can be considered to have origin due to the interaction between the organic polymer and inorganic silicate sheet. Thus, the nanocomposite has a microstructure that has never been seen in conventional composites.

Considering the properties of the nanocomposite may be, in a sense, an embodiment of the ideal polymer composite, or a completely novel composite.

## **1.2 Goals of This Research Work**

Considering the large improvement seen in nylon-6 nanocomposite as being such a great nanocomposite why do we need to do further research on it? Further research of this nanocomposite is conducted for a complete understanding of its behavior.

Specifically in this research we are looking at:

- Optimizing the molecular weight of the nanocomposite. Toyota reported nanocomposite had a low molecular weight as they treated the clay surface with maximum amount of initiator [10]. What we tried to do was to lower the amount of initiator in the nanocomposite to increase the molecular weight of the polymer. And to observe whether the high molecular weight of the polymer affects the properties of the nanocomposite.
- In this study we are also looking at the characteristic of the edge treated nanocomposite. As discussed above the edges of the clay plates are hydroxyl terminated that can be treated with an appropriate silane-coupling agent which can participate in the polymerization process. Thus we should have polymer growing from the edges of the clay plate, this particular nanocomposite would have different rheological properties than the Toyota nanocomposite.
- Edge treatment in conjunction with the surface treatment of the nanocomposite. As mentioned above Toyota researchers added some hexamethylenediamine to the nanocomposite to make the nanocomposite

tougher [29]. The question we wanted to answer is whether or not the impact properties of the nanocomposite are influenced by the added edge treatment of the clay.

- Different clays have different particle size thus in this research we have studied laponite which has a smaller aspect ratio than montmorillonite and to test whether particle size has an effect on the properties of the nanocomposite.

Conclusively the purpose of this research is to determine the effect of various surface modifications on the nanocomposite characteristic of nylon 6 from a fundamental point of view.

## CHAPTER 2

### 2.0 RESEARCH OUTLINE

#### 2.1 Case 1: To Optimize the Molecular Weight of the Polymer

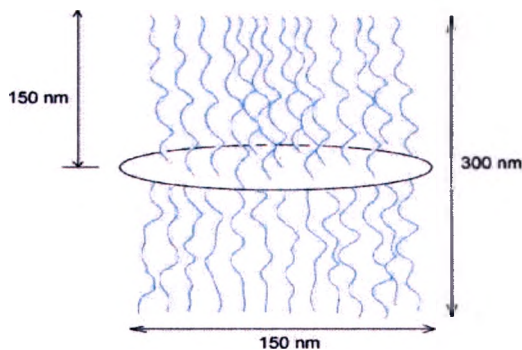
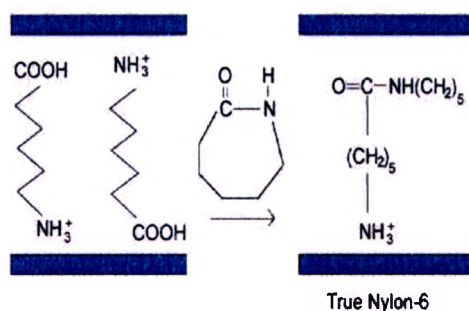


Figure 15: 6-Aminocaproic acid is used which improves intercalation and optimizes the number of acid initiators to get a 25000 mol. wt. Polymer

Figure 16: Dimensions of the nanocomposite.

In situ polymerization of nylon 6 is carried out in the presence of 6-aminocaproic acid that has a shorter alkyl chain ( $\text{C}_6$ ) than 12-aminolauric ( $\text{C}_{12}$ ) acid use previously by Toyota Researchers [10]. Due to the shorter alkyl chain the interaction between the polymer and the surface of the clay increase thus improving the process of intercalation.

Previously [13] a lot of initiator was added on the surface of the clay thus the molecular weight of the polymer was low around 15000 to 19000, it is has been discussed previously that high molecular weight polymer produce a good exfoliated nanocomposite and the mechanical and the thermal properties of the nanocomposite is also improved. Thus to maximize the molecular weight of the polymer the amount of initiator added to the surface of the clay is reduced to give 25,000 molecular weight polymer, the PDI (poly dispersity index) for nylon 6 nanocomposite is 1.5 for 5% montmorillonite which show a good distribution of the polymer on the surface of the clay. If 25000 molecular weight polymer/clay nanocomposite is obtained the dimensions of the nanocomposite would be as shown in figure 16, keep in mind that this is an idealistic view of the nanocomposite. Therefore the rheological properties of this nanocomposite would be different from the nanocomposite made by Toyota researchers.

## 2.2 Case 2: Surface & Edge Treatment

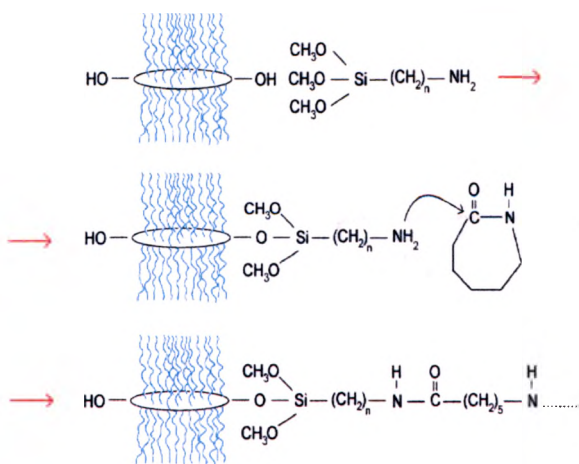


Figure 17: Edge interaction with silane coupling agent

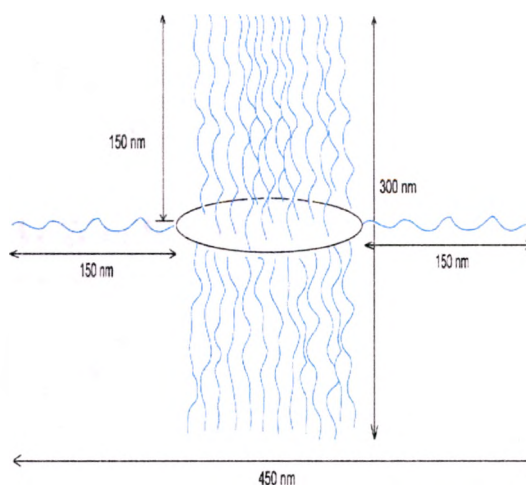


Figure 18: Dimensions for the surface and edge treated nanocomposite

Another aspect that has been studied is the surface and the edge treatment of the nanocomposite. It has been established that there are hydroxyl groups present on the edges of the clay plates which can interact with the silane coupling agent if these silane coupling agent are functionalized with an amine or a carboxyl group these functional groups would interact with the monomer and the polymer would grow from the edges of the clay plates which is illustrated [Figure 17](#). These clay plates are also treated with 6-aminocaproic acids on the surface, which also participates in the process of polymerization. [Figure 18](#) illustrated the idealistic dimension of this nanocomposite.

### 2.3 Case 3: Building a House of Cards

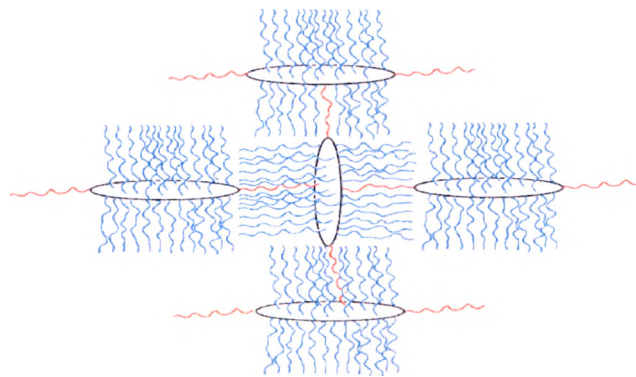


Figure 19: Interconnection of the edges with the carboxyl terminated surface to give a house of cards

Building a house of cards with interconnecting clay plates is another aspect that is studied. It is determined that the polymer growing from the edges of the clay plates is amine terminated and the polymer growing from the surface is carboxyl terminated. The amine terminated polymer on the edges of the clay can interact with the carboxyl terminated polymer growing from the surface of the clay plates, in such a way that it looks like a house of cards. What we are trying to do here is to create a similar effect that

the Toyota researcher created [29] when they treated the nanocomposite with hexamethylenediamine to recover the impact property of the nanocomposite.

#### 2.4 Case 4: Edge Treated Nanocomposite

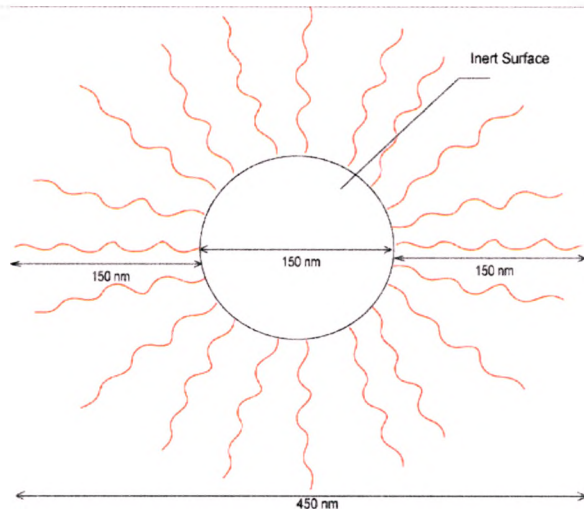


Figure 20: Clay treated with alkyl ammonium ion and the edges treated with silane coupling agent

Another kind of nanocomposite is also being looked at, in which an organoclay (93A) is used. This particular clay is not treated with the initiator on the surface although it is treated with silane-coupling agent on the edges of the clay, which participates in polymerization process. Thus the nanocomposite formed would have an inert surface and have polymer grow from the edges of the clay plates.

93A is smectic clay (montmorillonite) treated with a methyl dehydrogenated tallow ammonium ion on the surface, which should interact favorably with the polymer and produce a fairly well exfoliated nanocomposite. Thus, the property that we are specifically looking at is whether the polymer that is growing out of the edges of the clay

plates, aids in the process of exfoliation of the clay plates in the polymer matrix. Figure 20 shows the dimension of this particular nanocomposite

A comparative study of  $\text{Na}^+$  Cloisite edge treated is also conducted. To study the effect of the edge treated nanocomposite, that has  $\text{Na}^+$  ions on the surface of the clay plates.

## 2.5 Case 5: Nylon-6 Nanocomposite Using Laponite

To study the effect of particle size on the nanocomposite laponite is used and treated in a similar manner as montmorillonite.

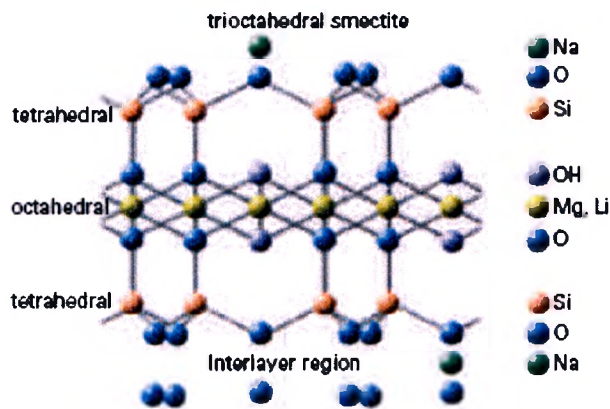


Figure 21: Idealistic structural formula of laponite [30]

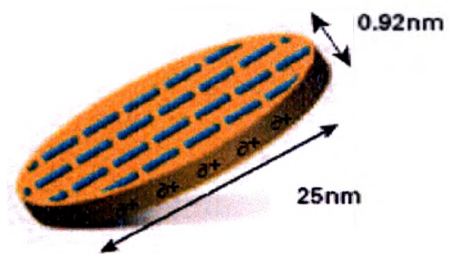


Figure 22: Single laponite plate crystal [30]

### **2.5.1 Laponite Clay Structure and Dimension**

Laponite is entirely synthetic clay. It has a layered structure six octahedral magnesium ions sandwiched in between two layers of silicon atoms. Some of the magnesium ions are substituted by lithium ions which gives a negative charge to the layer which is neutralized by sodium ion on the surface of the crystal laponite has a diameter of 25 nm as compared to montmorillonite which has a diameter of 150 nm.

### **2.5.2 Polymerization Using Laponite**

Polymerization of nylon 6 was conducted using laponite. Laponite was initially treated with the surface initiator (6-aminocaproic acid) and in-situ polymerization with  $\epsilon$ -caprolactam was then carried out. To make edge treated nanocomposite laponite was treated with 16% of 3-aminopropyltrimethoxysilane reagents as laponite contains 16% edges as compared to montmorillonite (2%). The silane reacts with the hydroxyl groups on the edges of the clay plates and takes part in the polymerization process. Edge and surface treated nanocomposite of laponite were also made by using the surface initiator 6-aminocaproic and edge initiator, 3-aminopropyltrimethoxysilane. Then the thermal and mechanical properties of this nanocomposite were studied.

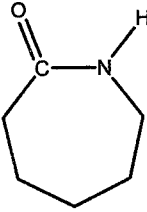
## CHAPTER 3

### 3.0 EXPERIMENTATION

#### 3.1 Materials

The materials used in this study are described in the table below:

Table 1 – Materials Used in the Study

Materials	Specification	Supplier
6-Aminocaproic acid	$\text{NH}_2(\text{CH}_2)_5\text{COOH}$	Aldrich
$\epsilon$ -Caprolactam		Aldrich
3-Aminopropyltrimethoxysilane	$(\text{MeO})_3\text{Si}(\text{CH}_2)_3\text{NH}_2$	United Chemical Technology
Hydrochloric Acid	HCl	
Closite® Na <sup>+</sup>	No organic modifier Cation exchange capacity 100meq/100g	Southern Clay
Closite®93 A [M2HT]	Methyl dihydrogenated tallow ammonium montmorillonite	Southern Clay
Laponite Grade B	Fluorosilicates Cation exchange capacity 60meq/100g	Southern Clay

### 3.2 Treatment of Clay with Initiator

$\text{Na}^+$  Cloisite is treated with 100 milliequivalent of 6-aminocaproic acid and hydrochloric acid by mixing first in a kitchen aid mixer for 20 min with water, the clay was passed through a Hobert commercial Auger extruder (Figure 24). The treated clay was then dried overnight at  $80^\circ\text{C}$  and grounded using a coffee grinder and sieved through a  $75\mu\text{m}$  mesh. Edge treated clay was made via the same procedure just adding 2% silane to the clay. Figure [23, 24, 26, 27] shows all the appliances used in the process described above. Table 2 clearly describes the different types of clay prepared in this study.

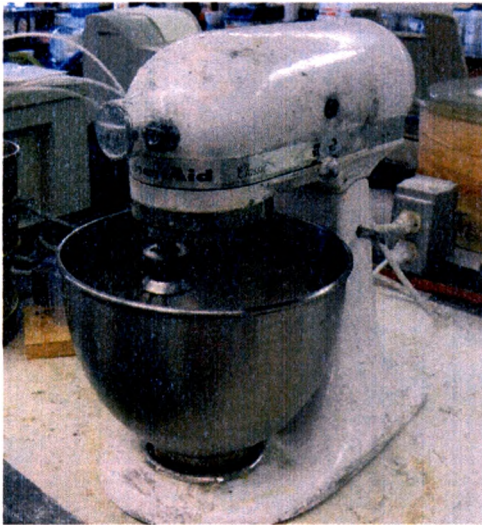


Figure 23: Kitchen Aid Mixer



Figure 24: Hobert Commercial Auger Extruder (model 4822)



Figure 25: Extruded material

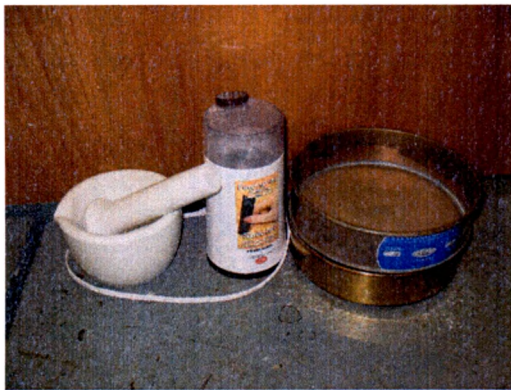


Figure 26: Coffee grinder and 75µm mesh

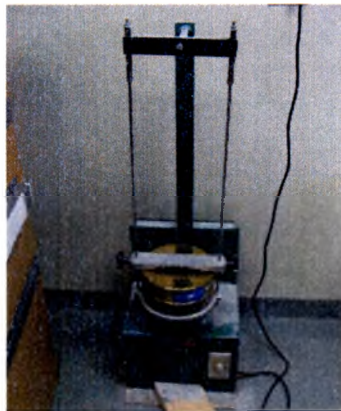


Figure 27: Clay sieving machine

Table 2 – Description of samples

<b>Sample</b>	<b>Aminocaproic acid (Surface Initiator)</b>	<b>3 Aminopropyl trimethoxy silane (Edge Initiator)</b>
Nylon 6	100 milleq	X
Surface Toyota	100 milleq	X
Surface Toyota & Edge	100millieq	2%
Surface Optimized	70millieq	X
Surface Optimized & Edge	70milleq	2%
Na+ Closite Edge	X	2%
93 A Edge	X	2%
Laponite Surface	60 milleq	X
Laponite Surface & Edge	60 milleq	16%
Laponite Edge	X	16%
[X = not added]		

### 3.3 In-situ Polymerization

Bulk polymerization is taken place in a 500-mL round bottom flask with a magnetic stirrer 15g of the modified clay, 275g of  $\epsilon$ -caprolactam (5% clay by weight) was added. The mixture was then heated to 230°C for 48 hours under an inert atmosphere. After cooling the products were mechanically crushed and washed with water at 85°C for 1 hour. All the samples were prepared by this procedure except the edge treated clay, which was heated for 72 hours and 100 milliequivalent of the aminocaproic acid was added to the reaction mixture in case of montmorillonite nanocomposite to improve the rate polymerization.

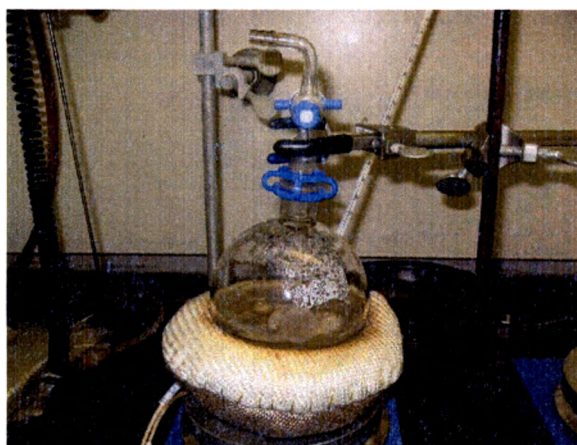


Figure 28: Bulk Polymerization Process

### 3.4 Characterization of the Clay Nanocomposite

Whenever a sample of material is to be studied, one of the easiest tests to perform is to heat it. The observation of the behavior of the sample and the quantitative measurement of the changes on heating can yield a great deal of useful information on the nature of the material.

### 3.4.1 Thermogravimetric Analysis (TGA)

The technique has been defined as a technique in which the mass change of a substance is measured as a function of temperature while the substance is subjected to a controlled temperature program TGA's of the nylon-6 nanocomposite were carried out on a TGA Q50 instrument (Figure 29) with a heating rate of 20°C/min in Ar atmosphere from room temperature up to 800°C.

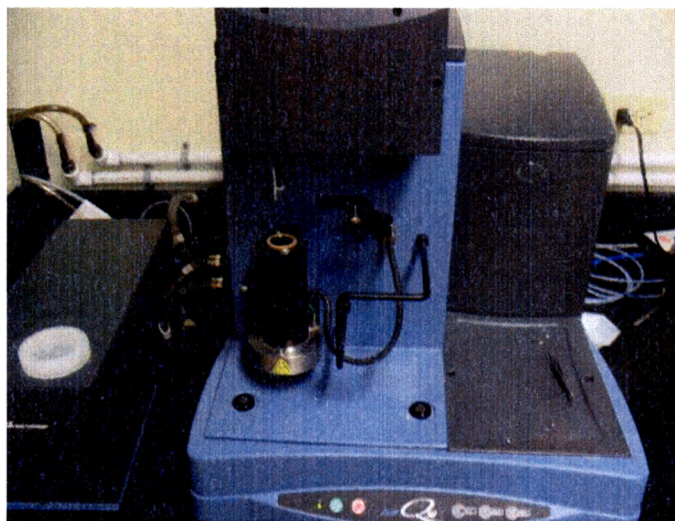


Figure 29: TGA Q50

#### 3.4.1.1 *Derivative Thermogravimetry (DTG)*

Overlapping reactions are sometimes difficult to resolve a DTG curve can be used to resolve overlapping reactions. The area under the DTG curve is proportional to the mass change and the height of the peak at any temperature gives the rate of the mass change at that temperature.

### 3.4.2 Modulated Temperature Differential Scanning Calorimetry (mt-DSC)

Differential scanning calorimetry was conducted in a Modulated DSC 2920 by TA instruments (figure 30), at a ramp rate of  $15^{\circ}\text{C}/\text{min}$  from room temperature up to  $300^{\circ}\text{C}$ . DSC is a technique we used to study the thermal transitions of the polymer component. The thermal transitions are the change that takes place in a polymer when it is heated (i.e crystallization, melting point,  $T_g$ ). The mt-DSC approach differs from that of the classical route in that it depends on the comparison between the thermal powers recorded at different heat rates. In mt-DSC the heating rate is continuously changing as a result of temperature modulation and the heat capacity is obtained by dividing the modulating heat flow by the modulated heating rate.

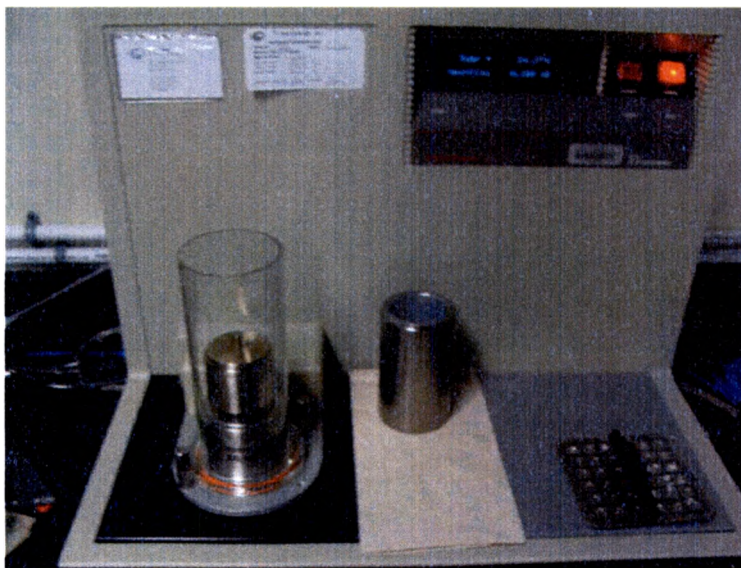


Figure 30: Modulated DSC 2920

### 3.4.3 Dynamic Mechanical Analysis (DMA)

Dynamic mechanical properties of nylon-6 nanocomposites were measured with a DMA Q800 from TA instruments (figure 32 & 33). The storage modulus  $E'$  and the loss modulus  $E''$  were determined at 1Hz in the temperature range between 50 and 150°C. The specimens were heated at a rate of 3°/min. Specimens were prepared for mechanical tests by Carver Model C Platen Press. The crushed nanocomposite was made into a plaques using Carver Model C Platen Press (figure 31) and standard size bar were cut out of these plaques, and DMA was conducted on these bars.

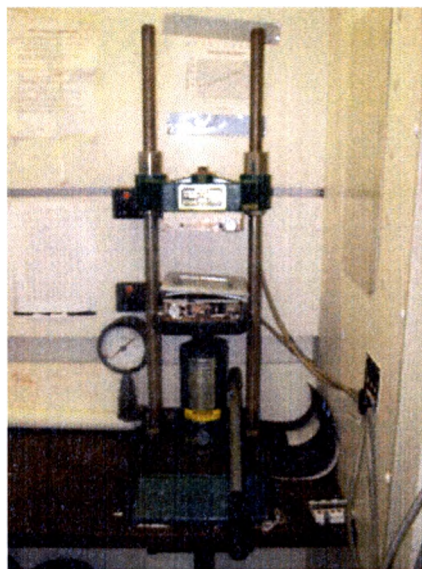


Figure 31: Carver Model C Platen Press

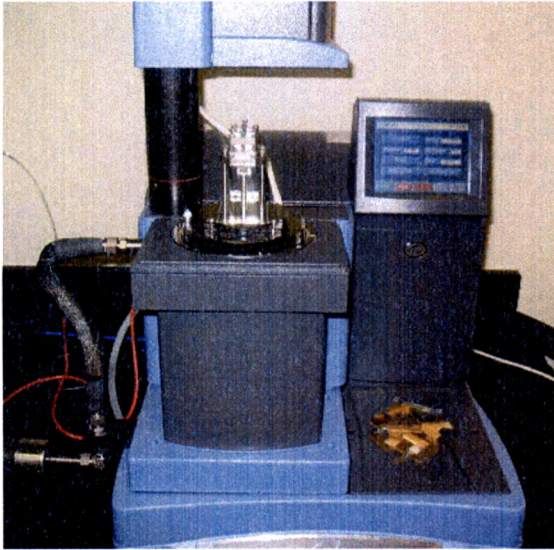


Figure 32: DMA Q800

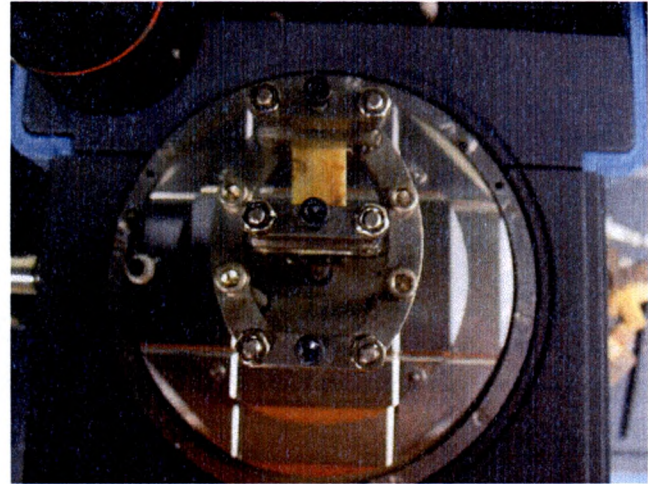


Figure 33: Specimen loaded on DMA Q800

#### 3.4.4 Notched Izod Impact Testing

Specimen's bars were then notched by the Notching Cutter Model TMI 22-05 and impact testing was done in a TEI Impact Testing Instrument Model # 48-0D-01, ASTM D256-04 [32].



Figure 34: Impact testing machine

### 3.4.6 Wide Angle X-ray Diffraction (WAXD)

WAXD was conducted in the reflective mode on selected nanocomposite at a scan rate of  $1^\circ/\text{min}$  using Bede XDS 2000 diffractometer using Ni filtered  $\text{CuK}\alpha$  X-ray radiation ( $\lambda = 1.54 \text{ \AA}$ ). The sample bars were oriented such that the incident beam reflected off the major surface of the bar. Samples were measured scanning  $2\theta$  angle from  $0.5$ - $20$  degree. The only d- spacing of interest in the diffractogram is the basal spacing along the c-axis.

Traditionally powder diffraction is used to characterize the structure of polymer/clay nanocomposite. Powder diffraction is used to monitor the position, full width at half maximum (fwhm) and intensity of the (001) basal reflection corresponding to the repeat distance perpendicular to the layers. A decrease in the degree of coherent layer stacking (i.e a more disordered system) results in peak broadening and intensity loss. In contrast, the extensive layer separation, beyond the resolution of Bragg Brentano geometry, of exfoliated structures does not result in a new observable, basal reflection, but leads to intensity loss and eventual disappearance of the unintercalated basal reflection. Real-time evolution of these scattering patterns provides detailed information on the dynamics of structural formation and intercalation, such as demonstrated by Vias and coworkers examining the kinetics of polymer melt intercalation [33].

## CHAPTER 4

### 4.0 RESULTS & DISCUSSION

Thermal and Mechanical characterization of the nylon 6 nanocomposites was carried out using TGA (Thermalgravimetric Analysis), DSC (Differential Scanning Calorimetry), DMA (Dynamic Mechanical Analysis) and Izod Impact Testing.. X-ray diffraction is used to determine the structure of the nanocomposites.

#### 4.1 Thermal Properties

The thermal properties of nylon 6 and various kinds of nanocomposites were determined by Differential Scanning Calorimetry (DSC) and Thermo Gravimetric Analysis (TGA). Table 3 and 4 provides a summary of the results.

Table 3 – Differential scanning calorimetry data of nanocomposites

Sample	T <sub>m</sub> °C	T <sub>c</sub> °C	ΔH <sub>c</sub> (J/g)
Nylon 6	219.00	182.00	71.56
Surface Toyota	220.34	187.22	79.53
Surface Toyota & Edge	217.03	185.65	84.42
Surface Optimized	214.67	186.17	91.65
Surface Optimized & Edge	217.26	181.06	87.64
Na+ Closite Edge	215.47	180.66	86.16
93 A Edge	220.94	184.68	65.57
Laponite Surface	210.52	177.56	95.61
Laponite Surface & Edge	212.51	179.57	88.84
Laponite Edge	215.06	185.40	77.95

The DSC measurement indicates that the melt point  $T_m$  of the nanocomposites is slightly lowered as compared to the Toyota nanocomposite and neat nylon 6 this is due to the crystalline behavior of the nanocomposite. The effect of the silicate platelets on the crystal structure of the nylon 6 matrix of nanocomposites has also been of interest.

Aliphatic polyamides such as nylon 6, well known for their strong hydrogen bonding (H-bonding) ability and seek to maximize the number of H-bonds within and between polymer chains. All possible H-bonds are satisfied in the crystalline regions and a vast majority consummated in the amorphous regions [34]. Furthermore a sizeable fraction of H-bonds remain even in the molten state. These strong H-bonding characteristics dominate some physical behavior of polyamides like nylon 6.

Maximizing of the H-bonds in the crystalline state of nylon 6 requires the polyamide chains to adopt either a fully extended or twisted configuration. In a fully extended configuration termed the  $\alpha$  form polymer chains are oriented in an antiparallel fashion, a monoclinic structure as shown in Figure 35, the  $\gamma$ -crystalline form of nylon 6 occurs, when H-bonds form between parallel polyamide chain and resembles a hexagonal structure. Wu and Lian examined the effect of thermal history and filler concentration on the crystal structure of nylon 6 nanocomposite formed by in-situ polymerization using saponite and natural montmorillonite. He concluded that nylon 6 nanocomposites at 5 % clay contains more of the  $\gamma$  form than  $\alpha$  form [35]. Thus it is due to the presence of these  $\gamma$ -crystals that the melting point of these nanocomposites was lower than the neat nylon 6.

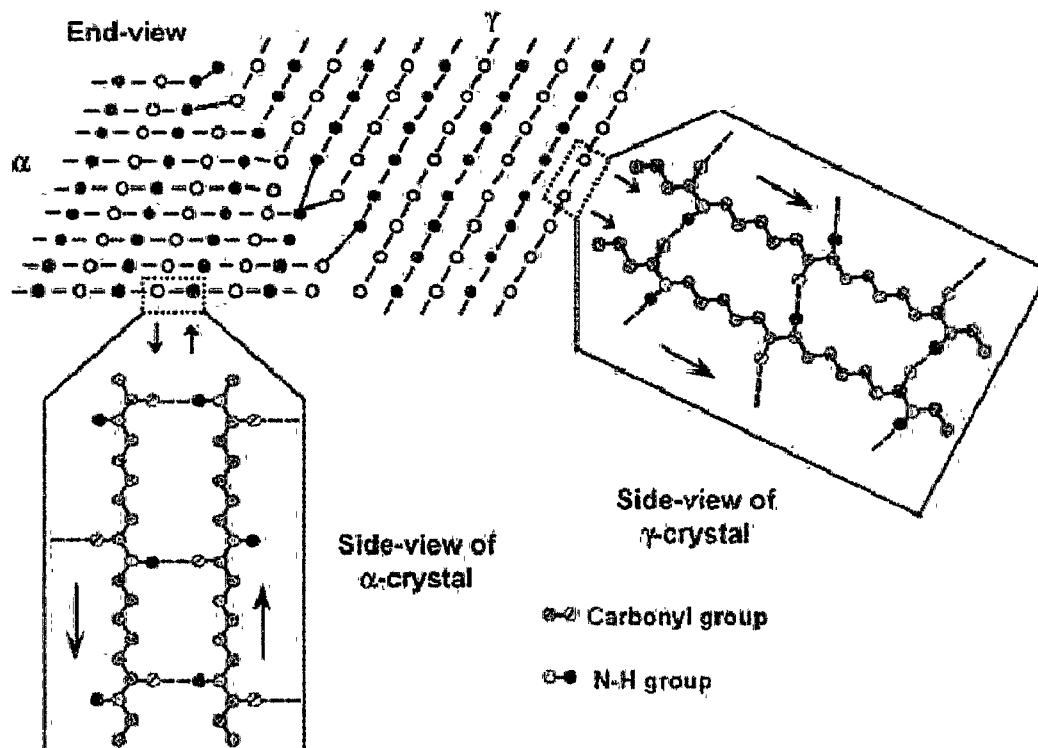


Figure 35: Schematic of hydrogen bonding within the  $\alpha$  and  $\gamma$  crystalline forms of nylon 6 as seen from end and side view of each crystal. Closed and open circles represent chain axes projecting out of and into the page respectively. Hydrogen bonds between polyamide chains are represented by dashed lines [36]

Degree of crystallinity is the single most important characteristic of a polymer in that it determines mechanical properties, such as yield stress, elastic modulus and impact resistance [37]. Of the various analytical methods used to determine the crystallinity of a polymer DSC is probably the most widely. The method that is employed in this study was to determine  $\Delta H_c$  (J/g) by integrating the area under the peaks. The heat of crystallization were determined by the cooling scans from 100 to 200 C° as shown in figure 36. The percent crystallinity is estimated through these values.

The above results indicate that the presence of filler increases the rate of crystallization of the nanocomposite as compared to neat nylon 6 this maybe due to the

fact that fillers can act as nucleating agents causing a higher degree of crystallinity. Smaller particles like laponite show high % crystallinity as compared to montmorillonite. This may be associated with an increase in the number of particles and thus nucleating sites on which crystals are able to originate and grow. Thus the above results prove that laponite, which has a smaller aspect ratio as compared to montmorillonite, behaves as an effective nucleating agent.

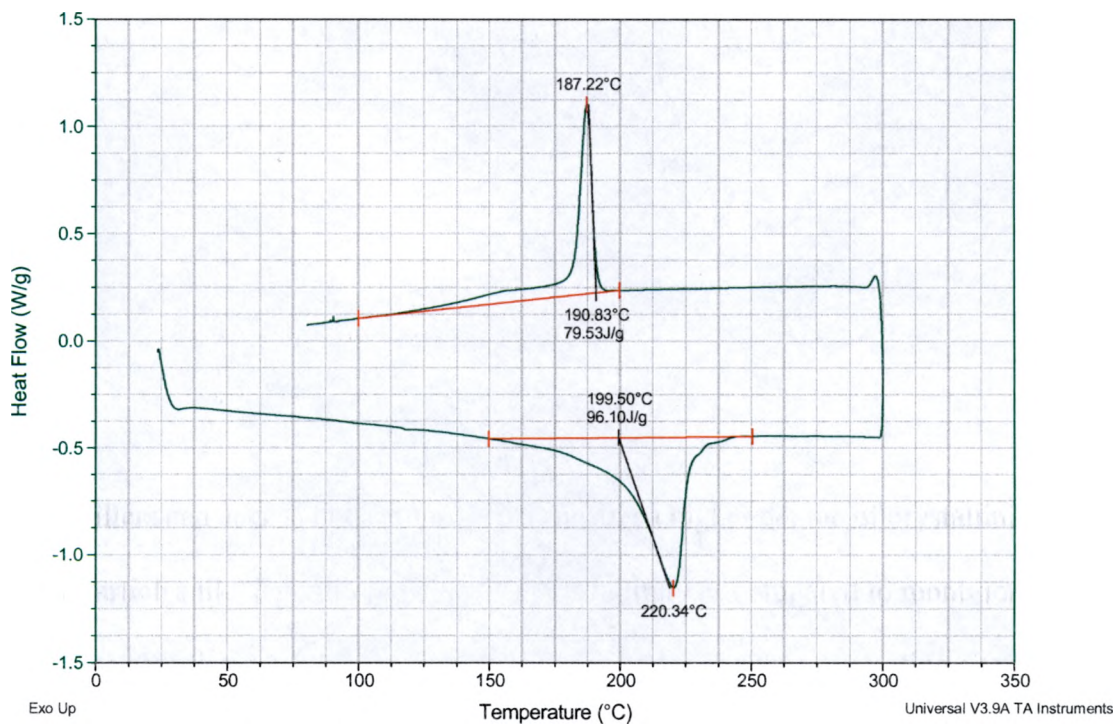


Figure 36: DSC of Surface Toyota Nanocomposite

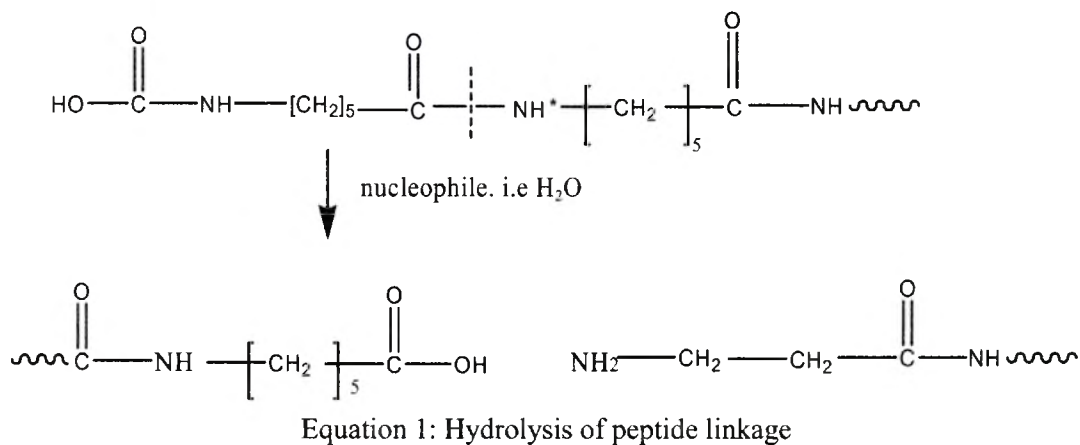
93A edge treated clay behaves peculiarly as it shows a comparable melting point to neat nylon 6, while the degree of crystallization is lower than neat nylon 6 and the crystallization temperature has increased. This behavior can be explained by the fact that 93A edge treated nanocomposite acts like a compounded organoclay nanocomposite and has similar characteristics as compared to the nylon 6 nanocomposites made previously via melt compounding by Paul et al [25].

As discussed above the polymer chains are growing from the edges of the clay plates and there are other polymer chains, which are growing in-between the clay plates as 100millivalent amount of initiator is added in the polymerization mixture to initiate polymerization. Thus this particular nanocomposite behaves as a compounded nanocomposite as compared to the other samples, the polymer chains are not tethered on the surface of the clay plates like surface treated nanocomposite.

The increase in crystallization temperature of this nylon 6 nanocomposite is a result of increasing chain mobility, this phenomenon is well known in the literature as summarized by Wunderlich[38]. The decrease in  $\Delta H_c$  is due to the rapid cooling of the plaque, the  $\text{Na}^+$  Cloisite edge treated clay does not show the same behavior as 93A because the hydrated  $\text{Na}^+$  ion on the surface does not interact well with the polymer and it can even result in the degradation of the polymer chain in the presence of water. X-ray diffraction data shows that the interaction between 93A and polyamide is favorable and results in well-exfoliated nanocomposite. Refer to Appendix A for all the DSC plots listed in table 3.

Sample	Decomposition Temperature °C	% Monomer
Nylon 6	473.10	9.66
Surface Toyota	462.60	5.68
Surface Toyota & Edge	457.98	5.81
Surface Optimized	459.37	3.71
Surface Optimized& Edge	459.74	2.17
Laponite Surface	469.64	0.00
Laponite Surface & Edge	461.97	3.66
Laponite Edge	451.52	10.04
Na+ Closite Edge	460.93	3.35
93 A Edge	461.44	5.42

According to the TGA result in table 4, the nanocomposites have somewhat lower stability than neat nylon 6. This is attributed to the degradation of the quaternary alkylammonium treated on the montmorillonite. Davis et al. [39] reported a significant level of nylon 6 degradation during high temperature melt processing i.e. at 300°C, of in situ formed nylon 6 nanocomposites. They proposed that the degradation was largely due to hydrolysis by water from the clay, either bound or from dehydroxylation of montmorillonite itself (equation 1).



However, Gilman et al. [40] observed that the fire retardant properties of nylon 6 nanocomposite were improved. In this case, the individual layers of clay act as an insulator and a mass transport barrier against oxygen or volatile degradation products generated as the nylon 6 decomposes. On the other hand they did not find any difference in stability. Figure 37 shows the TGA of all the nanocomposites and nylon 6. The weight loss at the initial stage ( $\leq 100^\circ\text{C}$ ) results from surface adsorption of water.

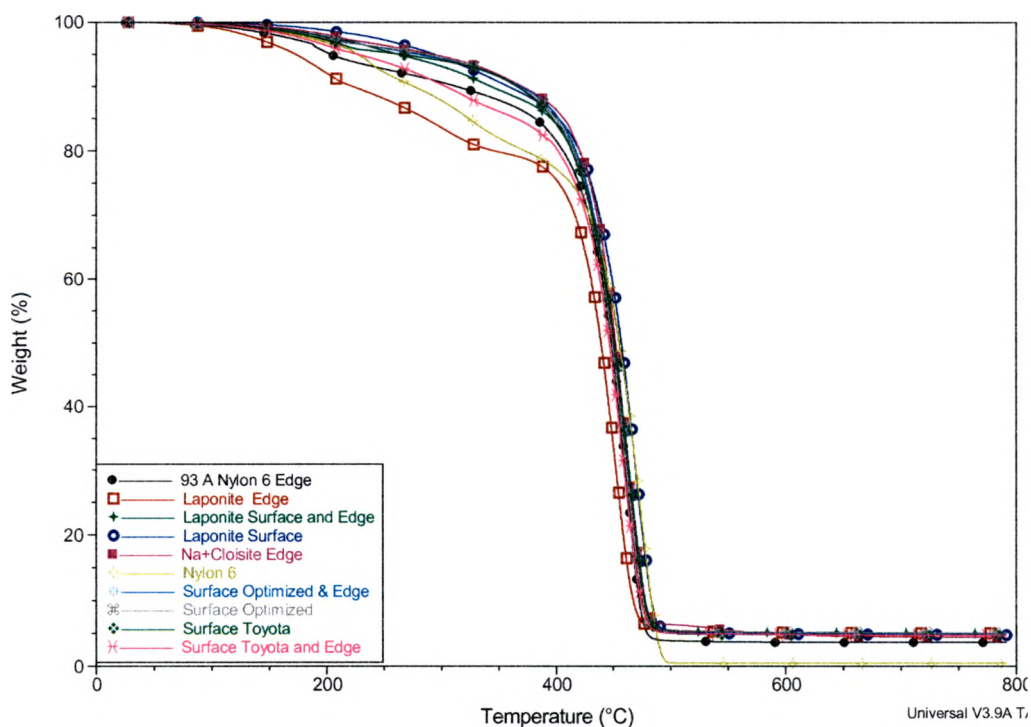


Figure 37: TGA curves of Nylon 6 and all the Different Nylon 6 Nanocomposite

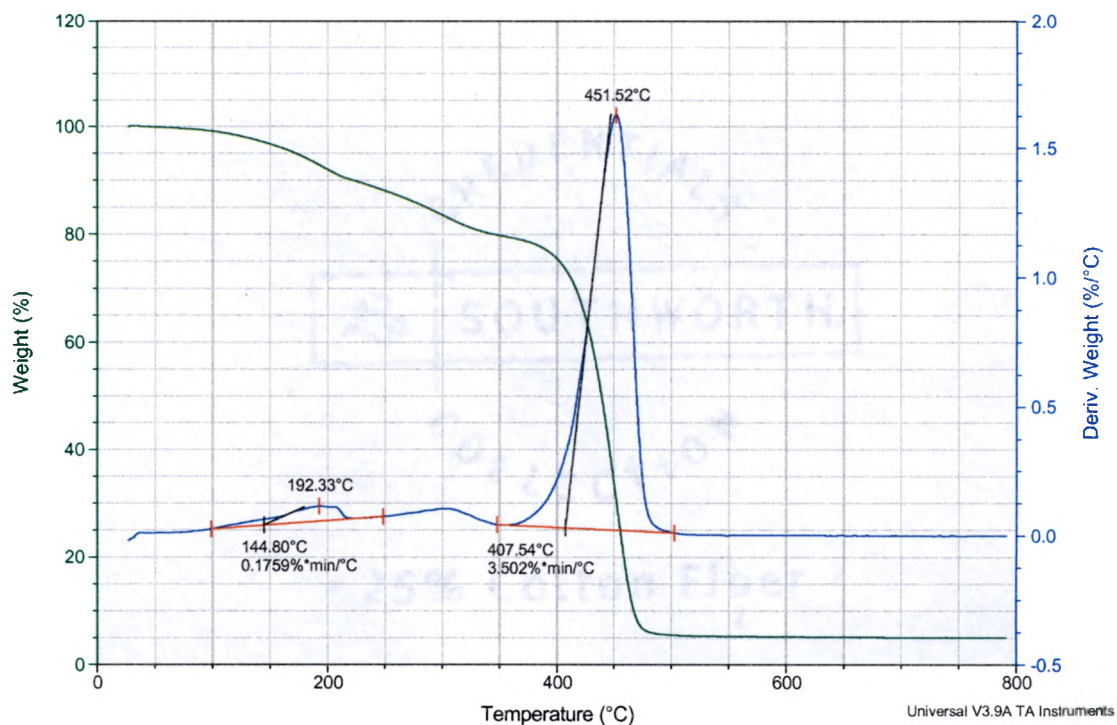


Figure 38: TGA curve and the 1<sup>st</sup> derivative curve of laponite edge treated nanocomposite

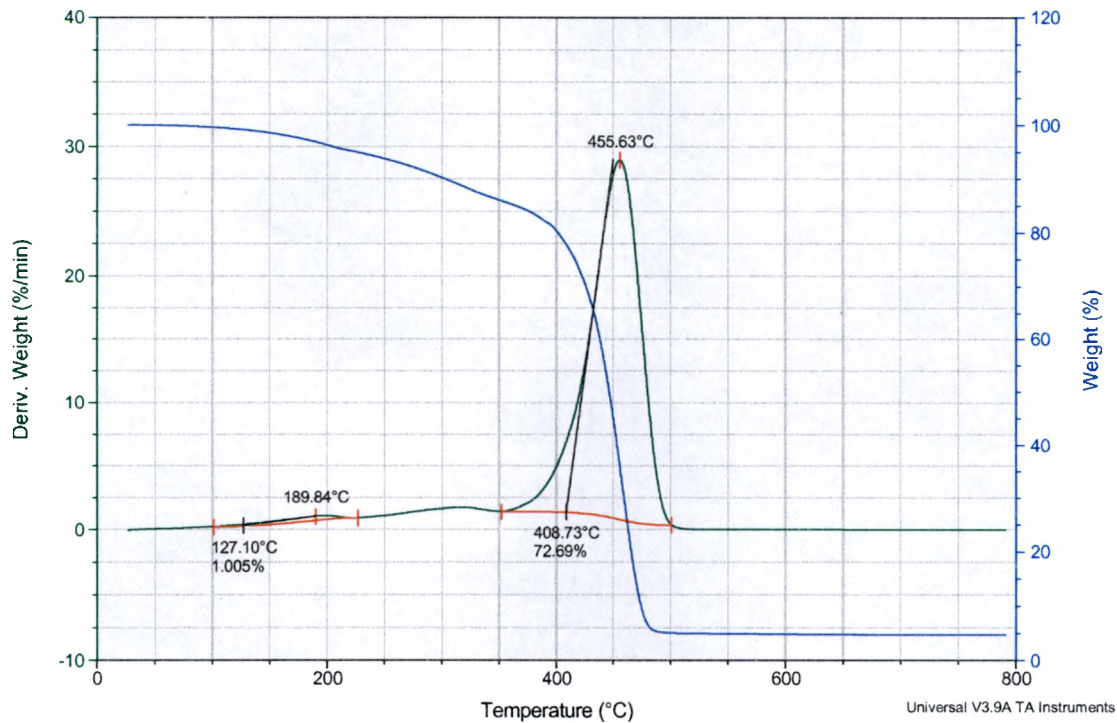
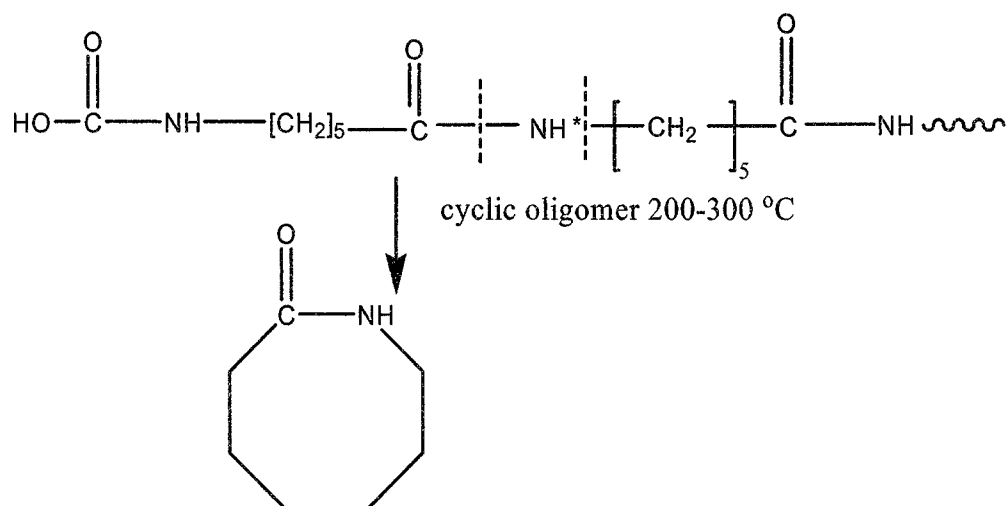


Figure 39: TGA and 1<sup>st</sup> derivative curve of Surface Toyota and Edge nanocomposite.

The weight loss associate at around 200 °C which is listed in table 4 is caused by the degradation of the un-reacted monomer present inside the polymer or of the monomer formed due to the intermolecular end-group cyclization reaction of the polymer chain at 200 -300 °C (equation 2) This cannot be well observed from the TGA curve but looking at the first derivative curve of some nanocomposite (shown in figure 38 & 39) it can be seen that there are two distinct peak associated with the weight loss of the nanocomposite. Degradation of the polymer causes a plasticizing effect in the nanocomposite as observed in the DMA results. Refer to Appendix B for the TGA plots listed in table 4.



Equation 2: Intramolecular cyclization of the oligomer to generate  $\epsilon$ -caprolactam [39]

## 4.2 Dynamic Mechanical Behavior of Nylon 6 Nanocomposite

The storage modulus of the nanocomposite has increased by 78.4%, which is not unusual as the presence of the filler dramatically improves the modulus of nylon 6 as reported earlier [23]. Table 5 and the bar diagram shows that the storage modulus of all the nanocomposites is significantly higher than neat nylon 6.

In general, the dynamic mechanical analysis of nylon 6 shows an  $\alpha$  peak in the  $\tan \delta$  curve that originates from the movement of the longer molecular chains in the amorphous region, corresponding to the glass transition temperature as can be seen from figure 40. Some of the  $T_g$ 's of the nanocomposite are comparable to neat nylon 6 but others are more than nylon 6 except the Surface Toyota and Edge treated nanocomposite, the  $T_g$  of this nanocomposite was not observed.

A similar characteristic should have been observed by Surface Optimized and Edge treated nanocomposite but due to the slow rate of polymerization, and low concentration of the initiator on the surface of the clay plates, there is no polymerization taking place in the galleries. The low concentration of initiator lowers the compatibility of the clay for the monomer this effect is observed in X-ray diffraction of the nanocomposite which shows a basal spacing of 14.85 Å which proves that no polymerization has taken place in the galleries.

The  $T_g$  of Surface Toyota and Edge treated clay was not observed in the DMA because of the peculiar behavior of the loss modulus. Figure 42 shows the different  $\tan \delta$  curves of selected nanocomposites it can be seen that the  $\tan \delta$  curve of the Surface Toyota and Edge treated nanocomposite shows a very different behavior than the other nanocomposite that is due to the interaction of the amine terminated polymer on the

edges of the clay plates with the carboxyl terminated polymer growing from the surface of the clay plates. It is because of this peculiar behavior of Surface Toyota and Edge treated nanocomposite that the Impact properties of the nanocomposite is improved as observed later. Refer to Appendix C for the DMA plots of the nanocomposites listed in table 5.

Table 5 – Dynamic Mechanical data of nanocomposite

Sample	Tg °C	E' at Tg (MPa)	E' at 30°C(MPa)
Nylon 6	59.54	744.5	972.8
	57.95	756.7	976.7
	58.75	648.6	837.5
Surface Toyota	52.55	1061	1676
	55.80	1447	1568
	56.29	1335	1729
Surface Toyota & Edge	Not observed		1066
			1315
			1417
			1181
Surface Optimized	58.13	1156	1607
	58.83	1026	1435
	60.42	934.0	1315
Surface Optimized & Edge	58.13	927.1	1232
	58.13	912.2	1219
	59.01	1051	1456
Na+ Cloisite Edge	60.25	866.7	1177
	58.87	1066	1513
	61.16	970.5	1371
Laponite Surface	62.19	845.3	1248
	63.43	728.5	1088
	63.55	764.0	1114
Laponite Surface & Edge	60.25	795.2	1040
	60.10	791.9	1092
	60.09	911.1	1261
Laponite Edge	80.68	745.4	1112
	74.23	762.2	1114
	65.01	797.4	1070
93 A Edge Treated	60.40	1148	1655
	60.42	838.8	1223
	61.19	1209	1813

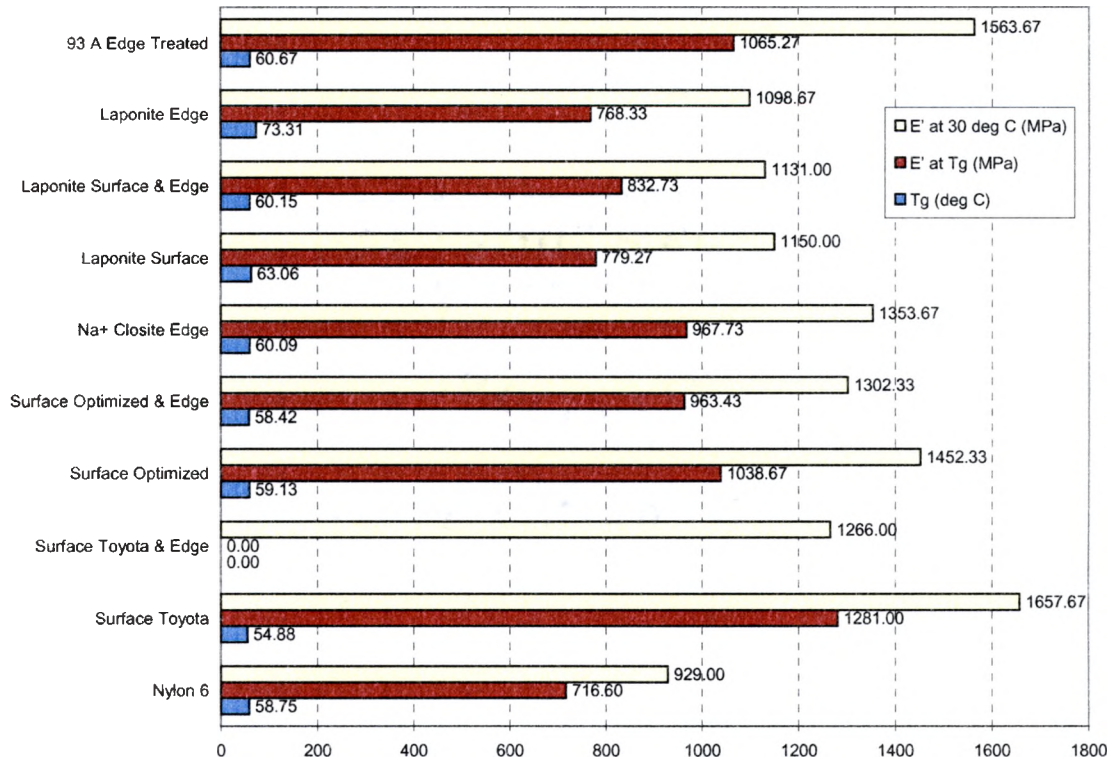


Figure 40: Bar Diagram of Dynamic mechanical behavior of nanocomposites

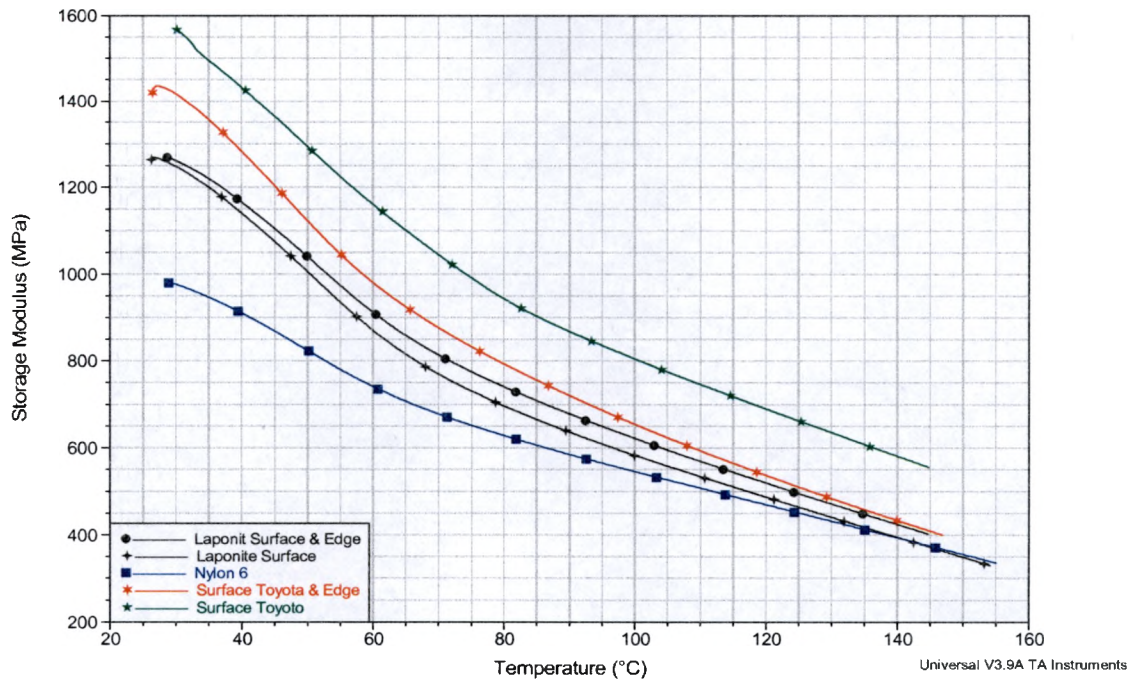


Figure 41: Storage modulus plots of nylon 6 and nylon 6 nanocomposites

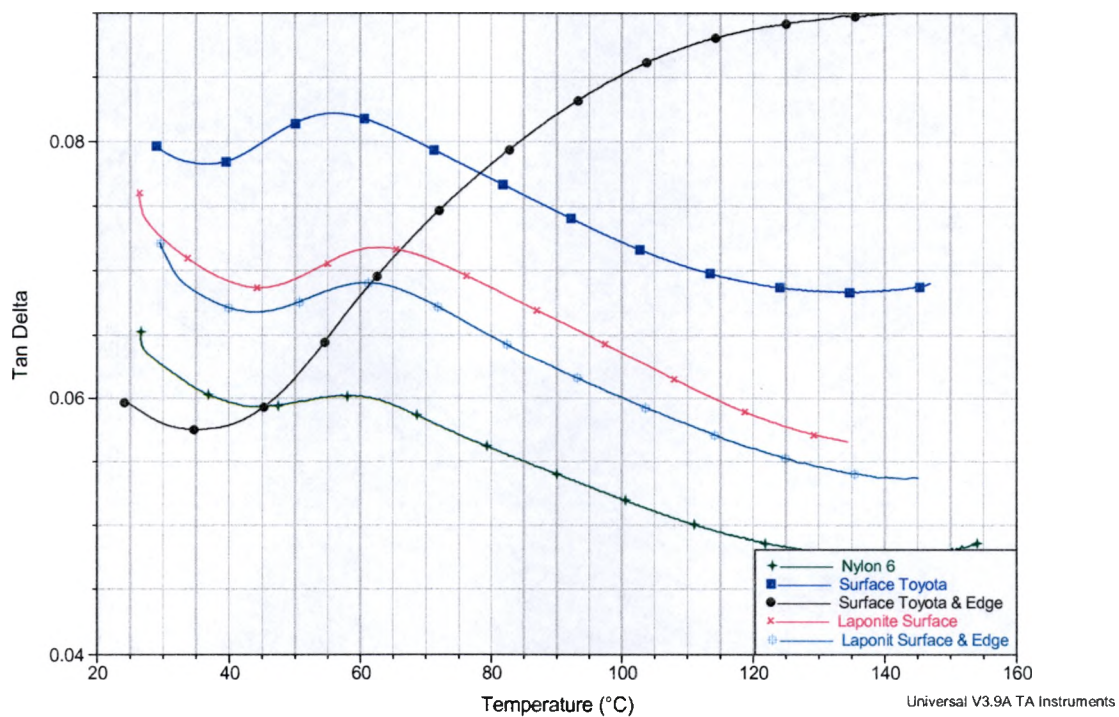


Figure 42: Tan  $\delta$  plots of nylon 6 and selected nylon 6 nanocomposites

### 4.3 Mechanical Properties of Nylon 6 Nanocomposite

In general, the addition of rigid particle to a thermoplastic matrix results in an increase in strength, modulus and dimensional stability. A summary of the mechanical properties of these materials is shown in table 6. As evident from figure 43 (see next page), regardless of the type of filler, the strength and modulus were substantially increased relative to neat nylon 6. As discussed previously, the nanocomposite is treated with hexamethylenediamine by Toyota researchers A.Okada *et al* [29] to regain the toughness of the material. As this research is comparative between the different kinds of nanocomposite, in which the amount of clay is maintained but the treatment of the clay is different, hexamethylenediamine was not added, as can be seen from table 4. The Impact property of the nanocomposite is sacrificed as compared to nylon 6, meaning that the materials toughness deteriorates.

Table 6 – Impact test data

Sample	Izod Impact Testing
Nylon-6	NB
Laponite Surface	0.98+/-0.06
Laponite Surface & Edge	0.96+/-0.125
Laponite Edge treated	0.76+/-0.1
Surface Optimized	1.20+/-0.06
Surface Optimized & Edge	1.00+/-0.14
Na <sup>+</sup> Cloisite Edge	1.04+/-0.1
Surface Toyota & Edge	4.62+/-0.737
Surface Toyota	2.28+/-0.38
93 A Edge Treated	1.85+/-0.04

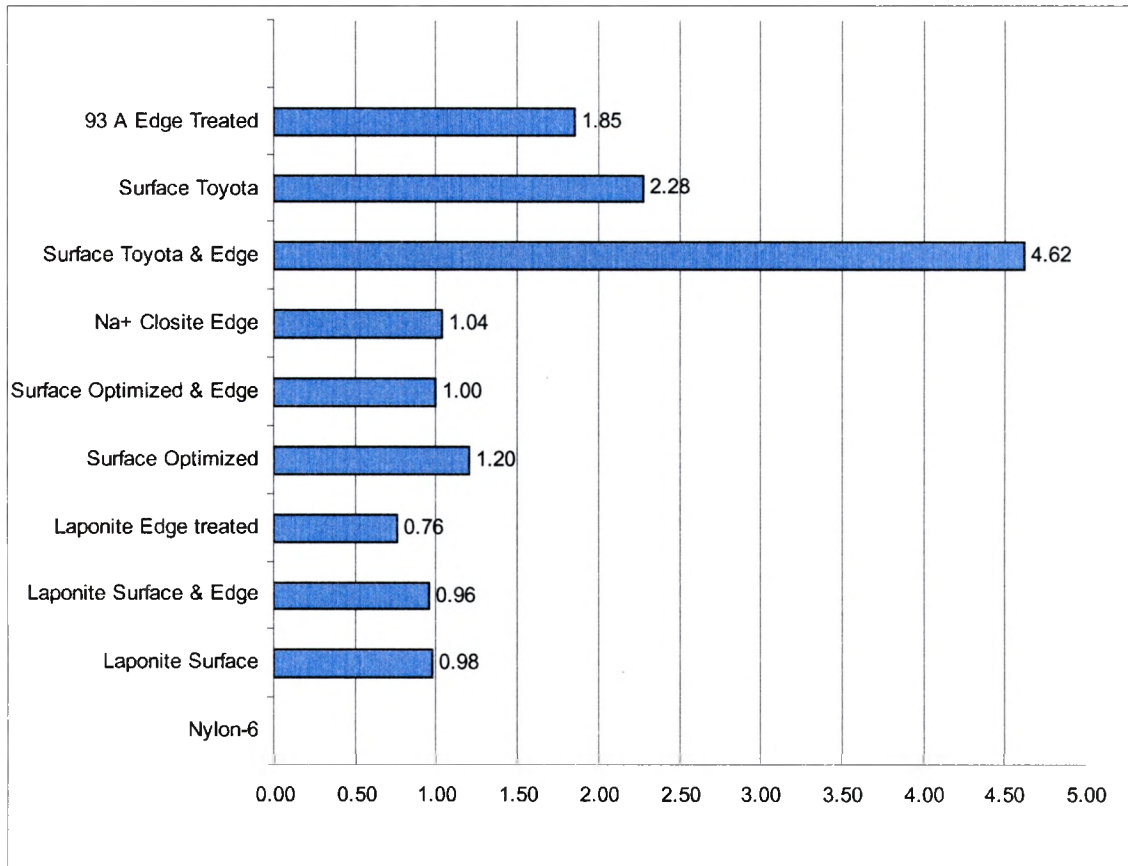


Figure 43: Impact test data graph

But comparatively it is observed that all the nanocomposites show a lower Notched Izod Impact averaging around 1.0 except the Surface Toyota and the Surface Toyota and Edge treated and 93A. This results show that the impact strength of the Surface Toyota and Edge has increased by 102.6 % relative to the Surface Toyota treated. This is due to the interaction of the polymer growing from the edges of the clay plates which is amine terminated with the polymer growing from the surface of the clay plates which is carboxyl terminated. The different  $\tan \delta$  curves observed in the DMA for the Surface Toyota and Edge treated nanocomposite correlates to these results. 93 A, as explained earlier, acts as an intercalated nanocomposite thus showing higher impact property than the rest. It is illustrated in the literature that the melt compounded clay has

slightly different characteristic than nanocomposites made via in-situ polymerization. This is due to the fact that nanocomposite made via in-situ polymerization are tethered on the surface of the clay plates while those nanocomposite made via melt compounded have polymer chains intercalated in between the clay plates hence having high chain mobility.

#### 4.4 Wide Angle X-ray Diffraction

Wide angle X-ray diffraction (WAXD) pattern of the sample prepared in this study are given in [table 7](#). For montmorillonite a diffraction peak can be seen at  $9.2$  and  $7.1^\circ$  ( $2\theta$ ), which corresponds to basal distance of  $9.6$  and  $12.5\text{\AA}$  respectively. The basal distance of  $12.5\text{\AA}$  is attributed to hydration of the silicate sheet. For the samples the peak at  $31.3\text{\AA}$ - $18.49\text{\AA}$  is due to the formation of oligomer-clay complex the degree of polymerization depends upon the basal distance of the clay plates. The peaks around  $14.85\text{\AA}$ - $16.38\text{\AA}$  are due to the presence of 6-aminocaproic acid and  $\epsilon$ -caprolactam present in between the clay plates. [Figure 44](#) illustrates all the stages in the polymerization process.

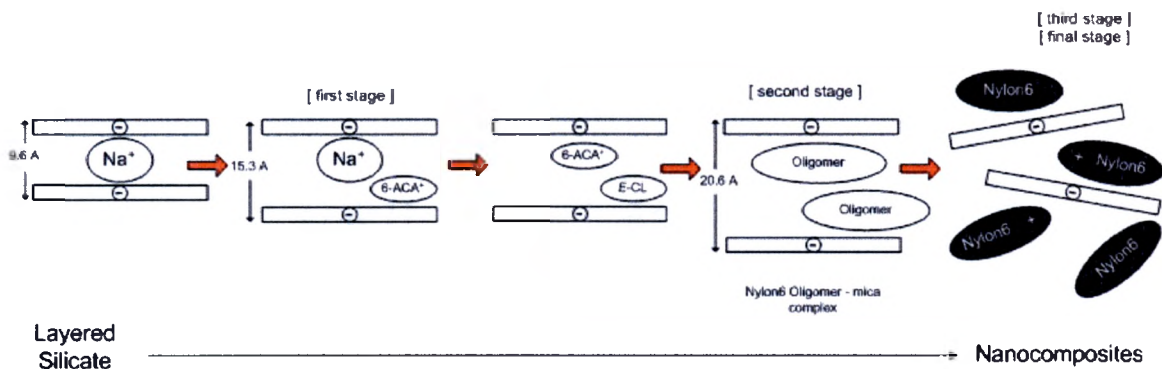


Figure 44: Schematic illustration of the nanocomposite formation process

It has already been discussed that a decrease in the degree of coherent layer stacking (i.e. a more disordered system) results in peak broadening and intensity loss. Some of the nanocomposite formed in this study shows a well-exfoliated structure while some show a more disordered system. Surface Optimized and Edge treated clay as discussed previously does not show the same property as the Surface Toyota and Edge treated nanocomposite this is due to that there is no polymerization taken place in the galleries of the clay plates reducing the concentration of the initiator on the surface of the clay plates reduces the compatibility of the clay plate for the monomer thus show no exfoliation in the polymer matrix as observed by X-ray this particular nanocomposite shows a d-spacing of 14.85 Å which is due to the presence of  $\epsilon$ -caprolactam and the initiator. Those samples that show no peak or a very broad peak are superior in quality than others, which is explained in the discussion above. Refer to Appendix D for X-rays of nanocomposites listed in table 7.

Table 7 – Wide Angle X-ray Diffraction data

Sample	d A°	Intensity(cps)
Nylon 6	X	1078.15
Surface Toyota	19.14	851.59
Surface Toyota & Edge	19.44	3839.84
Surface Optimized	16.38	1649.34
Surface Optimized & Edge	14.85	3016.14
Na+ Cloisite Edge	15.09	2994.62
93 A Edge	X	X
Laponite Edge	18.49	998.79
Laponite Surface	X	X
Laponite Surface & Edge	31.3	1317.55

## CHAPTER 5

### 5.0 CONCLUSIONS

#### 5.1 Optimizing Molecular Weight of the Nanocomposite

The treatment of the nanocomposite with fewer numbers of initiators does not improve the properties of the nanocomposite. This is probably due to the fact that the presence of the filler dominates the characteristic of the nanocomposite. Lowering the amount of initiators also resulted in increasing the reaction time of the nanocomposite, which lead to further degradation as dissipation of heat is a big problem in bulk polymerization. It is clearly observed in X-ray diffraction that optimizing the number of initiators on the surface of the clay lowers the compatibility of the clay plates for the monomer thus the swelling of the clay plates does not take place. The results show that no polymerization is observed in galleries of the clay plates. Thus overall lowering the number of initiators does not improve the properties of the nanocomposite as predicted earlier.

## 5.2 Effect of the Edge Treatment on Nanocomposite

Treatment of the clay with functional silane did not bring about significant differences in the thermal properties as shown by the TGA and DSC. The Tg of Surface Toyota and Edge nanocomposite was obscured due to the unusual behavior of the nanocomposite. The storage modulus of the nanocomposite did not show any dramatic improvement but dramatically affected the impact properties of the nanocomposite. This is attributed to the interaction of the amine-terminated polymer at the edges of the clay plates with the surface carboxyl terminated polymer of another clay plate and building a house of cards. What we tried to do here is to look at the properties of the nanocomposite that Toyota researchers made and see how the impact properties improved with the addition of hexamethylenediamine which converts some of the carboxyl groups of the polymer chain end on the surface of the clay plates into amine terminated, thus the interaction of these amine end groups with the carboxyl end groups of another polymer chain cause the impact property to go up.

Our research took the same concept but in a different manner instead of adding hexamethylenediamine we added silane-coupling agents on the edges of the clay plates which as established previously are amine terminated thus a similar interaction between the amine terminated polymer on the edges of the clay plates with the carboxyl terminated polymer on the surface caused an increase in impact property of the nanocomposite. Toyota group observed a 185% increase in the impact property of the unnotched nanocomposite with an addition of 0.3 % of hexamethylenediamine While we observed a 102.63% increase in the impact property of the notched nanocomposite with

the addition of 2% silane by weight of the clay which would be equal to 0.1% silane in the reaction mixture. The results prove that the composite material made using a different method is equally effective in increasing the impact property of the nanocomposite. The conceptual model of building a house of cards is proven well by these results Surface Optimized and Edge treated nanocomposite should behave in a similar manner as Surface Toyota and Edge does this was not observed due to the absence of exfoliation in the nanocomposite lowering the amount of initiator lowered the compatibility of the clay plates towards the monomer thus the polymerization does not take place in the galleries. Therefore it does does behave in a similar manner as Surface Toyota and Edge nanocomposite.

### **5.3 Edge Treated Nanocomposite**

The conceptual model that we predicted for the organoclay edge treated holds true. 93A organoclay, which has polymer growing out of the edges of the clay plate's show a well exfoliated structure, thus the polymer growing from the edges of the clay plates helps in the exfoliation of the clay plates in the polymer matrix. The polymer chains as in surface Toyota nanocomposite are not tethered on the clay surface. Thus it acts as a compounded nanocomposite which is why it shows different characteristic than the other nanocomposites made in this research project.

### **5.4 Effect of Particle Size on the Nanocomposite**

For polymer composite system size, shape and concentration of the filler can have a significant effect on the rheological properties. The comparative study of the laponite and montmorillonite nanocomposite show that laponite, having a smaller particle size, does not perform as a better nanocomposite than montmorillonite. This is due to the

presence of larger number of hydroxyl groups in the laponite nanocomposite. Laponite is fluorinated clay which has a lot of fluorines instead of hydroxyl groups on its edges. These fluorine edges do not interact well with the silane coupling agent thus there are a lot of un-reacted hydroxyl groups present due to the silane in the treated clay. These hydroxyl groups acts as nucleophilies and breaks the peptide linkage of the polymer thus resulting in an increase in degradation of the polymer chains.

## APPENDICES

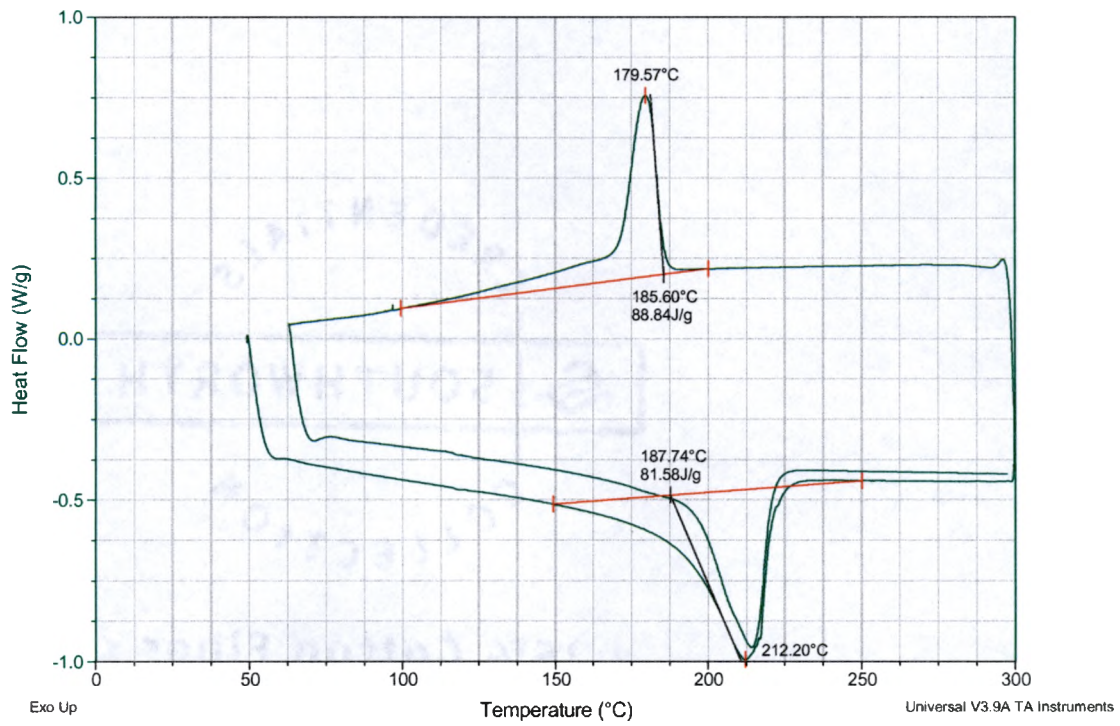
**APPENDIX A – DSC GRAPHS OF NYLON 6 NANOCOMPOSITES**

## Appendix A1 – DSC of Laponite Surface & Edge

Sample: Laponite Surface & Edge Again  
Size: 16.3000 mg  
Method: Heat/Cool/Heat

DSC

File: C:\...Laponite Surface & Edge Again.001  
Operator: stew  
Run Date: 5-Jul-04 15:33  
Instrument: 2920 MDSC V2.6A

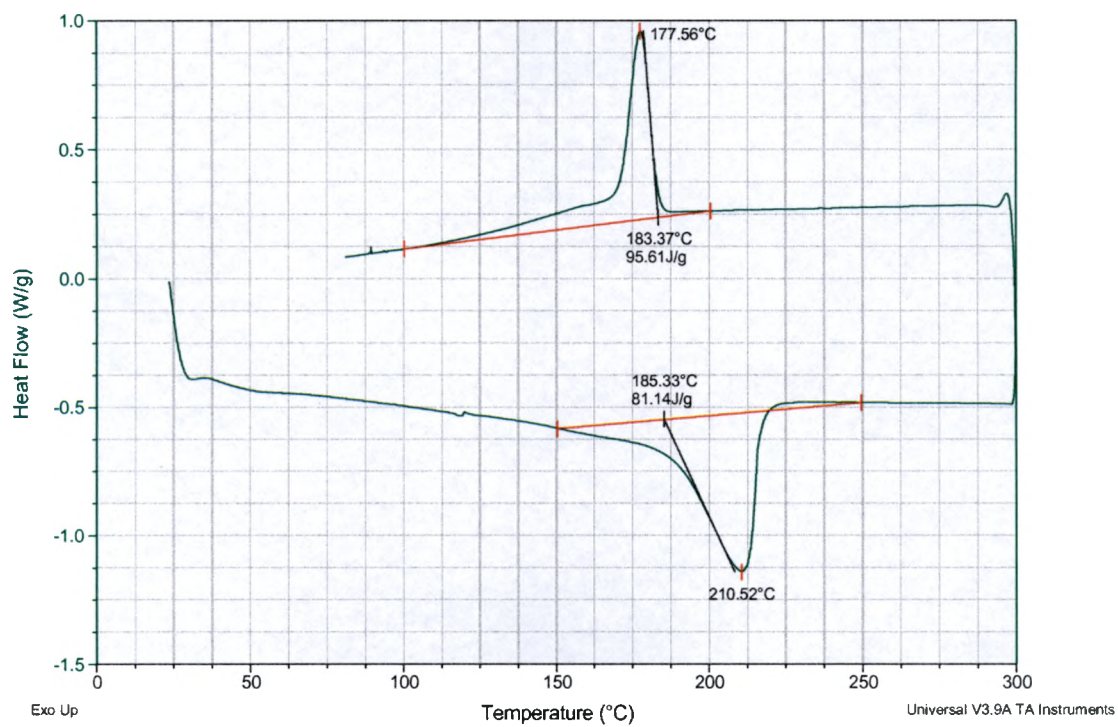


## Appendix A2 – DSC of Laponite Surface

Sample: Laponite Surface  
Size: 10.5000 mg

DSC

File: C:\...\Beall\Goofy\Laponite Surface.001  
Operator: stew  
Run Date: 1-Jul-04 10:52  
Instrument: 2920 MDSC V2.6A

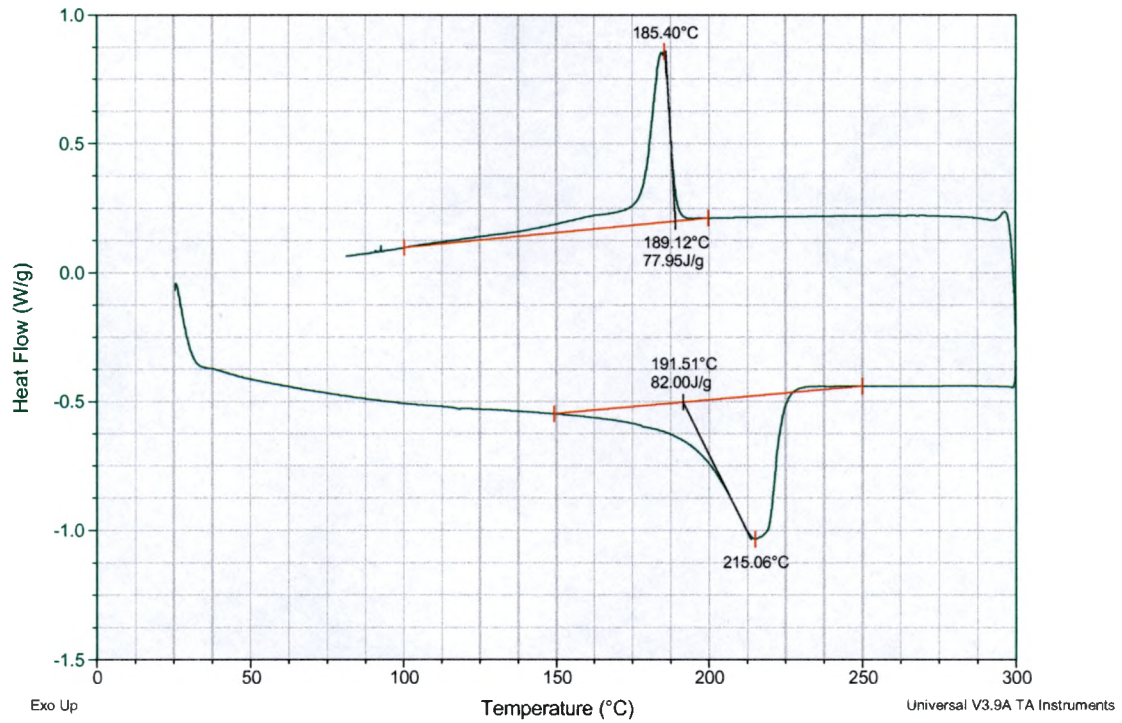


## Appendix A3 – DSC of Laponite Edge

Sample: Laponite Edge 2nd run  
Size: 13.7000 mg

DSC

File: C:\...\Goofy\Laponit Edge 2nd Run.001  
Operator: stew  
Run Date: 2-Jul-04 16:39  
Instrument: 2920 MDSC V2.6A

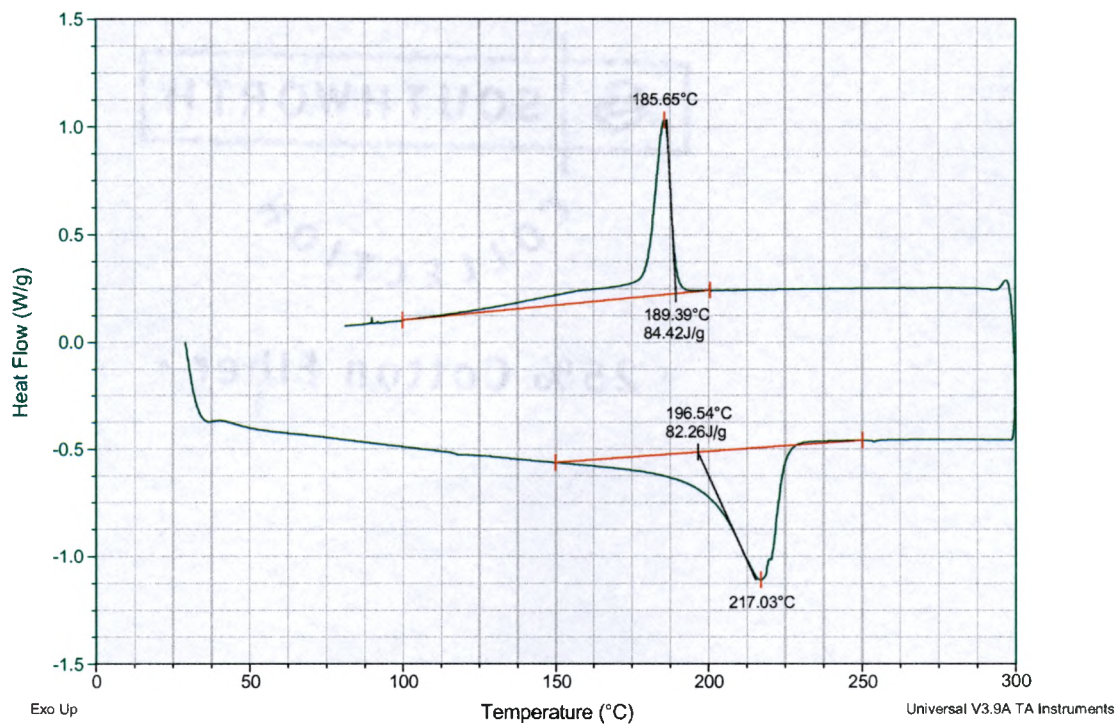


## Appendix A4 – DSC of Surface Toyota & Edge

Sample: Surface toyota & edge  
Size: 10.1000 mg

DSC

File: C:\...\Goofy\Surface toyota & edge.001  
Operator: stew  
Run Date: 30-Jun-04 17:32  
Instrument: 2920 MDSC V2.6A

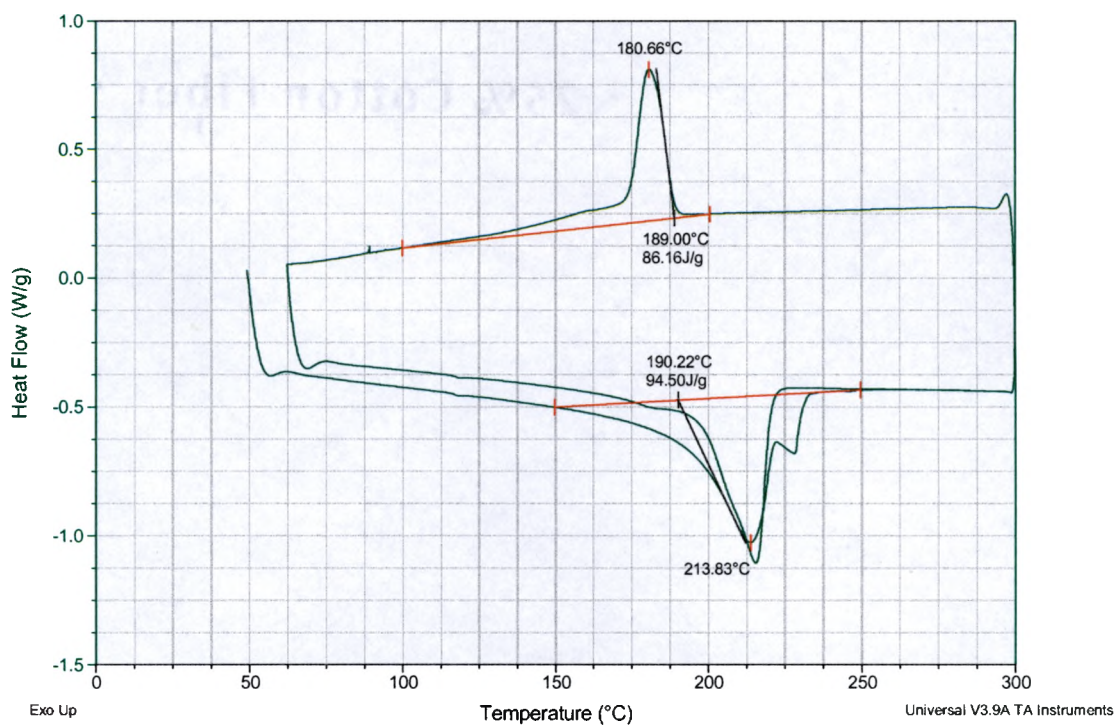


## Appendix A5 – DSC of Na+ Cloisite Edge

Sample: Na+ Cloisite Edge 2nd  
Size: 10.2000 mg  
Method: Heat/Cool/Heat

DSC

File: C:\...\Goofy\Na+ Cloisite Edge 2 nd.001  
Operator: stew  
Run Date: 5-Jul-04 11:22  
Instrument: 2920 MDSC V2.6A

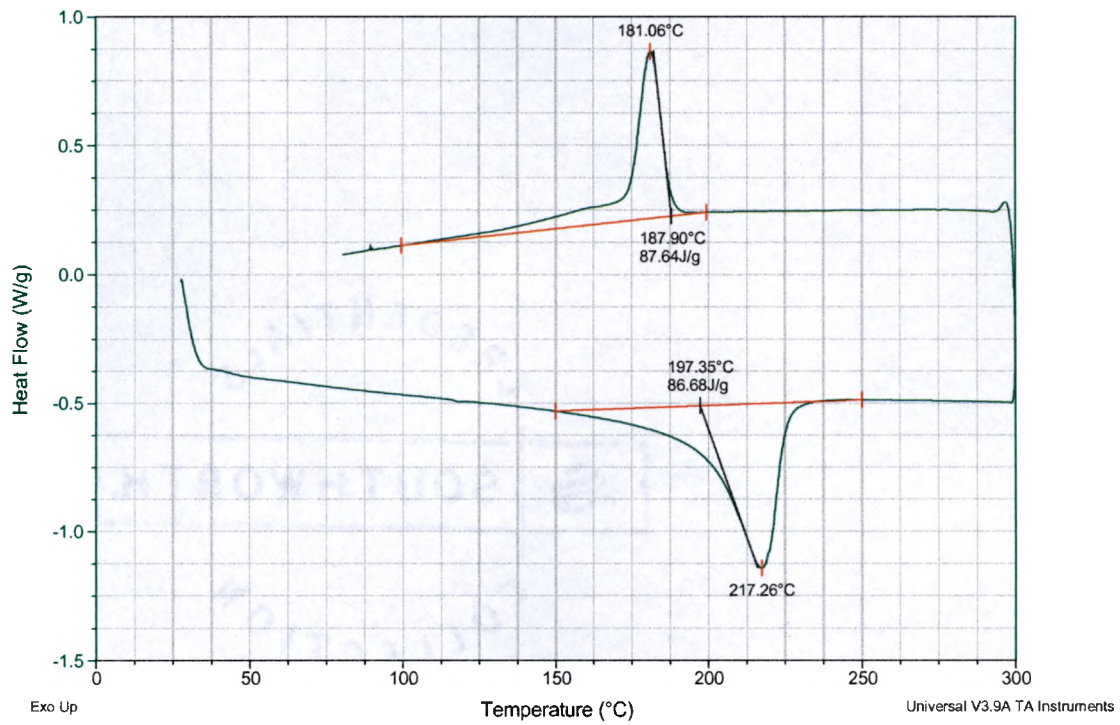


## Appendix A6 – DSC of Surface Optimized & Edge

Sample: Surface Optimized & Edge  
Size: 13.1000 mg

DSC

File: C:\...\Goofy\Surface Optimized & Edge.001  
Operator: stew  
Run Date: 1-Jul-04 15:52  
Instrument: 2920 MDSC V2.6A

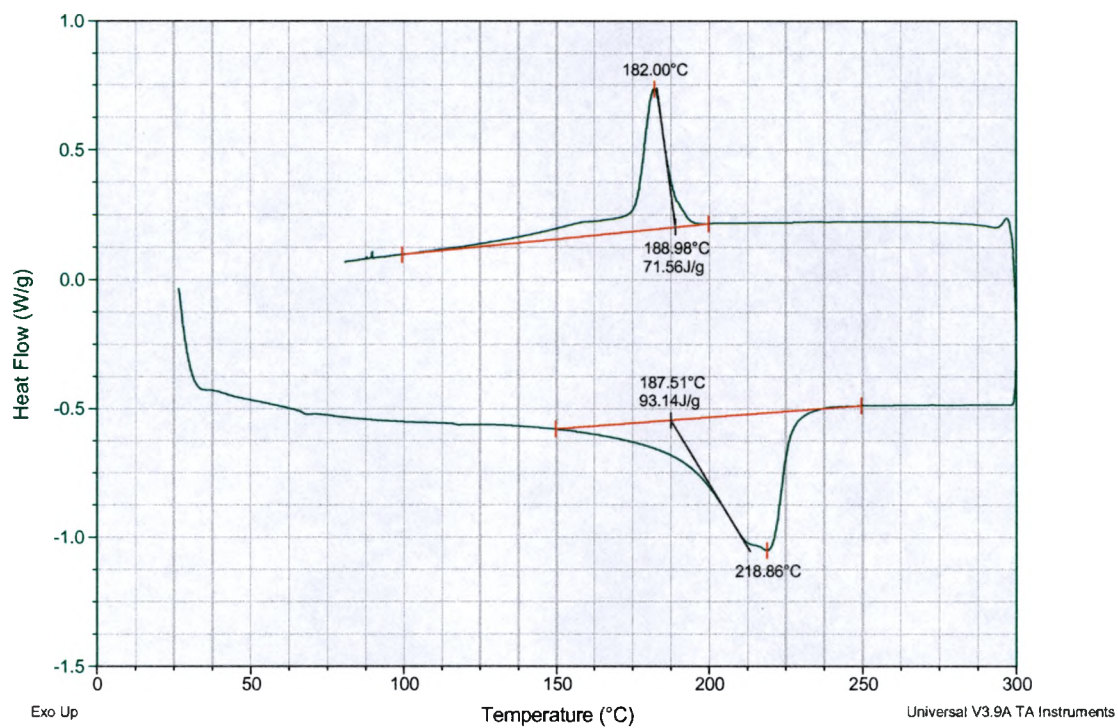


## Appendix A7 – DSC of Nylon 6

Sample: Nylon 6  
Size: 12.4000 mg

DSC

File: C:\TA\Data\DSC\Beall\Goofy\Nylon 6.001  
Operator: stew  
Run Date: 1-Jul-04 13:23  
Instrument: 2920 MDSC V2.6A

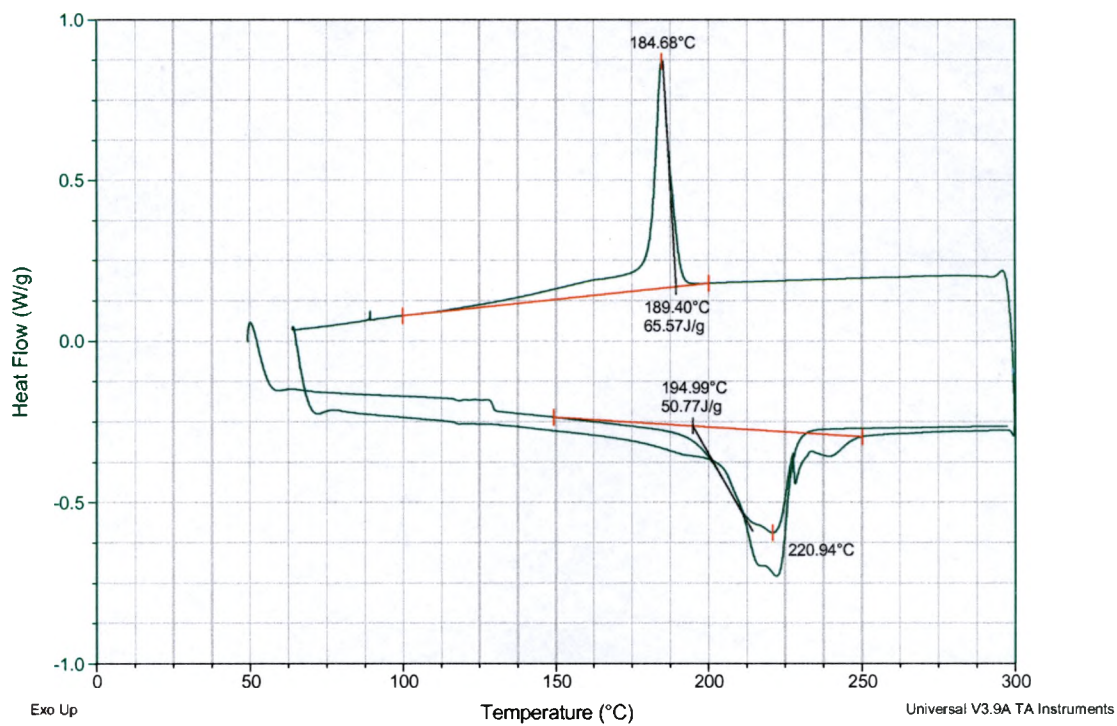


## Appendix A8 – DSC of 93 A Edge Treated

Sample: 93 A Edge Treated New  
Size: 12.0000 mg  
Method: Heat/Cool/Heat

DSC

File: C:\Goofy\93 A Edge Treated New.001  
Operator: stew  
Run Date: 5-Jul-04 18:53  
Instrument: 2920 MDSC V2.6A

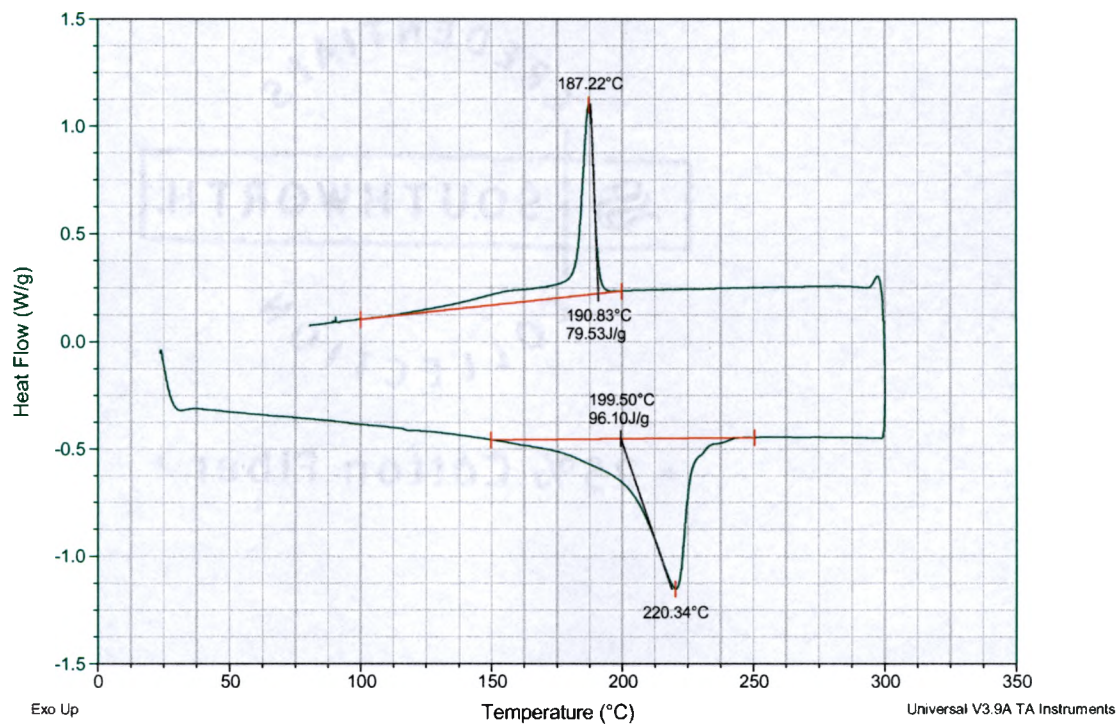


## Appendix A9 – DSC of Surface Toyota

Sample: Surface Toyota New  
Size: 10.3000 mg

DSC

File: C:\...\Beall\Goofy\Surface Toyota New.001  
Operator: stew  
Run Date: 2-Jul-04 14:29  
Instrument: 2920 MDSC V2.6A

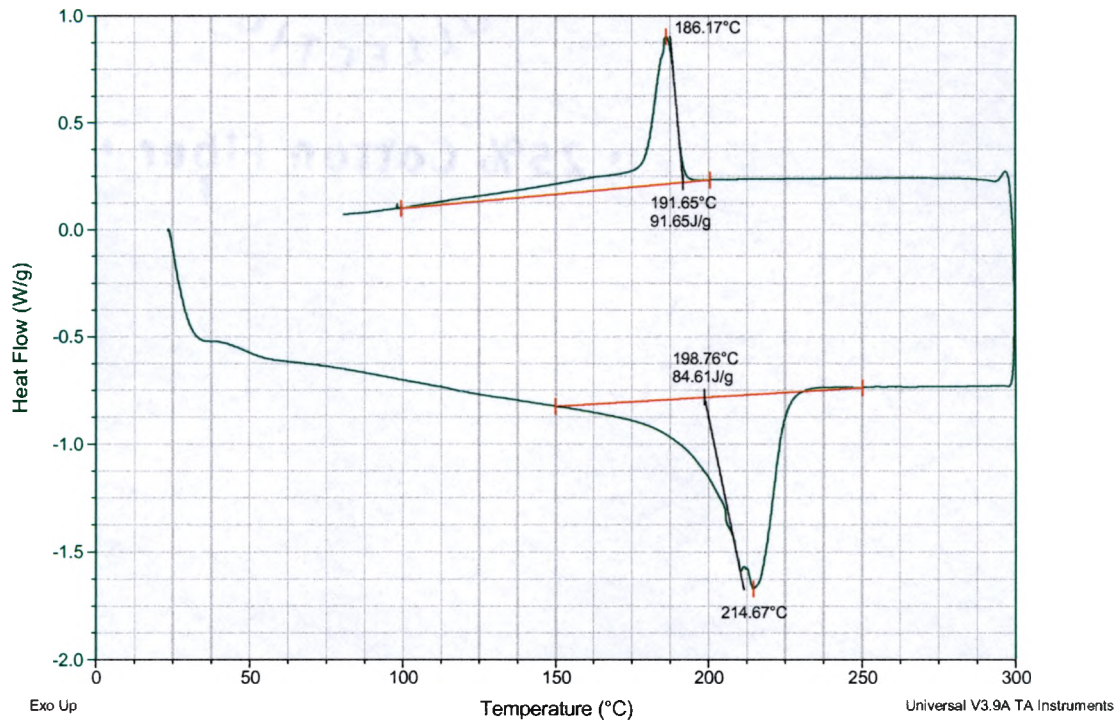


## Appendix A10 – DSC of Surface Optimized

Sample: Surface Optimized  
Size: 11.8000 mg

DSC

File: C:\...\Beall\Goofy\Surface Optimized.001  
Operator: stew  
Run Date: 30-Jun-04 15:13  
Instrument: 2920 MDSC V2.6A



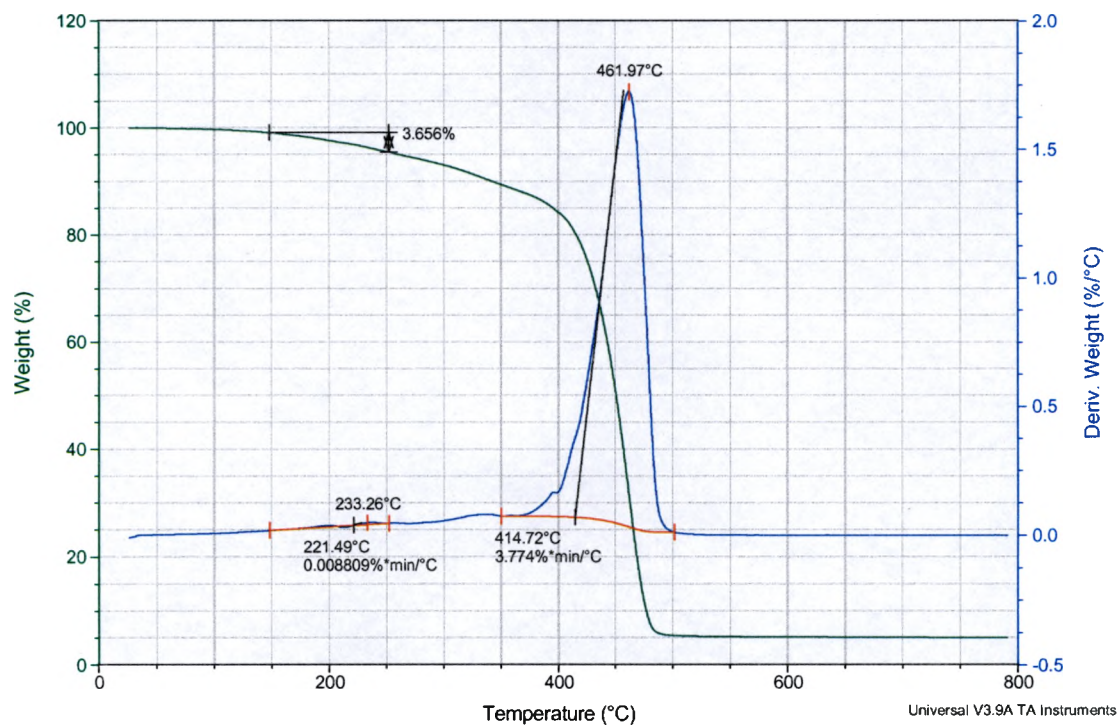
**APPENDIX B – TGA OF NYLON 6 NANOCOMPOSITES**

## Appendix B1 – TGA of Laponite Surface & Edge

Sample: Laponite Surface and edge new  
Size: 28.3000 mg  
Method: Ramp

TGA

File: C:\...\Laponite Surface and edge new.001  
Operator: stew  
Run Date: 24-Jun-04 11:04  
Instrument: TGA Q50 V6.1 Build 181

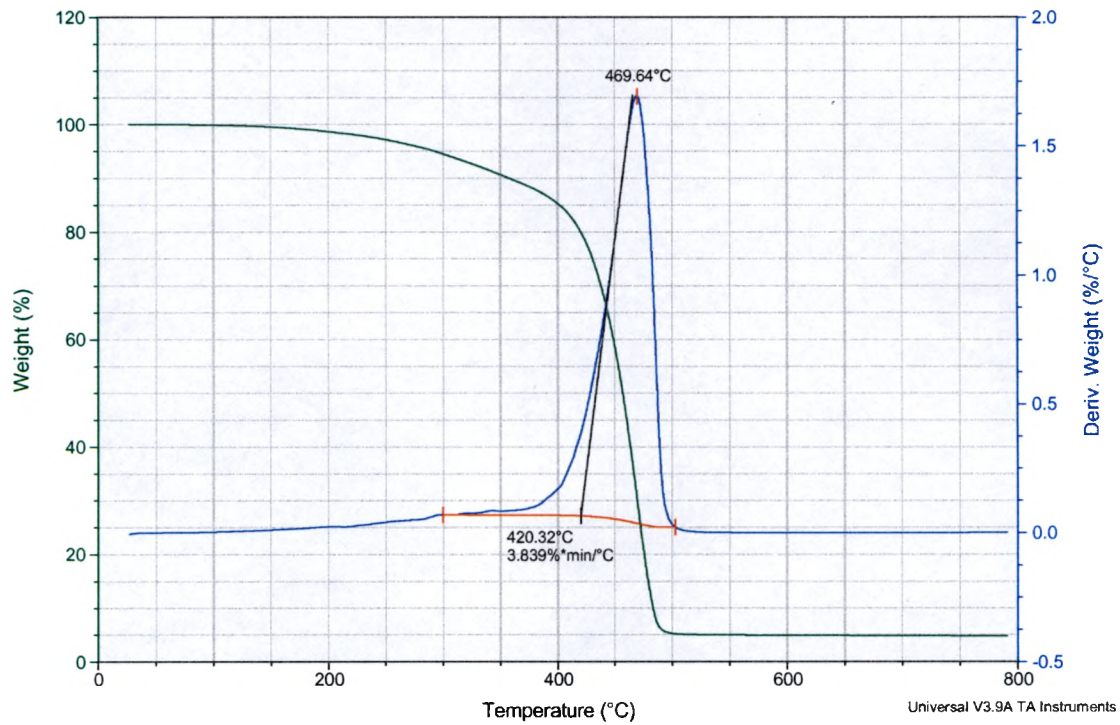


## Appendix B2 – TGA of Laponite Surface

Sample: Laponite Surface  
Size: 62.1560 mg  
Method: Ramp

TGA

File: C:\...\Beall\Goofy\Laponite Surface.001  
Operator: stew  
Run Date: 23-Jun-04 16:32  
Instrument: TGA Q50 V6.1 Build 181

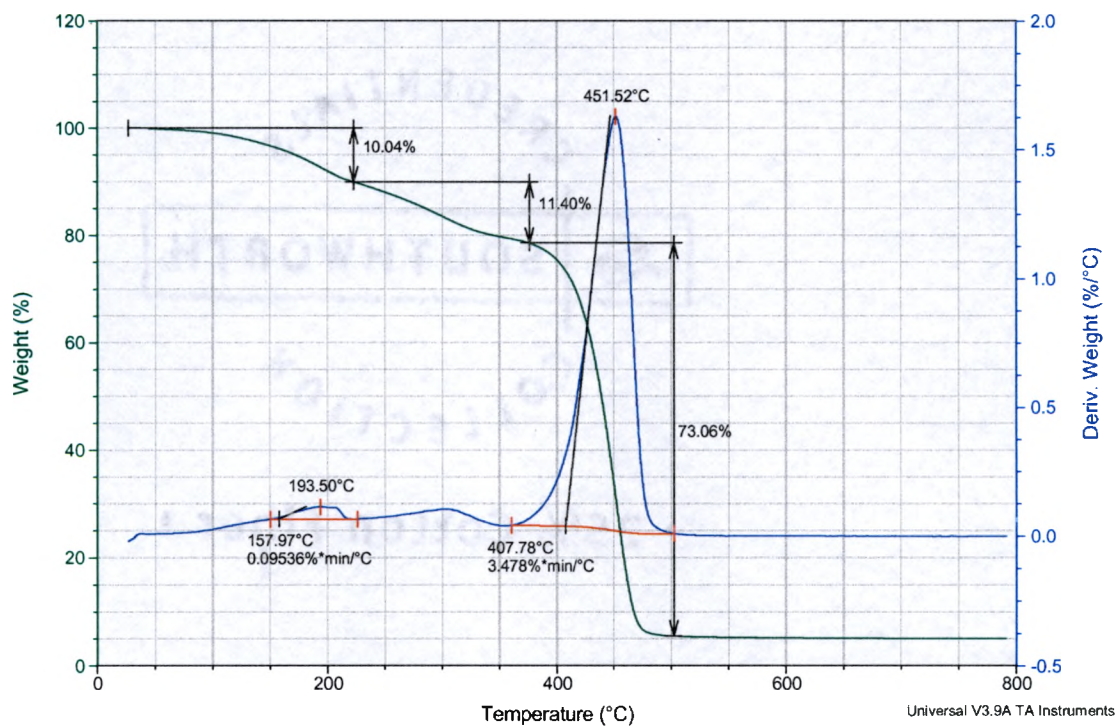


## Appendix B3 – TGA of Laponite Edge

Sample: Laponite Edge  
Size: 9.8700 mg  
Method: Ramp

TGA

File: C:\...TGA\Beall\Goofy\Laponit Edge.001  
Operator: Elizabeth  
Run Date: 24-May-04 13:54  
Instrument: TGA Q50 V6.1 Build 181



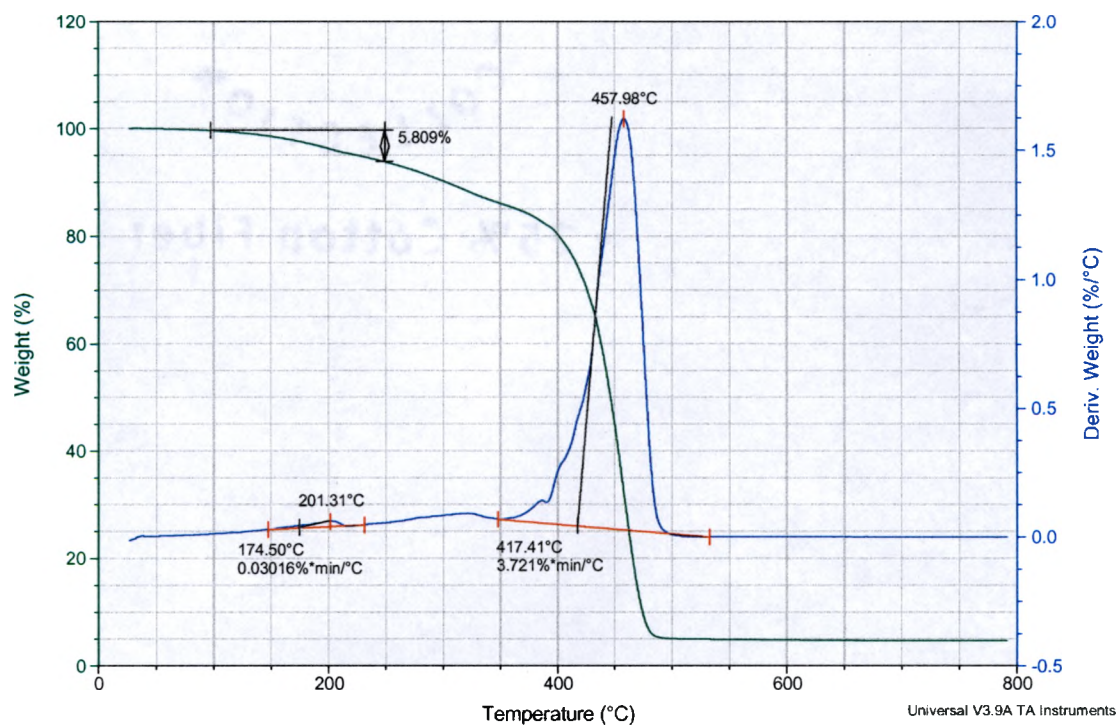
## Appendix B4 – TGA of Surface Toyota & Edge

Sample: Surface Toyota and Edge(16APR04)  
Size: 17.9990 mg

TGA

File: ...Surface Toyota and Edge(16APR04).001  
Operator: Stew  
Run Date: 16-Apr-04 13:00  
Instrument: TGA Q50 V6.1 Build 181

Comment: 5%

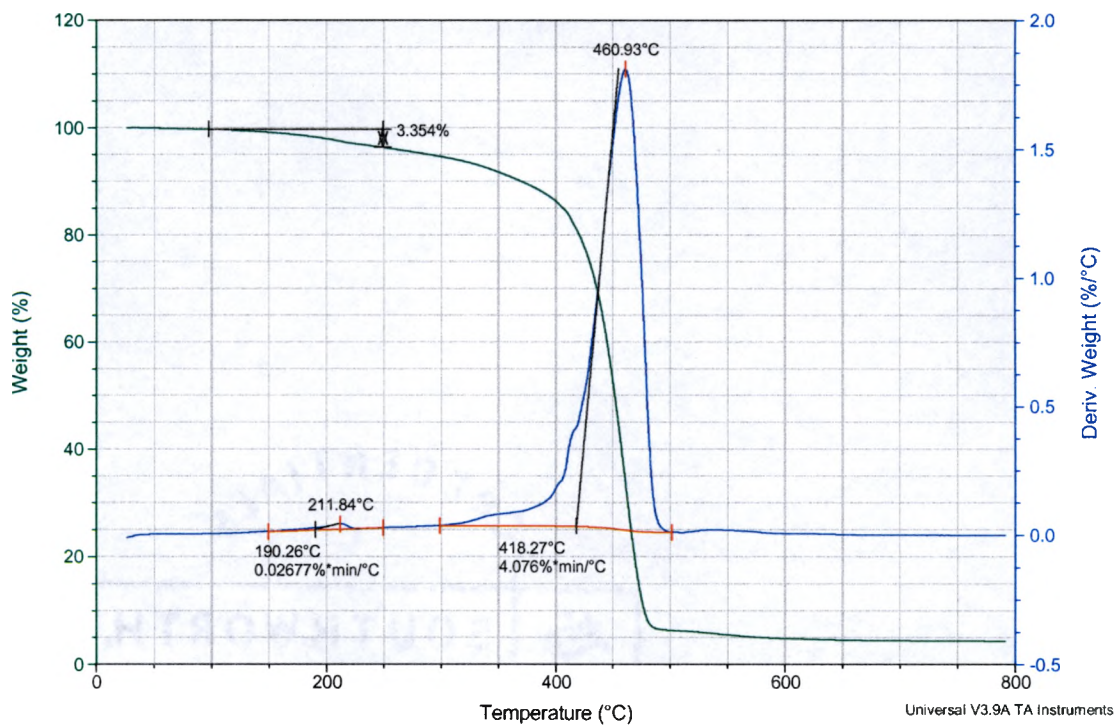


## Appendix B5 – TGA of Na+ Cloisite Edge

Sample: Na ET  
Size: 20.9090 mg  
Method: Ramp

TGA

File: C:\...TGA\Beall\Goofy\Na ET(22Jun04).001  
Operator: stew  
Run Date: 22-Jun-04 14:41  
Instrument: TGA Q50 V6.1 Build 181



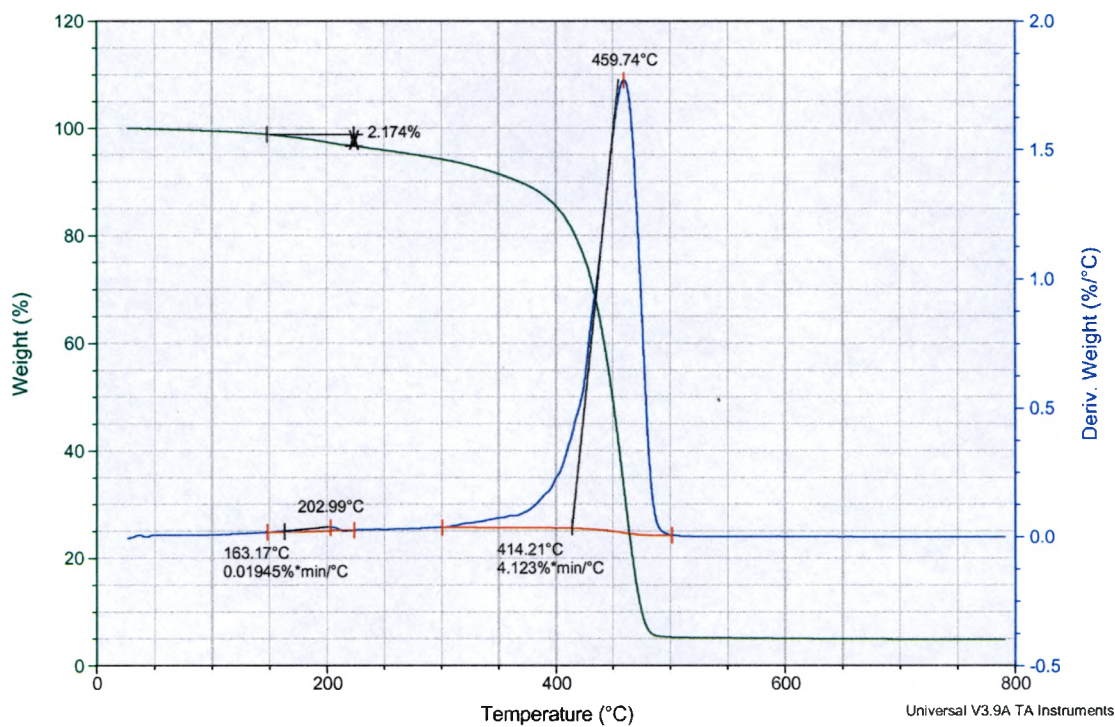
Universal V3.9A TA Instruments

## Appendix B6 – TGA of Surface Optimized & Edge

Sample: Surface Optimized & EdgeNew!  
Size: 16.0600 mg  
Method: Ramp

TGA

File: C:\...\Surface Optimized & Edge New!.001  
Operator: stew  
Run Date: 23-Jun-04 13:34  
Instrument: TGA Q50 V6.1 Build 181

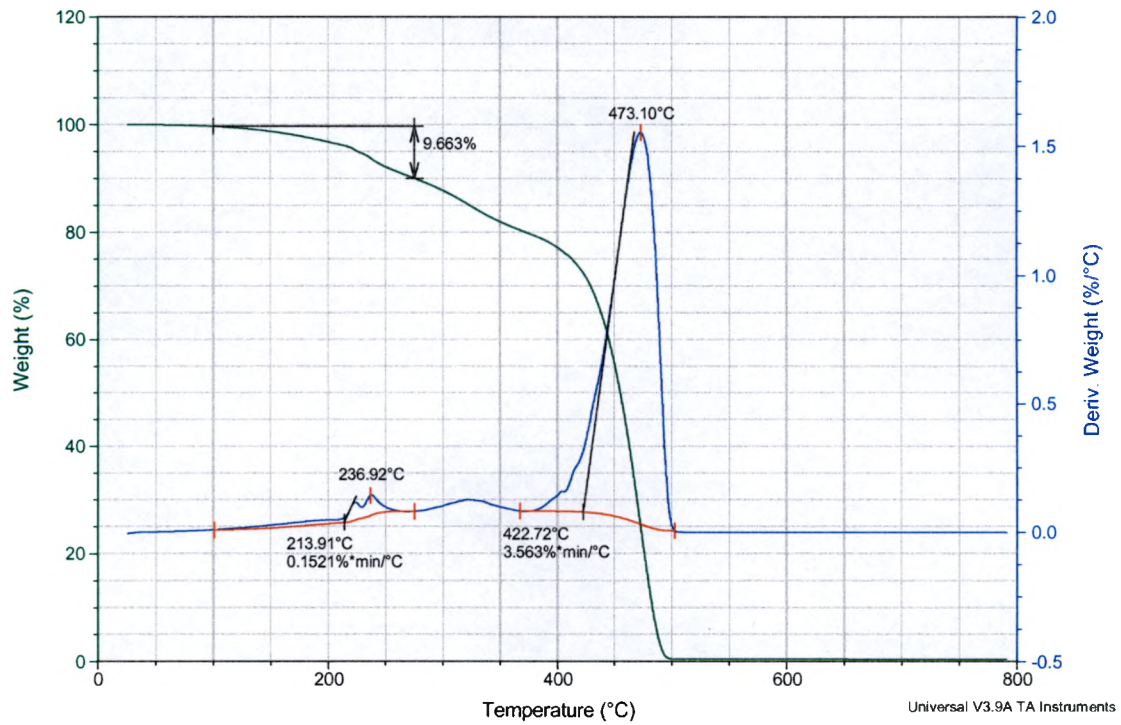


## Appendix B7 – TGA of Nylon 6

Sample: Nylon 6 New  
Size: 50.8520 mg  
Method: Ramp

TGA

File: C:\...TGA\Beall\Goofy\Nylon 6 New.001  
Operator: stew  
Run Date: 24-Jun-04 15:44  
Instrument: TGA Q50 V6.1 Build 181

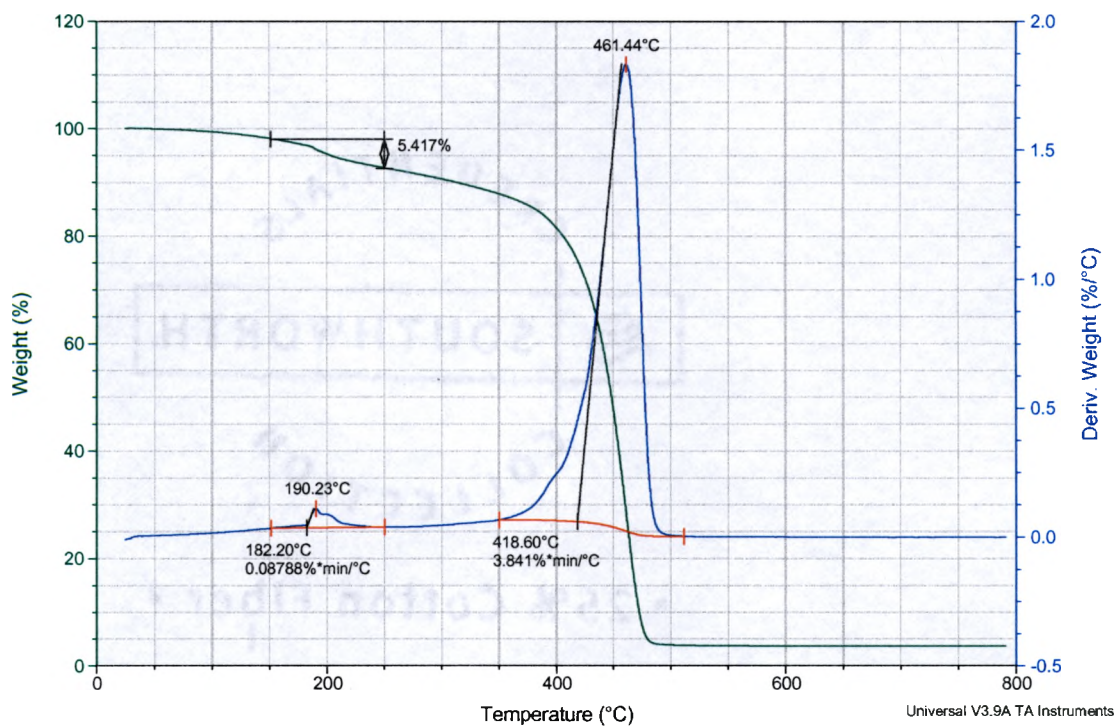


## Appendix B8 – TGA of 93 A Edge Treated

Sample: 93 A Nylon 6 Edge treated New  
Size: 21.7250 mg  
Method: Ramp

TGA

File: C:\...93 A Nylon 6 Edge treated New.001  
Operator: stew  
Run Date: 05-Jul-04 12:38  
Instrument: TGA Q50 V6.1 Build 181

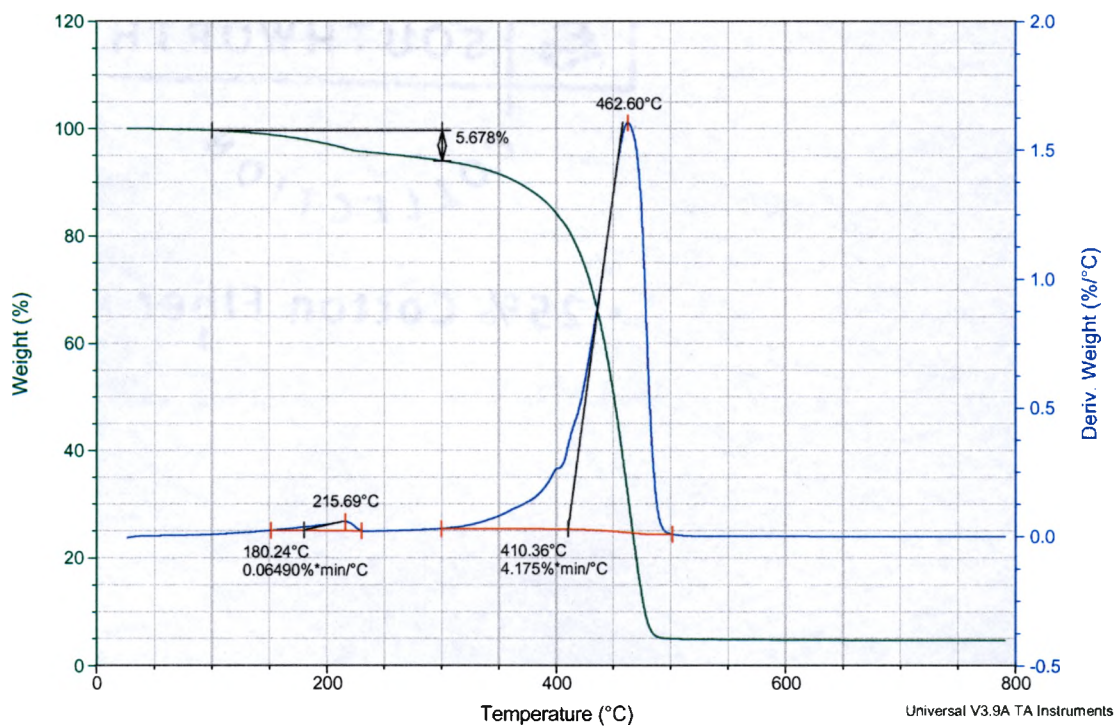


## Appendix B9 – TGA of Surface Toyota

Sample: Surface Toyota Last  
Size: 37.7900 mg  
Method: Ramp

TGA

File: C:\...\Goofy\Surface Toyota Last.001  
Operator: stew  
Run Date: 07-Jul-04 15:23  
Instrument: TGA Q50 V6.1 Build 181

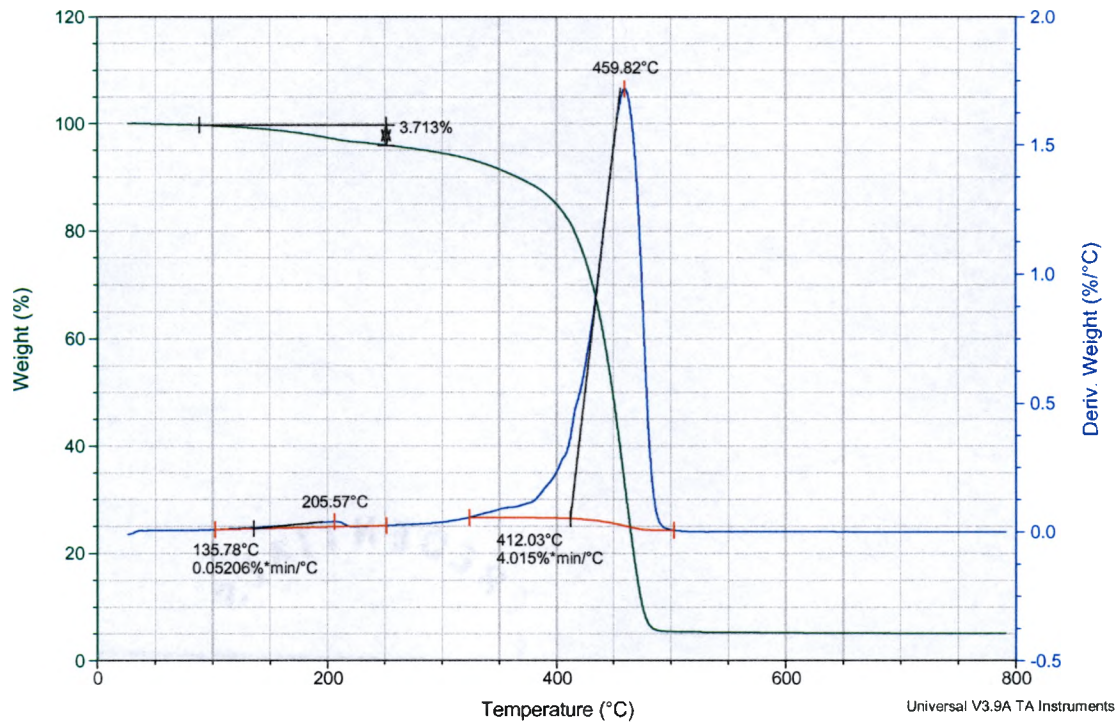


## Appendix B10 – TGA of Surface Optimized

Sample: Surface Optimized New!  
Size: 19.7030 mg  
Method: Ramp

TGA

File: C:\...\Goofy\Surface Optimized New!.001  
Operator: stew  
Run Date: 23-Jun-04 10:56  
Instrument: TGA Q50 V6.1 Build 181



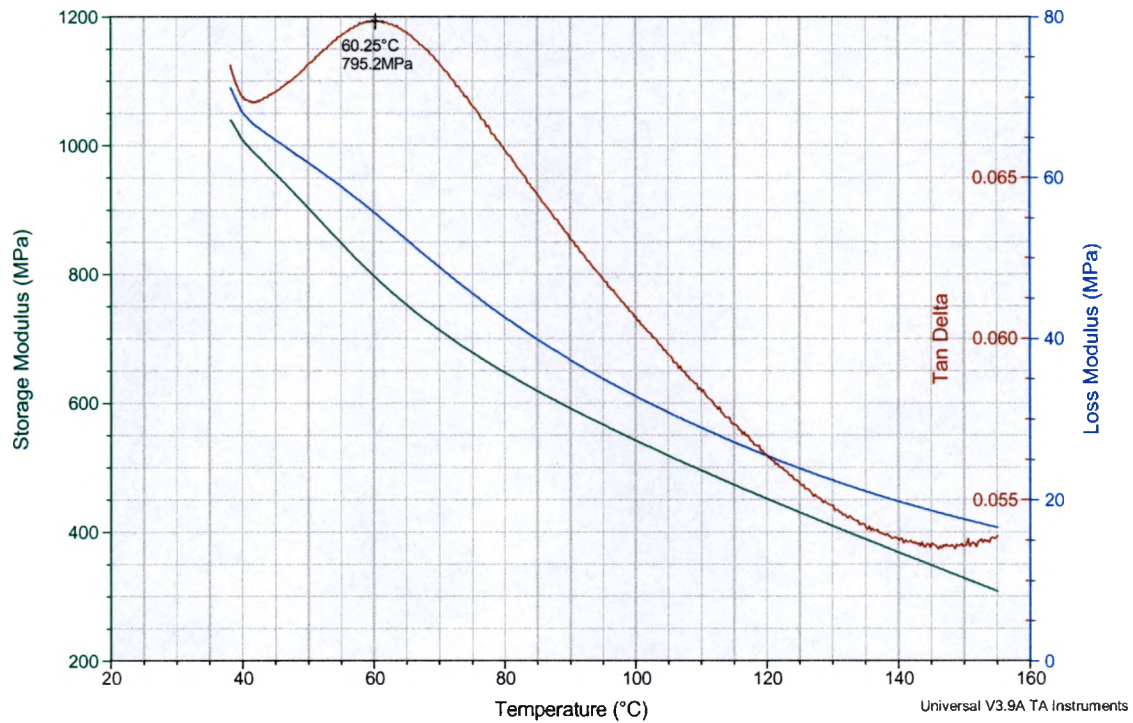
**APPENDIX C – DMA OF NYLON 6 NANOCOMPOSITES**

## Appendix C1-a – DMA of Laponite Surface & Edge – First Run

Sample: Laponite Surface & Edge New  
Size: 17.0400 x 13.6500 x 2.9800 mm  
Method: Temperature Ramp

DMA

File: C:\...Laponite Surface & Edge New.001  
Operator: Stew  
Run Date: 25-Jun-04 13:14  
Instrument: DMA Q800 V5.1 Build 92

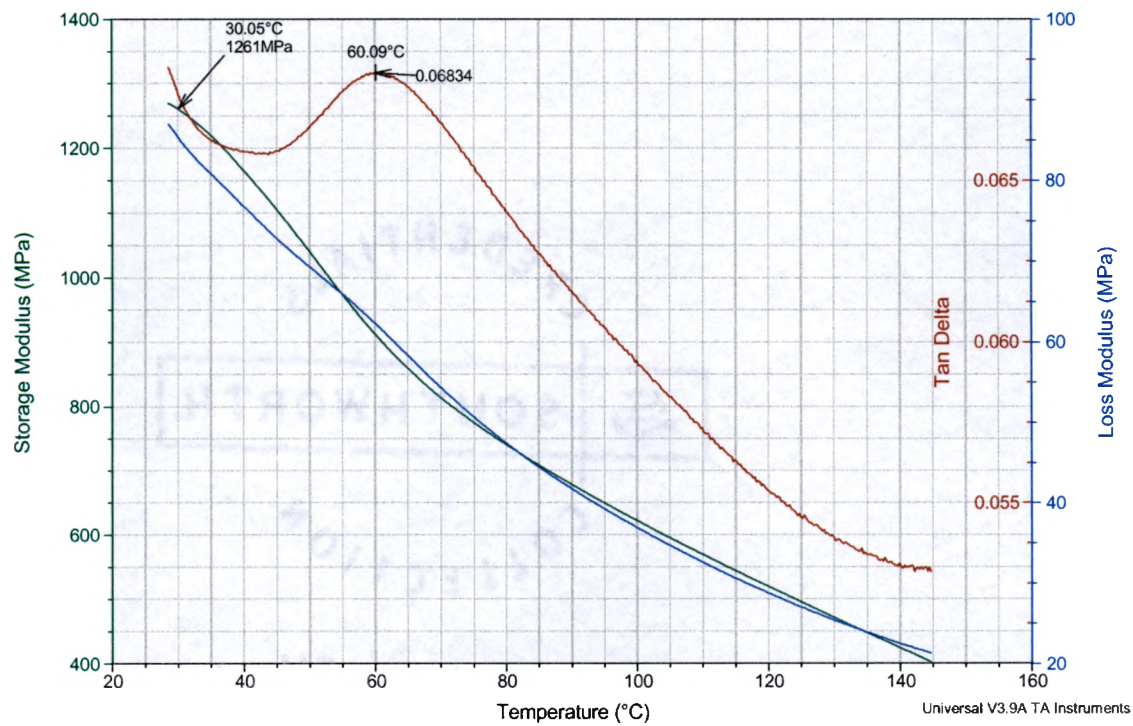


## Appendix C1-b – DMA of Laponite Surface & Edge – Second Run

Sample: Laponite Surface & Edge New #2  
Size: 17.1200 x 12.8000 x 2.8100 mm  
Method: Temperature Ramp

DMA

File: C:\...Laponite Surface & Edge New #2.001  
Operator: Stew  
Run Date: 25-Jun-04 13:14  
Instrument: DMA Q800 V5.1 Build 92

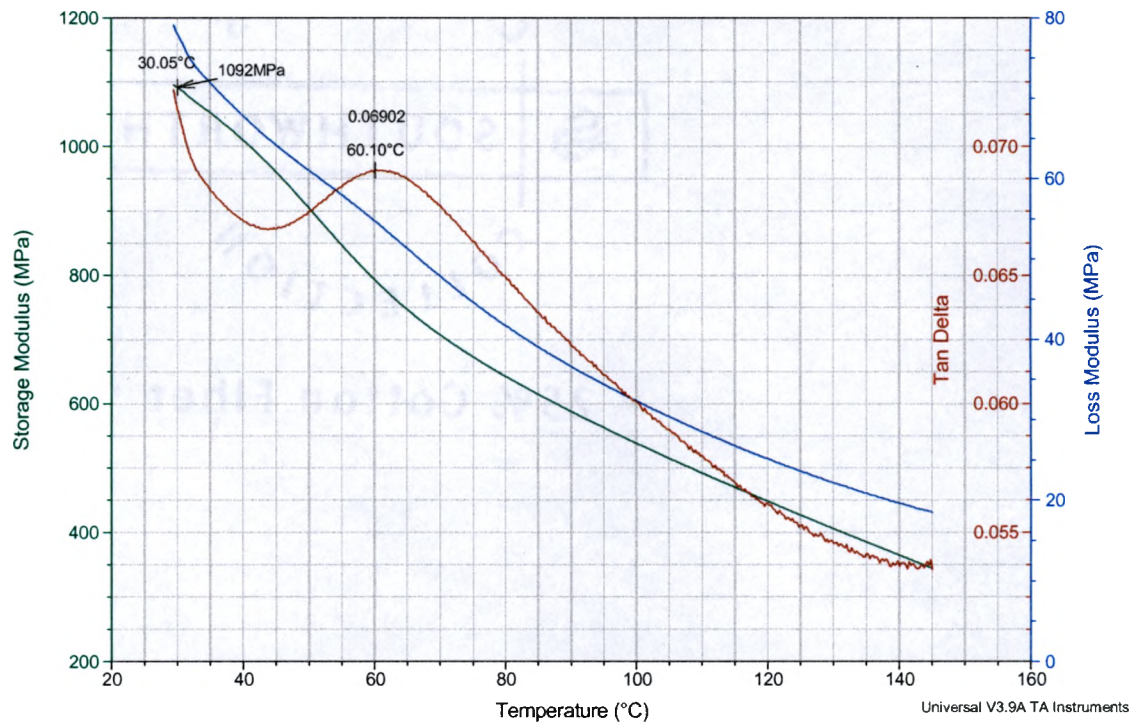


**Appendix C1-c – DMA of Laponite Surface & Edge – Third Run**

Sample: Laponite Surface & Edge New #3  
Size: 17.2700 x 11.8600 x 2.9000 mm  
Method: Temperature Ramp

DMA

File: C:\...\Laponite Surface & Edge New #3.001  
Operator: Stew  
Run Date: 25-Jun-04 13:14  
Instrument: DMA Q800 V5.1 Build 92

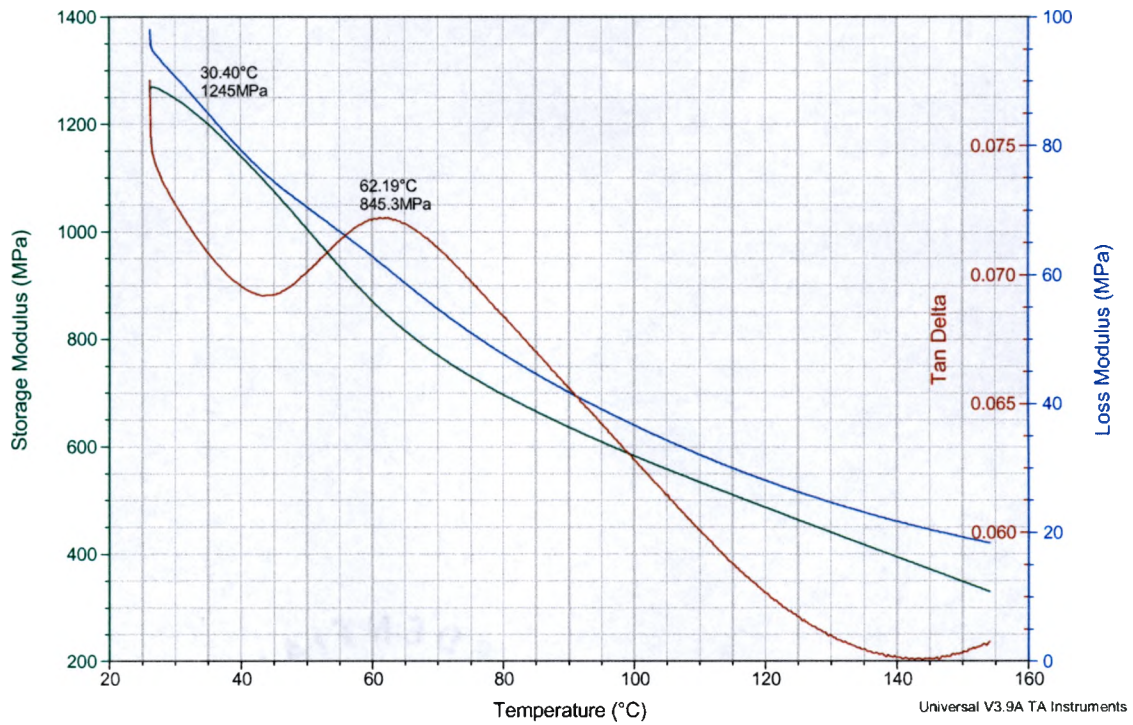


## Appendix C2-a – DMA of Laponite Surface – First Run

Sample: Laponite Surface New  
Size: 16.7800 x 13.8800 x 3.0800 mm  
Method: Temperature Ramp

DMA

File: C:\...\Shagufta\Laponite Surface New.001  
Operator: Stew  
Run Date: 25-Jun-04 13:14  
Instrument: DMA Q800 V5.1 Build 92

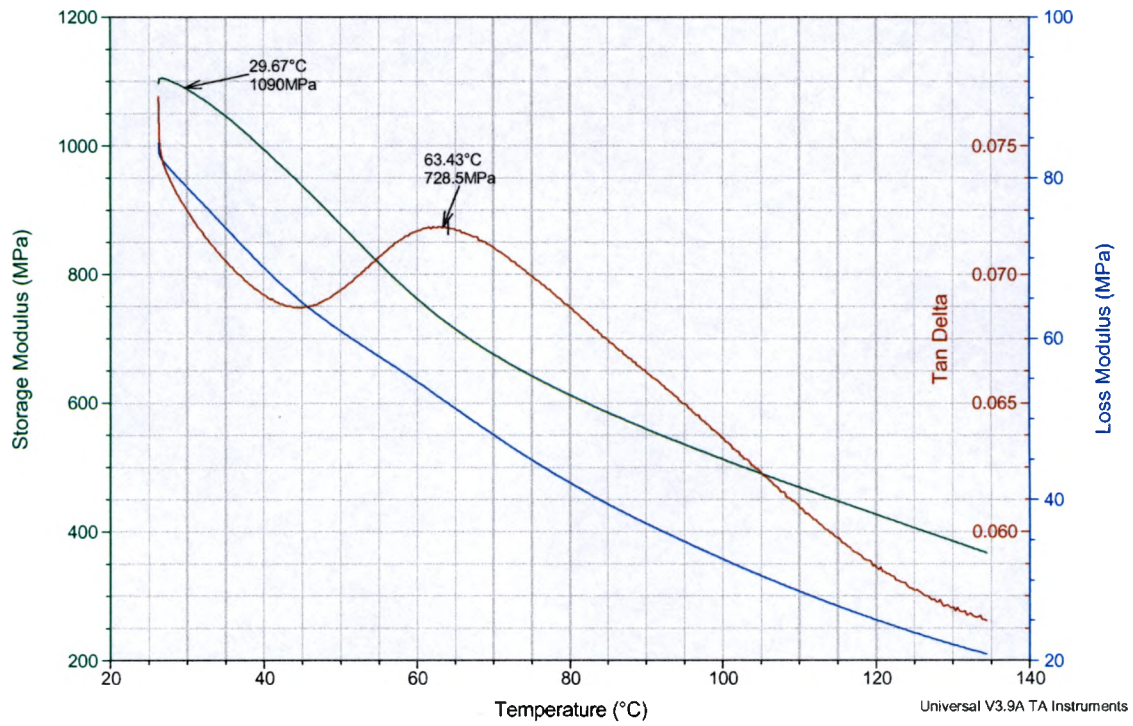


## Appendix C2-b – DMA of Laponite Surface – Second Run

Sample: Laponite Surface New #2  
Size: 17.0200 x 12.4300 x 2.9900 mm  
Method: Temperature Ramp

DMA

File: C:\...Laponite Surface New #2.001  
Operator: Stew  
Run Date: 25-Jun-04 13:14  
Instrument: DMA Q800 V5.1 Build 92

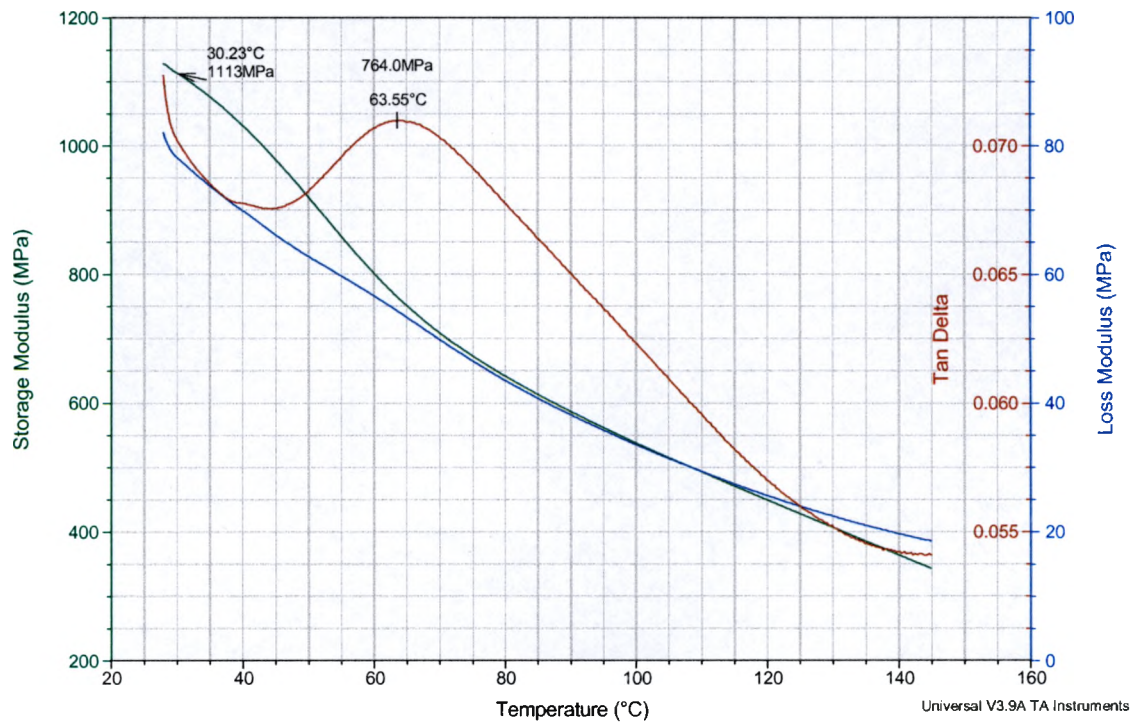


## Appendix C2-c – DMA of Laponite Surface – Third Run

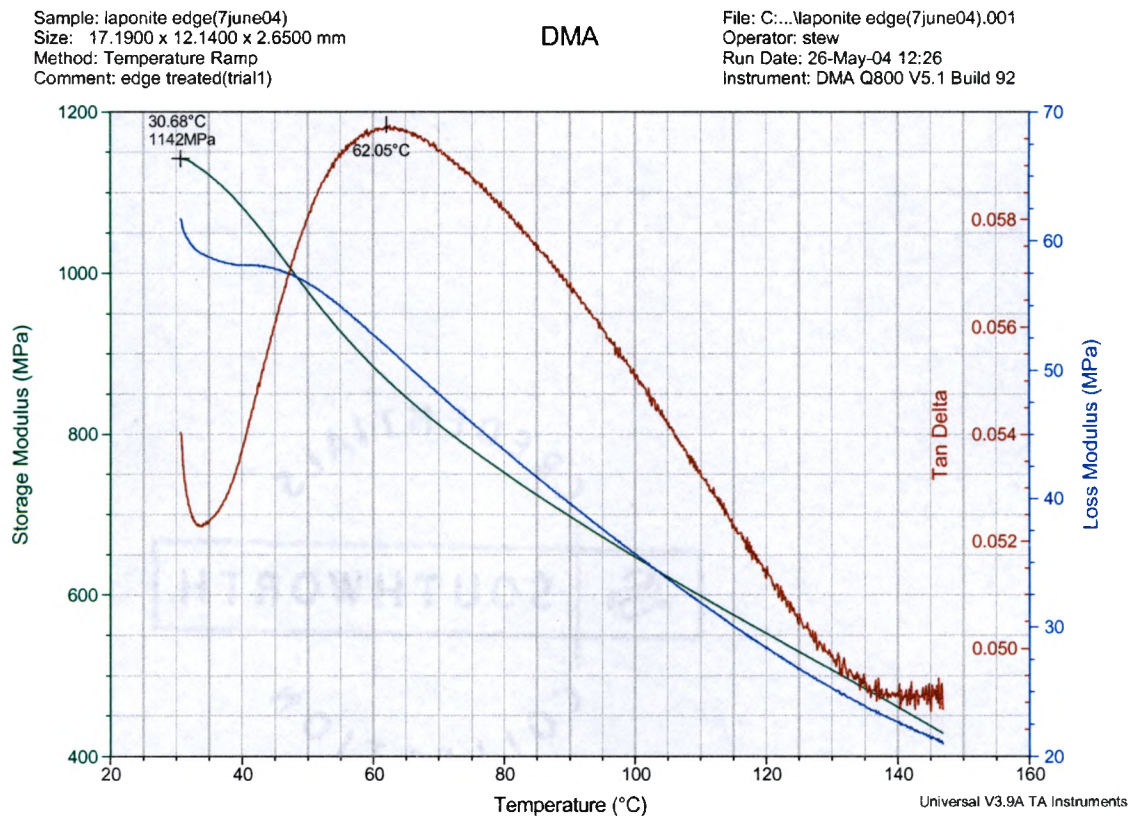
Sample: Laponite Surface New #3  
Size: 17.0900 x 13.3600 x 3.2900 mm  
Method: Temperature Ramp

DMA

File: C:\...Laponite Surface New #3.001  
Operator: Stew  
Run Date: 25-Jun-04 13:14  
Instrument: DMA Q800 V5.1 Build 92



## Appendix C3-a – DMA of Laponite Edge – First Run

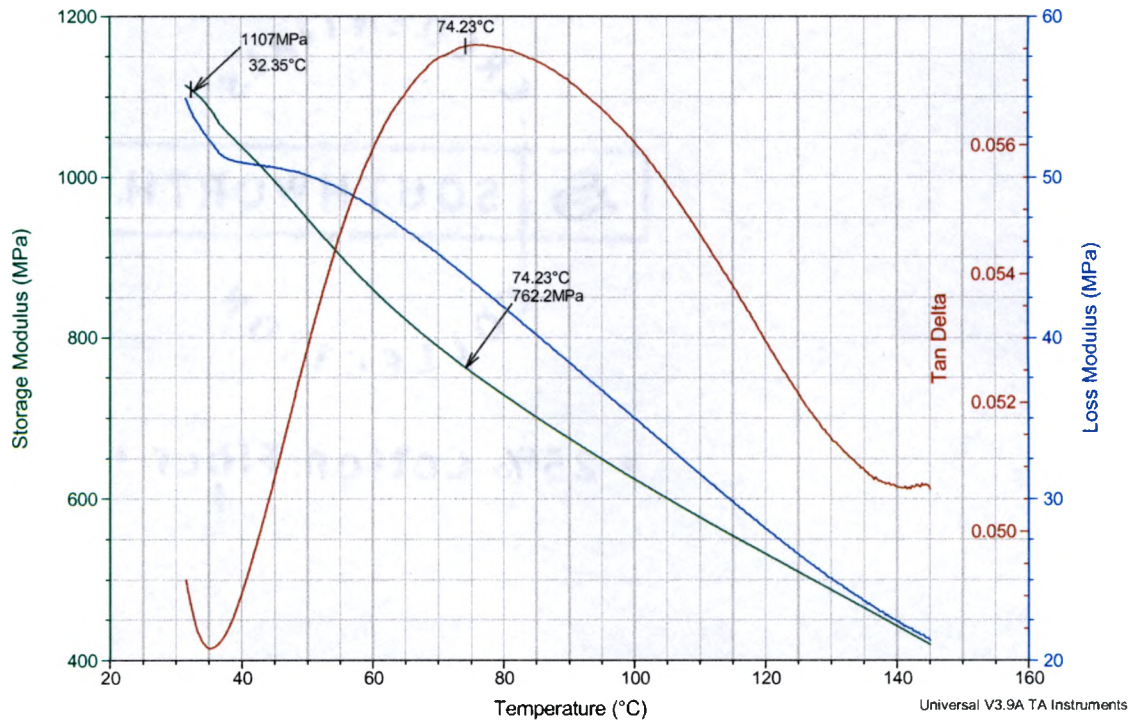


## Appendix C3-b – DMA of Laponite Edge – Second Run

Sample: Laponite Edge #3  
Size: 17.1600 x 12.2300 x 2.6900 mm  
Method: Temperature Ramp

DMA

File: C:\...\Shagufal\Laponite Edge #3.001  
Operator: Stew  
Run Date: 25-Jun-04 13:14  
Instrument: DMA Q800 V5.1 Build 92

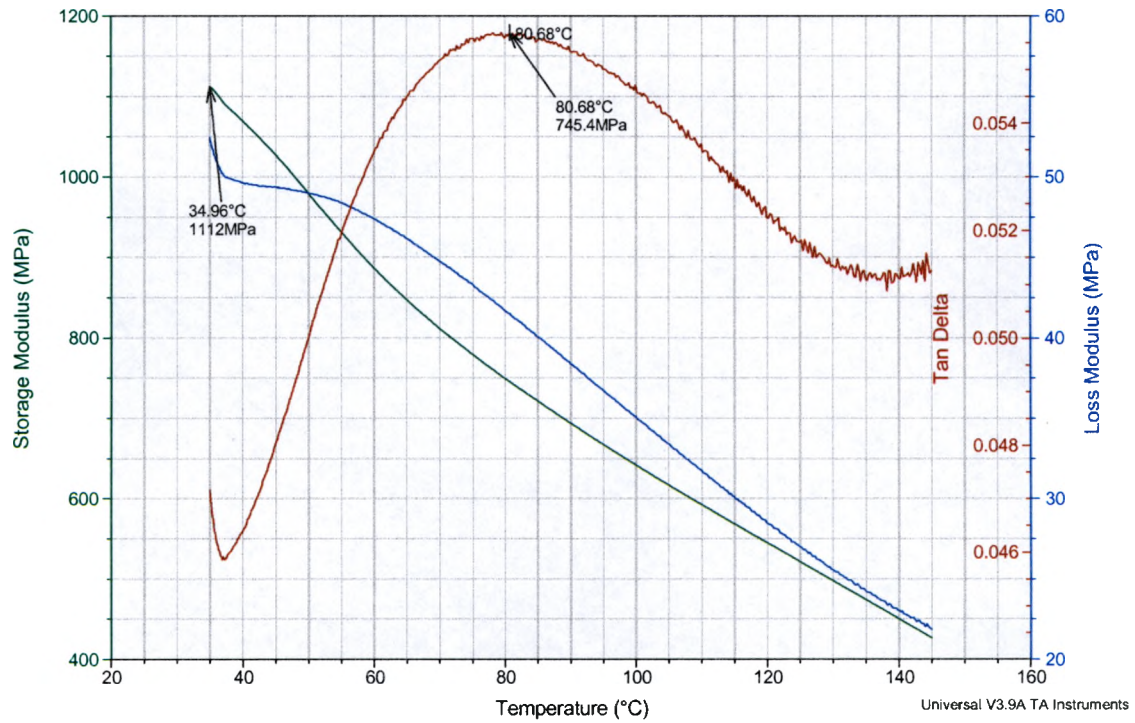


### Appendix C3-c – DMA of Laponite Edge – Third Run

Sample: laponite edge new #4  
 Size: 17.1900 x 12.1000 x 2.7100 mm  
 Method: Temperature Ramp

#### DMA

File: C:\...\Shagufalaponite edge new # 4.001  
 Operator: Stew  
 Run Date: 25-Jun-04 13:14  
 Instrument: DMA Q800 V5.1 Build 92

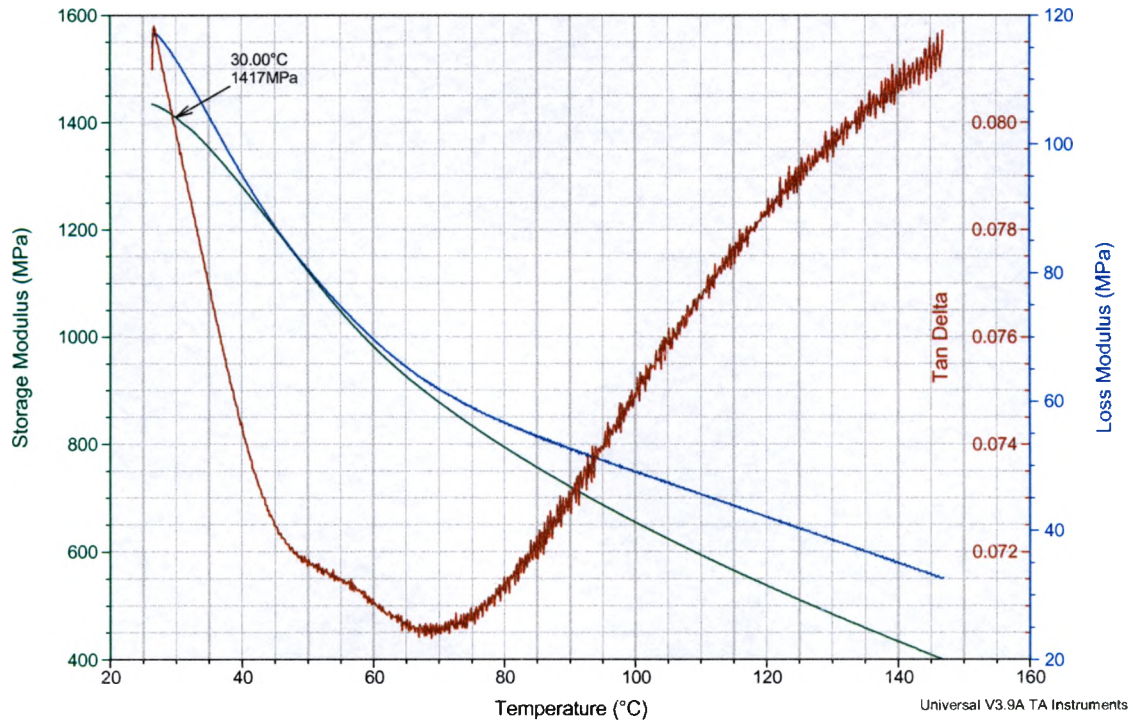


### Appendix C4-a – DMA of Surface Toyota & Edge – First Run

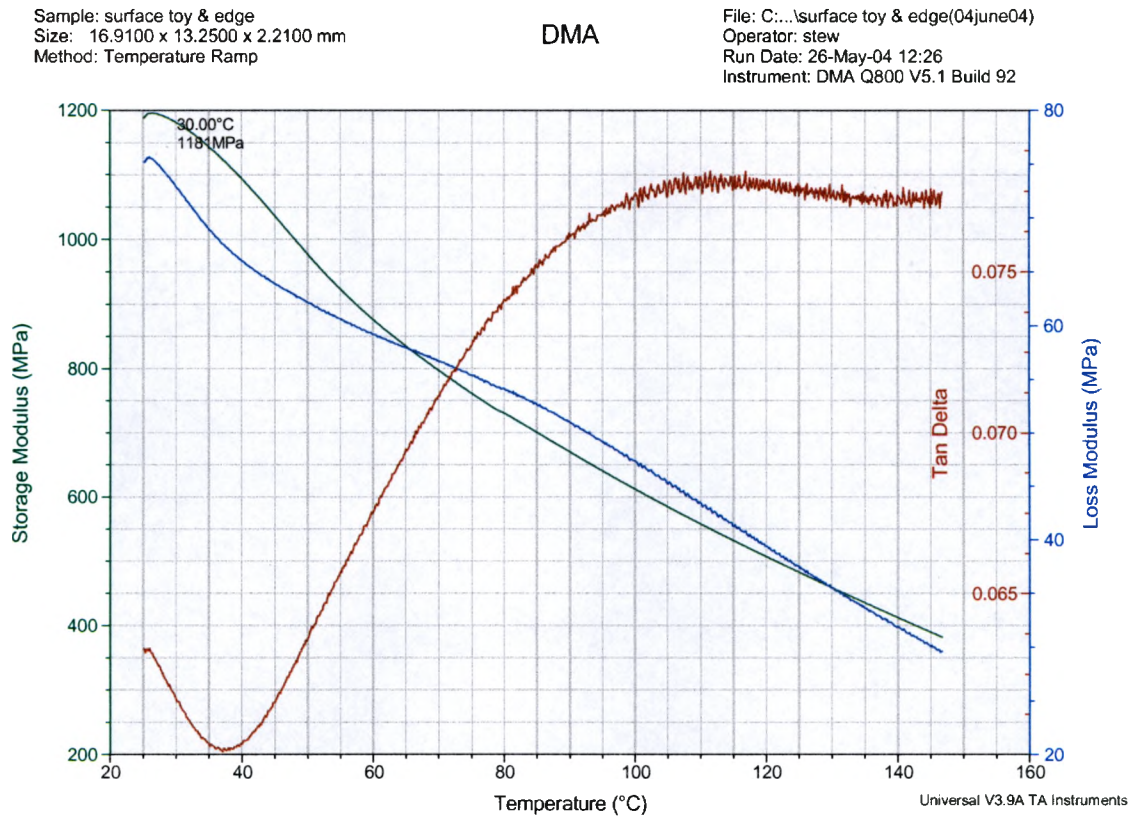
Sample: Surface treated toy and edge  
Size: 17.2500 x 10.6600 x 2.2700 mm  
Method: Temperature Ramp

DMA

File: C:\...\Surface treated toy and edge.001  
Operator: stew  
Run Date: 22-Apr-04 07:59  
Instrument: DMA Q800 V5.1 Build 92



## Appendix C4-b – DMA of Surface Toyota & Edge – Second Run

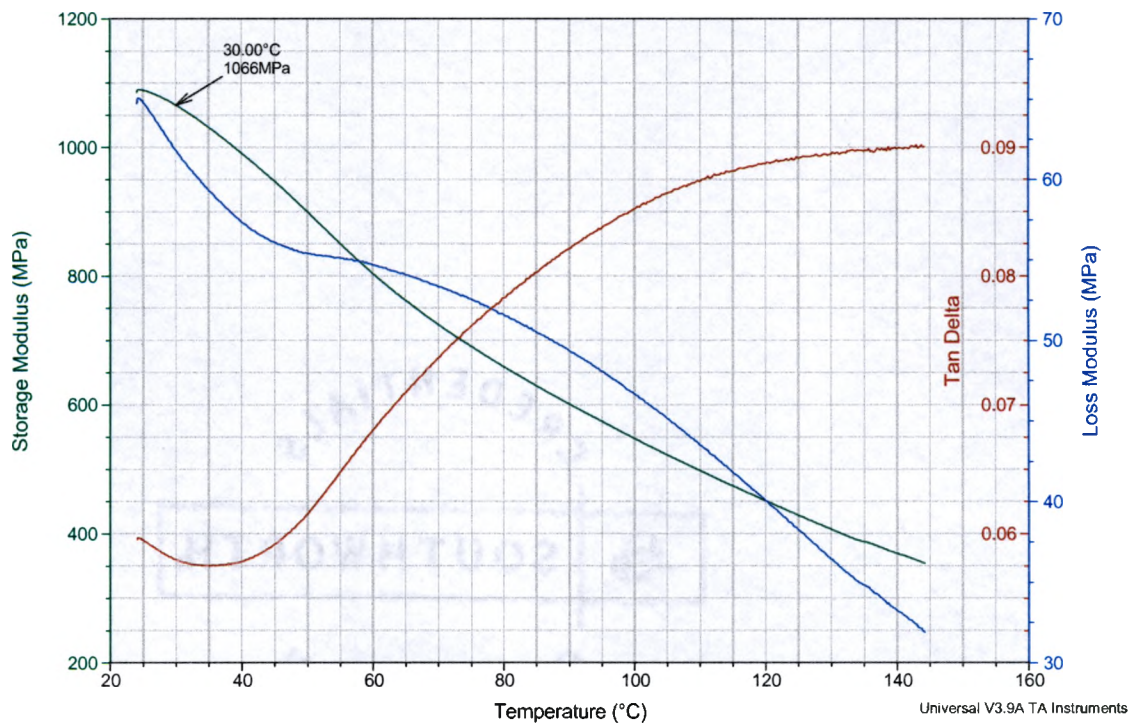


### Appendix C4-c – DMA of Surface Toyota & Edge – Third Run

Sample: Surface toyota & edge new  
Size: 17.0800 x 14.8900 x 2.5600 mm  
Method: Temperature Ramp

DMA

File: C:\...\Surface toyota & edge new.001  
Operator: Stew  
Run Date: 25-Jun-04 13:14  
Instrument: DMA Q800 V5.1 Build 92

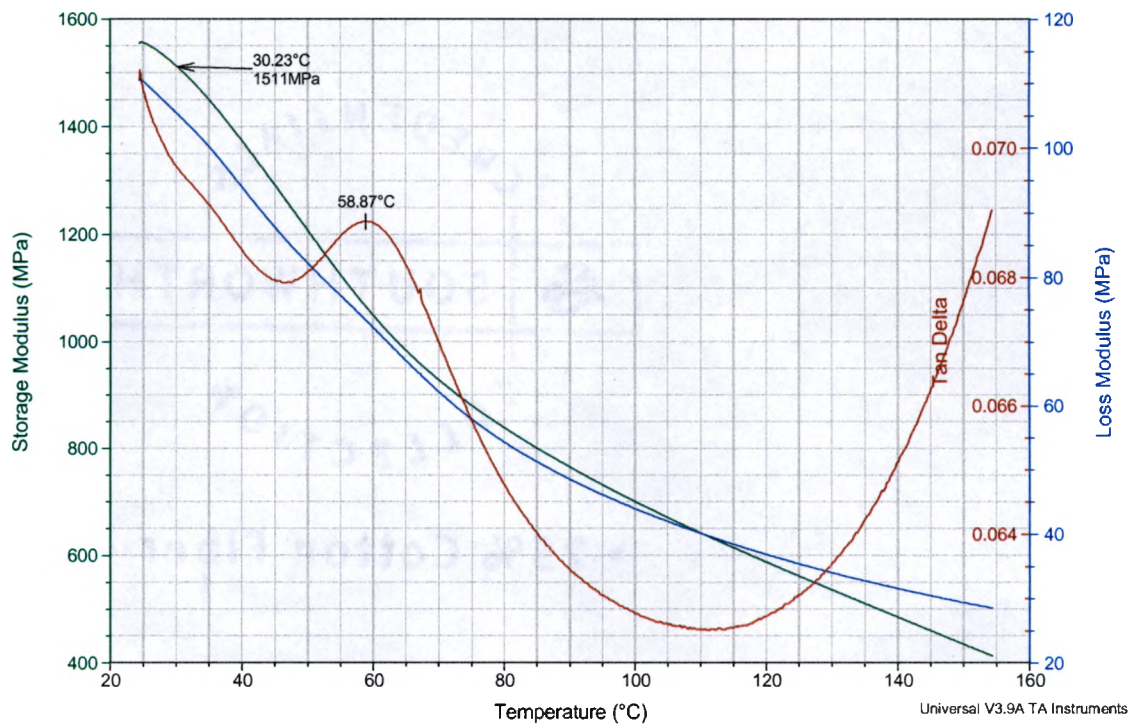


## Appendix C5-a – DMA of Na+ Closite Edge – First Run

Sample: Na+Closite Edge Treated  
Size: 17.0600 x 13.8900 x 3.5200 mm  
Method: Temperature Ramp

DMA

File: C:\...Na+Closite Edge treated.001  
Operator: Stew  
Run Date: 25-Jun-04 13:14  
Instrument: DMA Q800 V5.1 Build 92

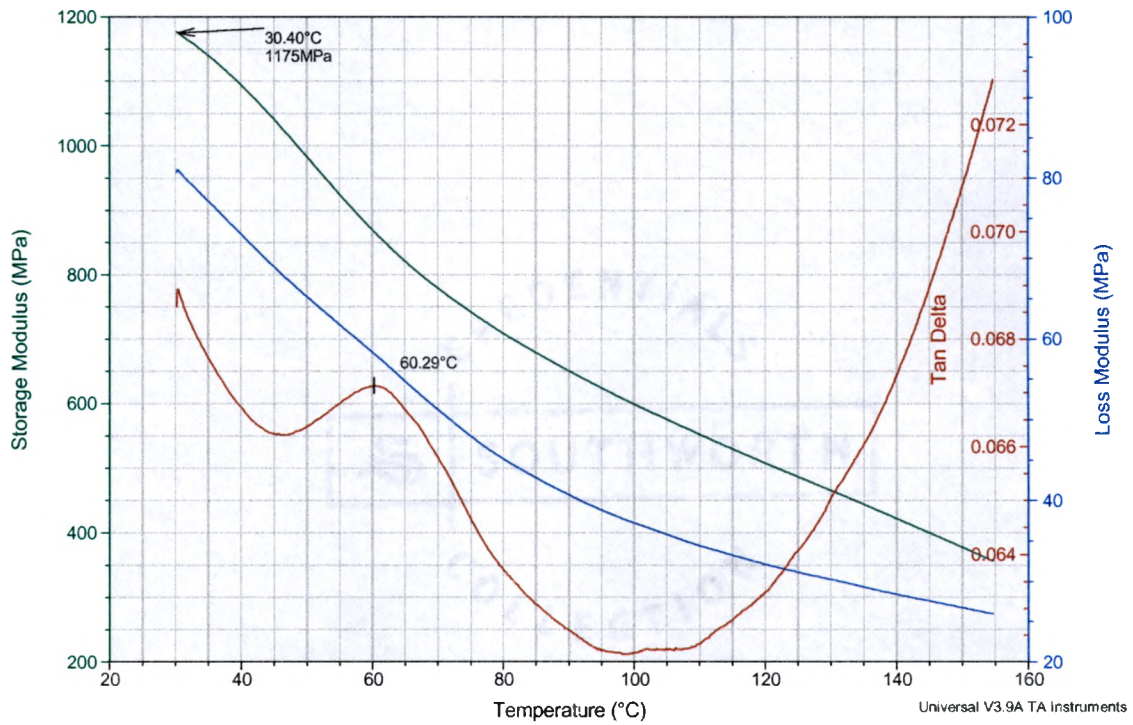


### Appendix C5-b – DMA of Na+ Cloisite Edge – Second Run

Sample: Na+ CLosite edge treated #2  
 Size: 17.1400 x 12.4300 x 4.0400 mm  
 Method: Temperature Ramp

DMA

File: C:\...Na+Cloisite Edge treated#2.001  
 Operator: Stew  
 Run Date: 25-Jun-04 13:14  
 Instrument: DMA Q800 V5.1 Build 92

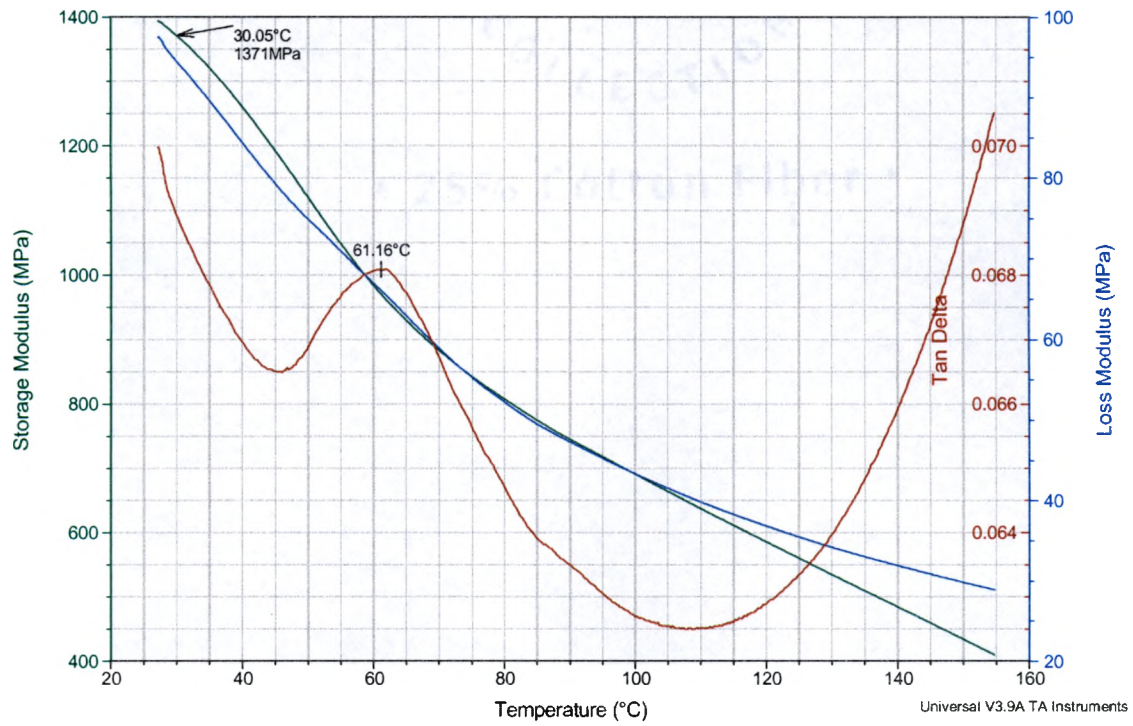


## Appendix C5-c – DMA of Na+ Closite Edge – Third Run

Sample: Na+ Closite edge treated #3  
Size: 17.0900 x 12.5200 x 3.6200 mm  
Method: Temperature Ramp

DMA

File: C:\...Na+Closite Edge treated#3.001  
Operator: Stew  
Run Date: 25-Jun-04 13:14  
Instrument: DMA Q800 V5.1 Build 92

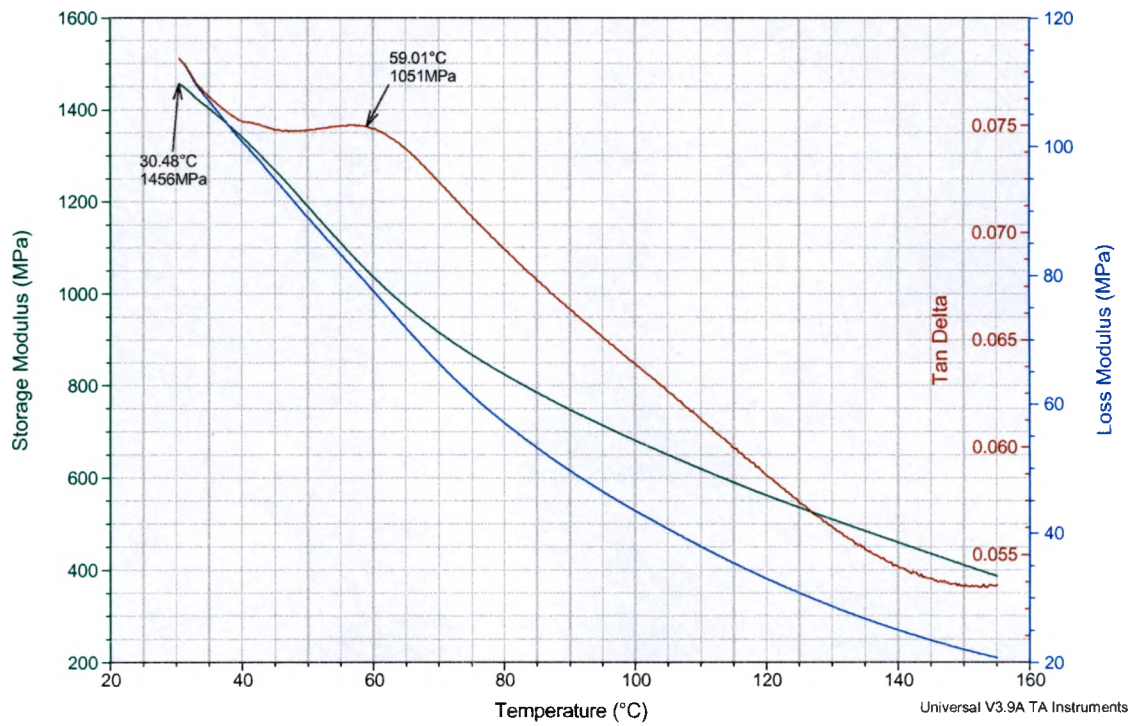


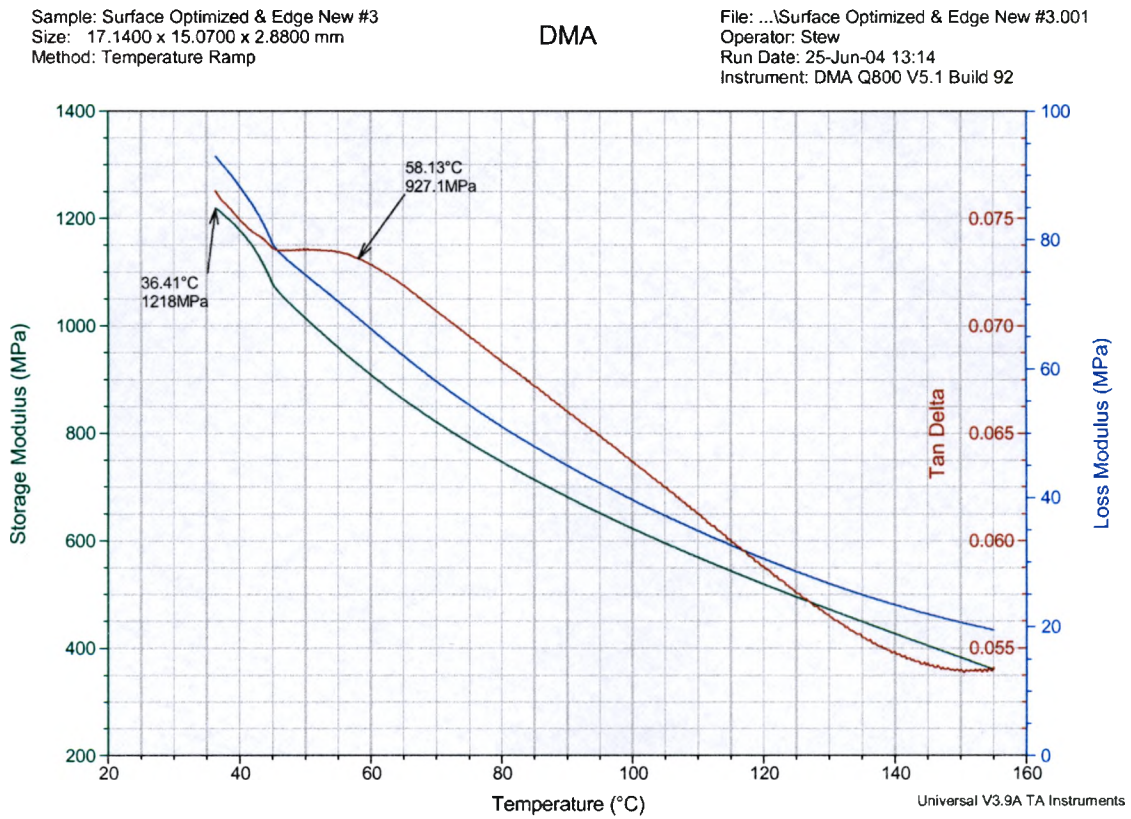
## Appendix C6-a – DMA of Surface Optimized & Edge – First Run

Sample: Surface Optimized & Edge New #2  
Size: 17.1400 x 13.8000 x 2.7700 mm  
Method: Temperature Ramp

DMA

File: ...Surface Optimized & Edge New #2.001  
Operator: Stew  
Run Date: 25-Jun-04 13:14  
Instrument: DMA Q800 V5.1 Build 92



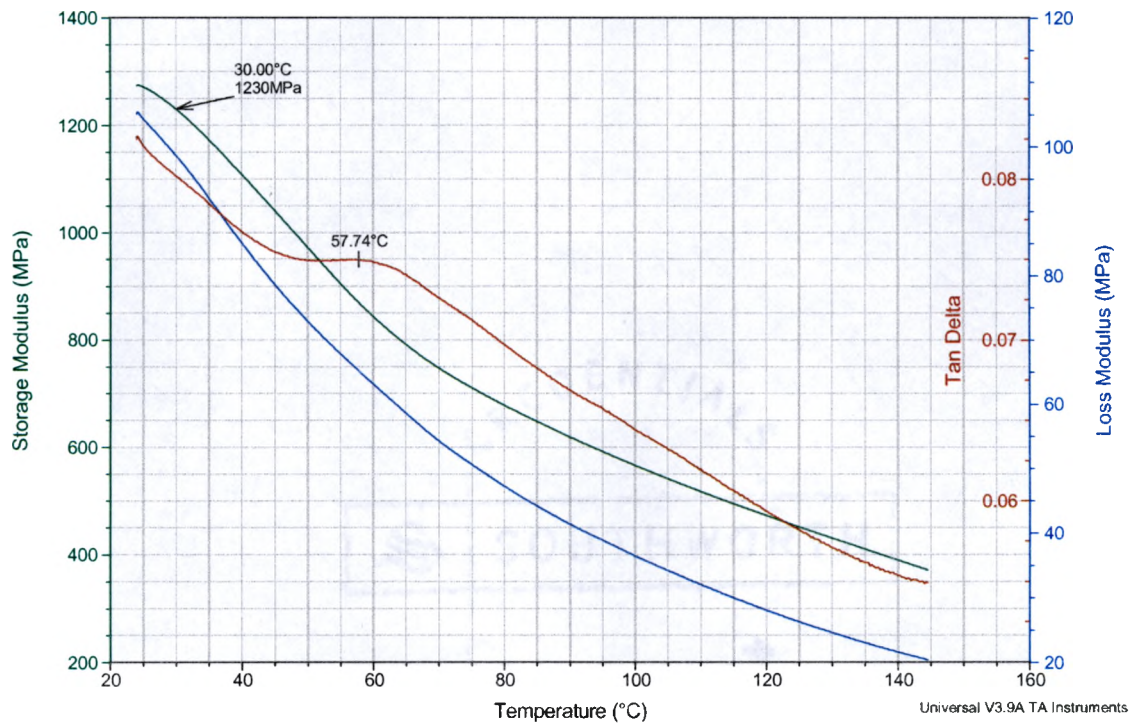
**Appendix C6-b – DMA of Surface Optimized & Edge – Second Run**

**Appendix C6-c – DMA of Surface Optimized & Edge – Third Run**

Sample: Surface optimized & edge new #4  
Size: 17.1100 x 11.8800 x 2.8300 mm  
Method: Temperature Ramp

DMA

File: ...Surface Optimized & edge new #4.001  
Operator: Stew  
Run Date: 25-Jun-04 13:14  
Instrument: DMA Q800 V5.1 Build 92

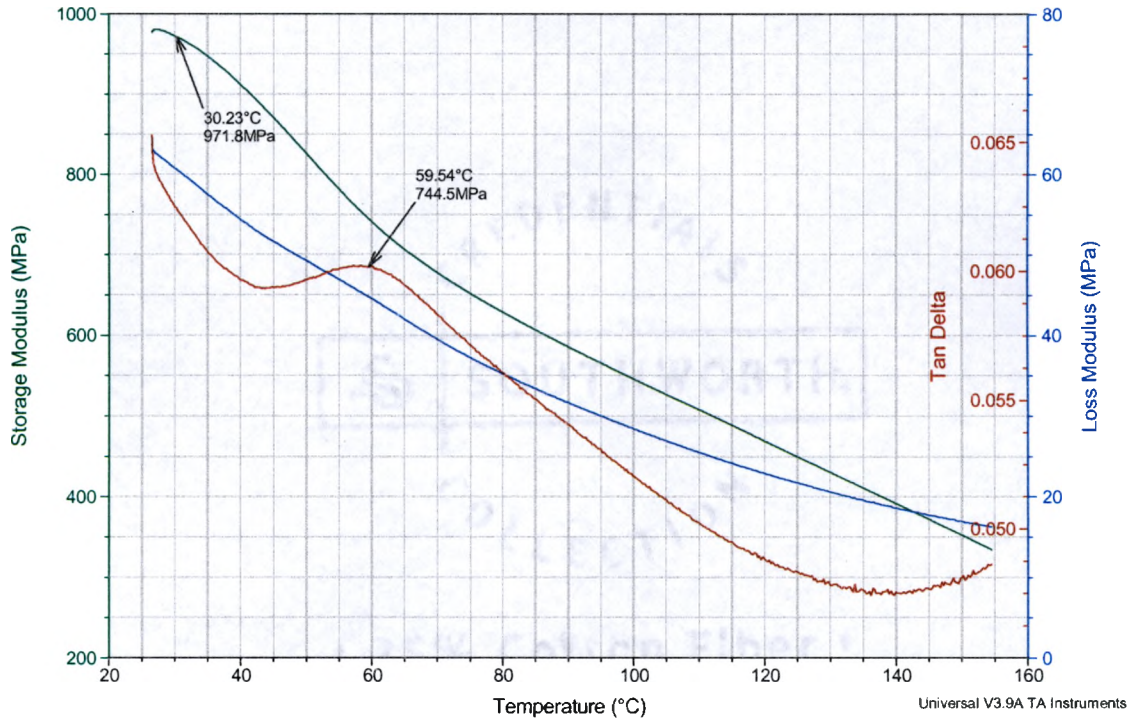


**Appendix C7-a – DMA of Nylon 6 – First Run**

Sample: Nylon 6 New  
 Size: 17.0600 x 13.2000 x 2.6200 mm  
 Method: Temperature Ramp

**DMA**

File: C:\...DMA\Beall\Shagufra\Nylon 6 New.001  
 Operator: Stew  
 Run Date: 25-Jun-04 13:14  
 Instrument: DMA Q800 V5.1 Build 92

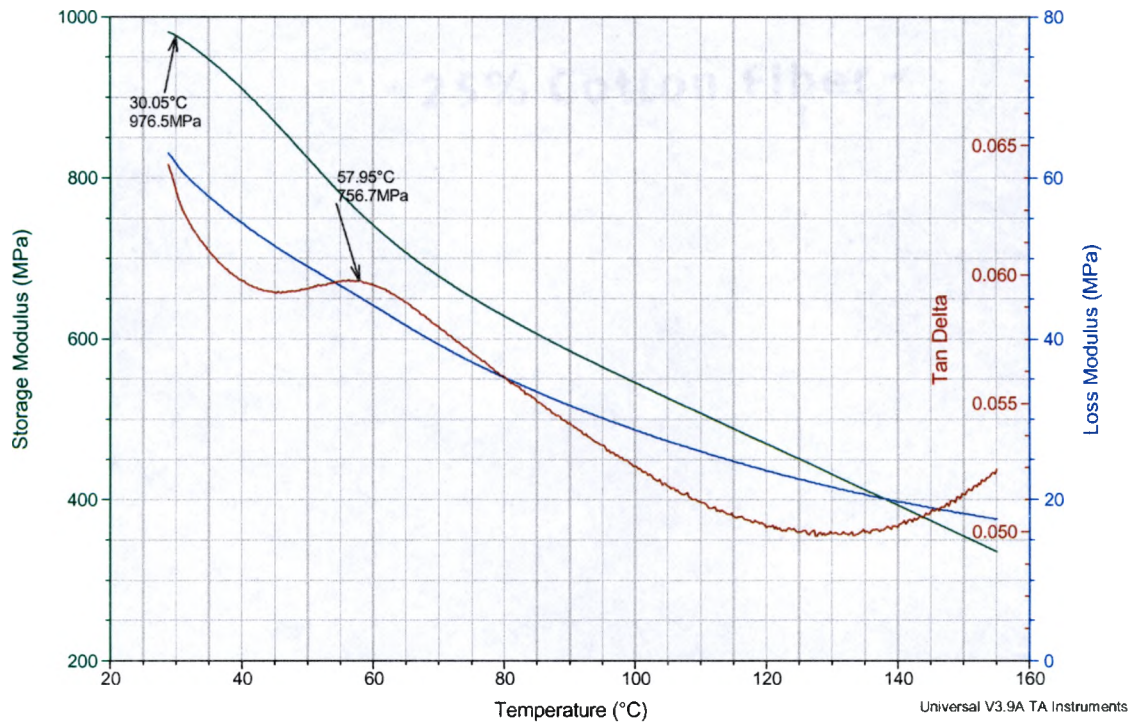


**Appendix C7-b – DMA of Nylon 6 – Second Run**

Sample: Nylon 6 New #2  
Size: 17.0900 x 14.1400 x 2.4700 mm  
Method: Temperature Ramp

DMA

File: C:\...Beal\Shagufa\Nylon 6 New #2.001  
Operator: Stew  
Run Date: 25-Jun-04 13:14  
Instrument: DMA Q800 V5.1 Build 92

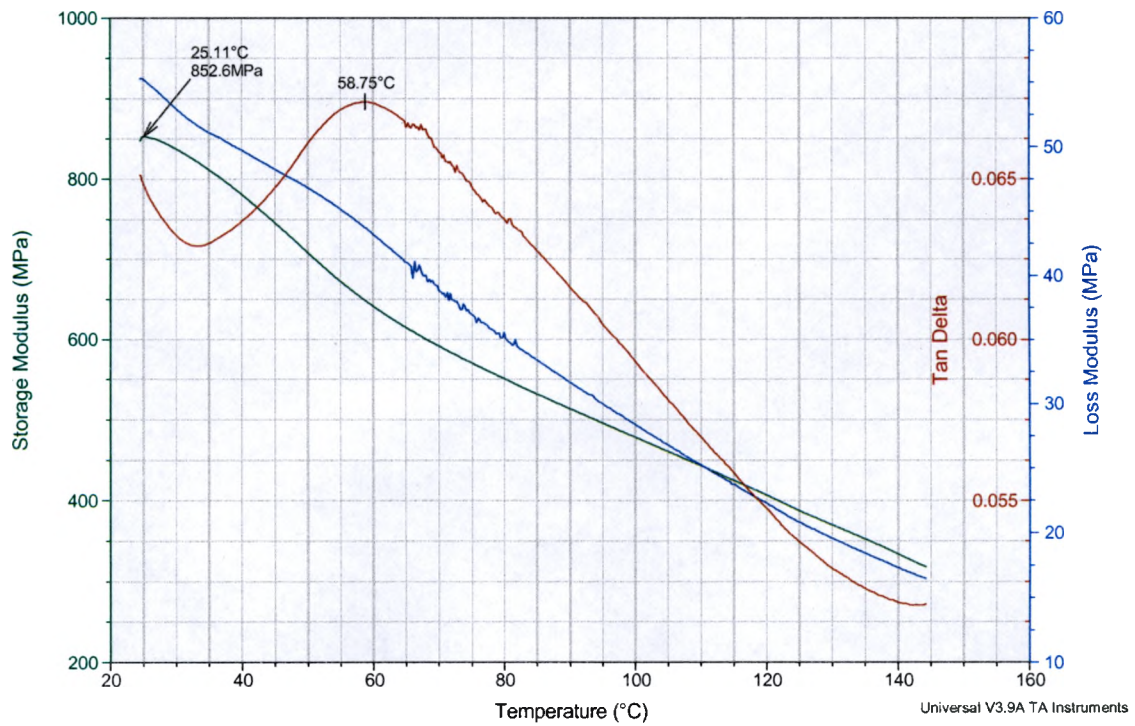


## Appendix C7-c – DMA of Nylon 6 – Third Run

Sample: Nylon 6 # 3  
 Size: 17.1800 x 14.3800 x 2.5500 mm  
 Method: Temperature Ramp

DMA

File: C:\...DMA\Beall\Shagufa\Nylon 6 # 3.001  
 Operator: Stew  
 Run Date: 25-Jun-04 13:14  
 Instrument: DMA Q800 V5.1 Build 92

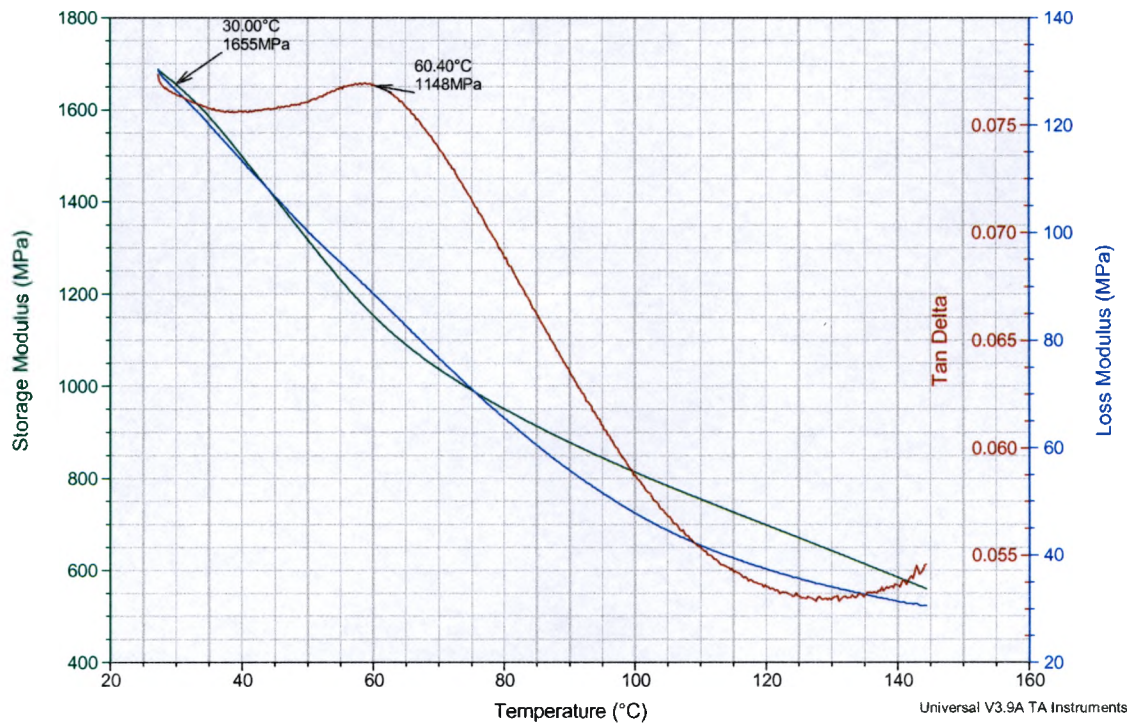


## Appendix C8-a – DMA of 93 A Edge Treated – First Run

Sample: 93 A Edge Treated New  
Size: 16.5500 x 13.0800 x 2.2900 mm  
Method: Temperature Ramp

DMA

File: C:\...\Shagufta\93 A Edge Treated New.001  
Operator: Stew  
Run Date: 25-Jun-04 13:14  
Instrument: DMA Q800 V5.1 Build 92

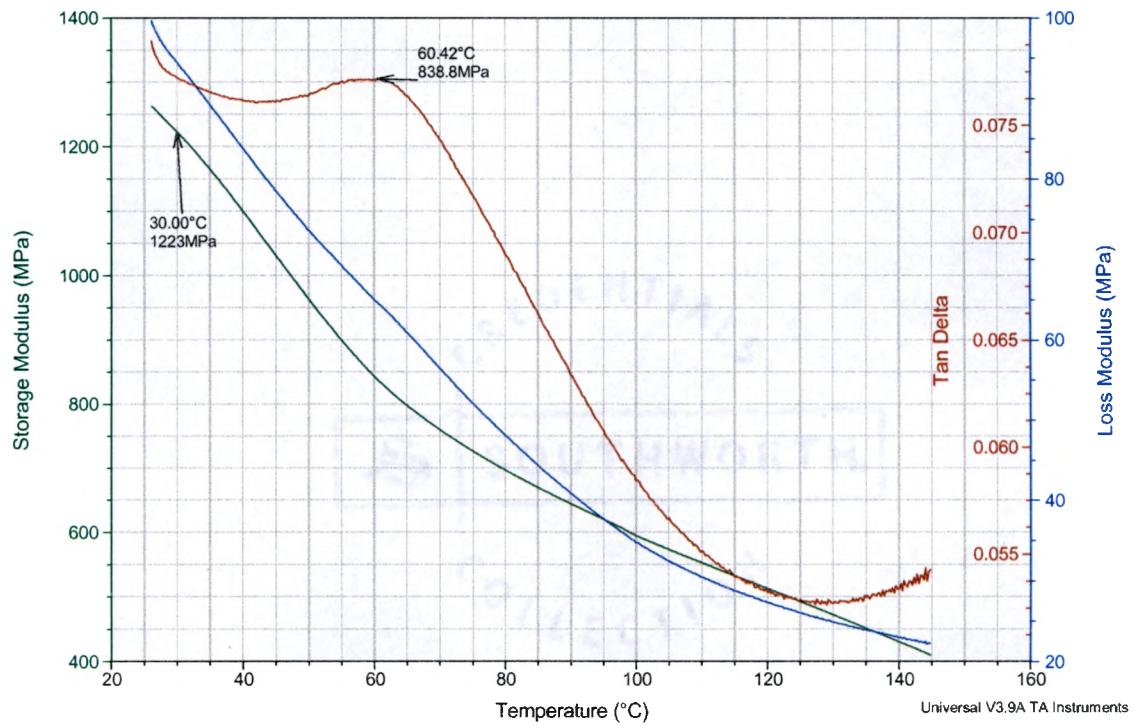


## Appendix C8-b – DMA of 93 A Edge Treated – Second Run

Sample: 93 A Edge Treated New 2nd  
Size: 16.9700 x 13.9400 x 2.5300 mm  
Method: Temperature Ramp

DMA

File: C:\...93 A Edge Treated New 2nd.001  
Operator: Stew  
Run Date: 25-Jun-04 13:14  
Instrument: DMA Q800 V5.1 Build 92

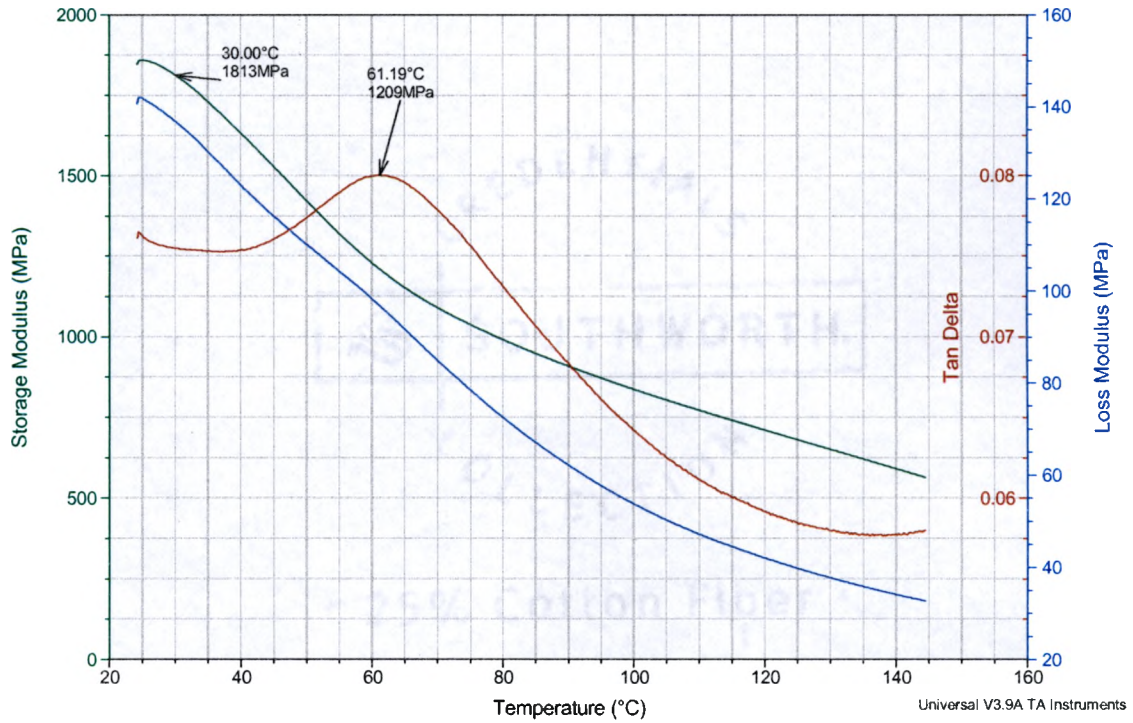


**Appendix C8-c – DMA of 93 A Edge Treated – Third Run**

Sample: 93 A Edge Treated New 2rd  
 Size: 17.0400 x 11.5800 x 2.6400 mm  
 Method: Temperature Ramp

DMA

File: C:\...93 A Edge Treated New 3rd.001  
 Operator: Stew  
 Run Date: 25-Jun-04 13:14  
 Instrument: DMA Q800 V5.1 Build 92

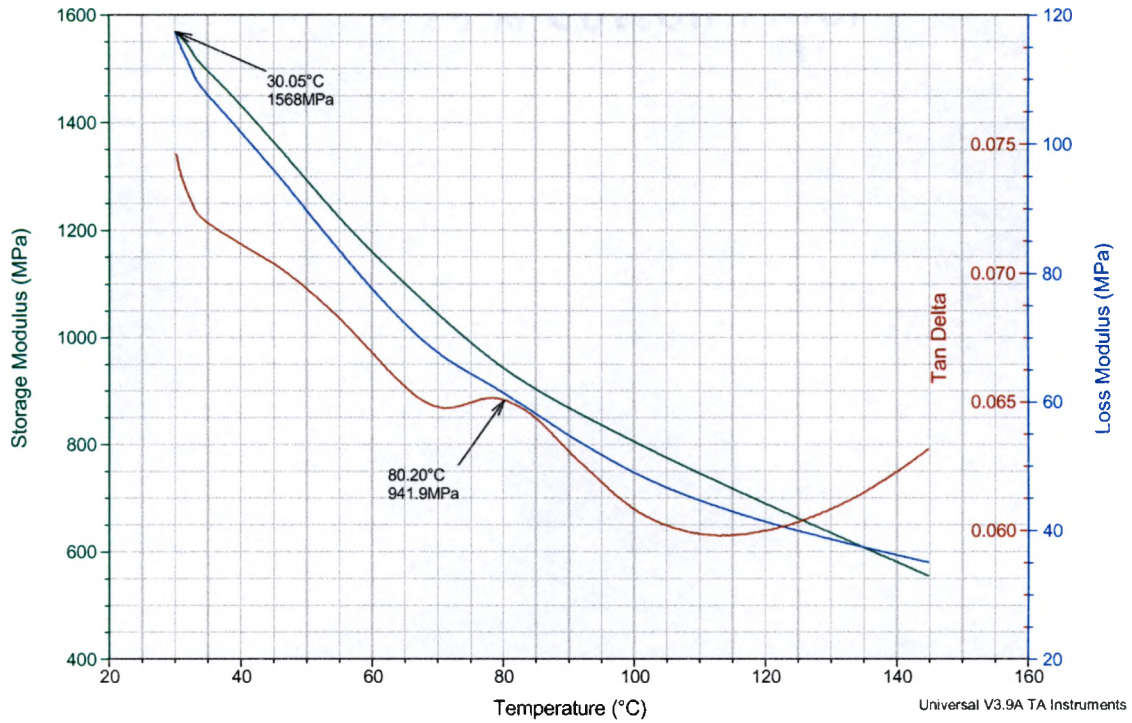


### Appendix C9-a – DMA of Surface Toyota – First Run

Sample: Surface Toyota Last 1st  
 Size: 17.2800 x 15.2700 x 3.7600 mm  
 Method: Temperature Ramp

DMA

File: C:\...\Surface Toyota Last 1st.001  
 Operator: Stew  
 Run Date: 25-Jun-04 13:14  
 Instrument: DMA Q800 V5.1 Build 92

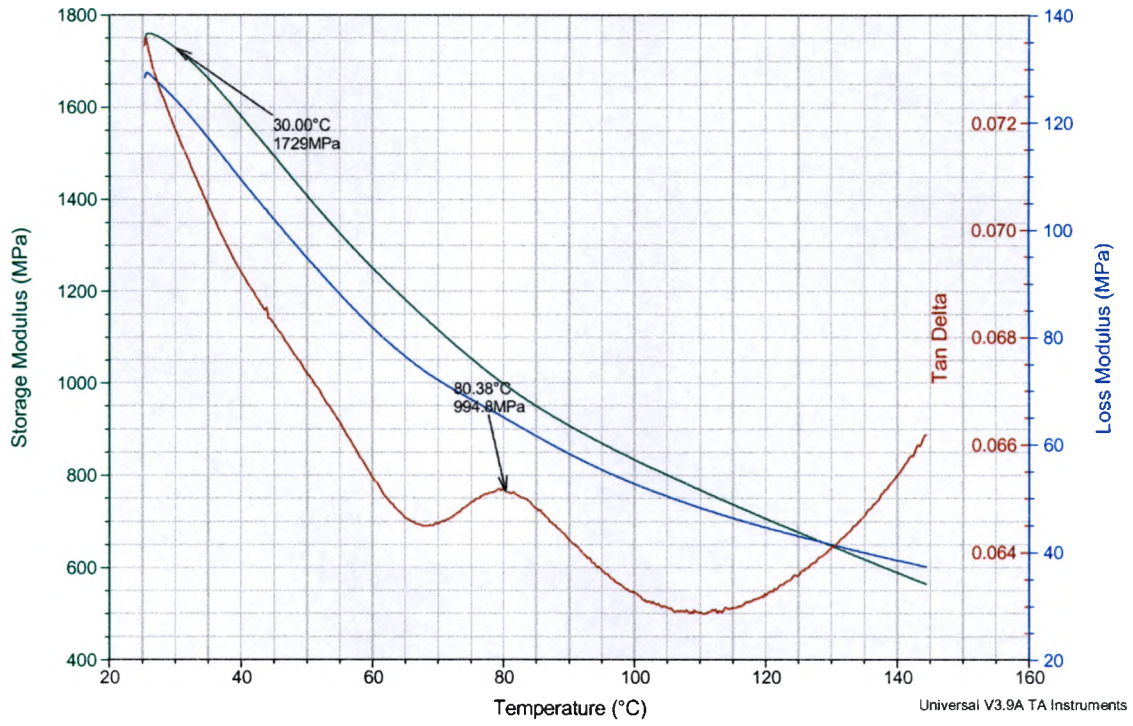


**Appendix C9-b – DMA of Surface Toyota – Second Run**

Sample: Surface Toyota Last 2n  
 Size: 17.0000 x 13.3500 x 2.9800 mm  
 Method: Temperature Ramp

DMA

File: C:\...\Surface Toyota Last 2nd.001  
 Operator: Stew  
 Run Date: 25-Jun-04 13:14  
 Instrument: DMA Q800 V5.1 Build 92

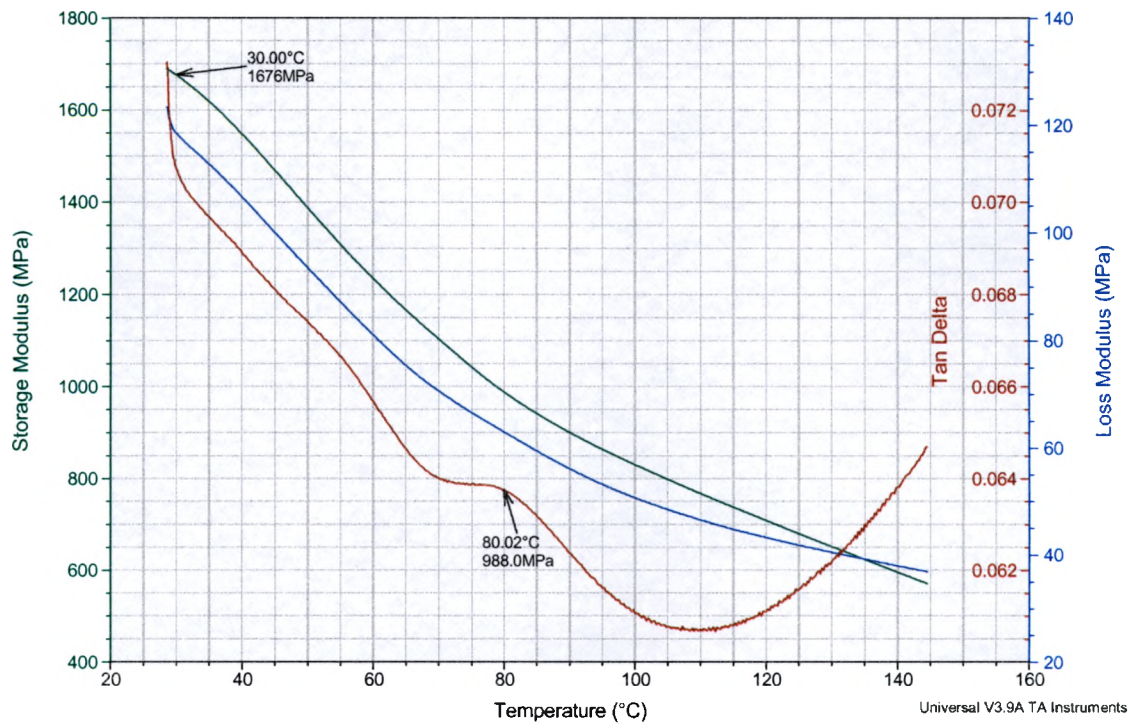


**Appendix C9-c – DMA of Surface Toyota – Third Run**

Sample: Surface Toyoto Last3rd  
Size: 17.3700 x 14.2200 x 3.6900 mm  
Method: Temperature Ramp

DMA

File: C:\...\Surface Toyota Last 3rd.001  
Operator: Stew  
Run Date: 25-Jun-04 13:14  
Instrument: DMA Q800 V5.1 Build 92

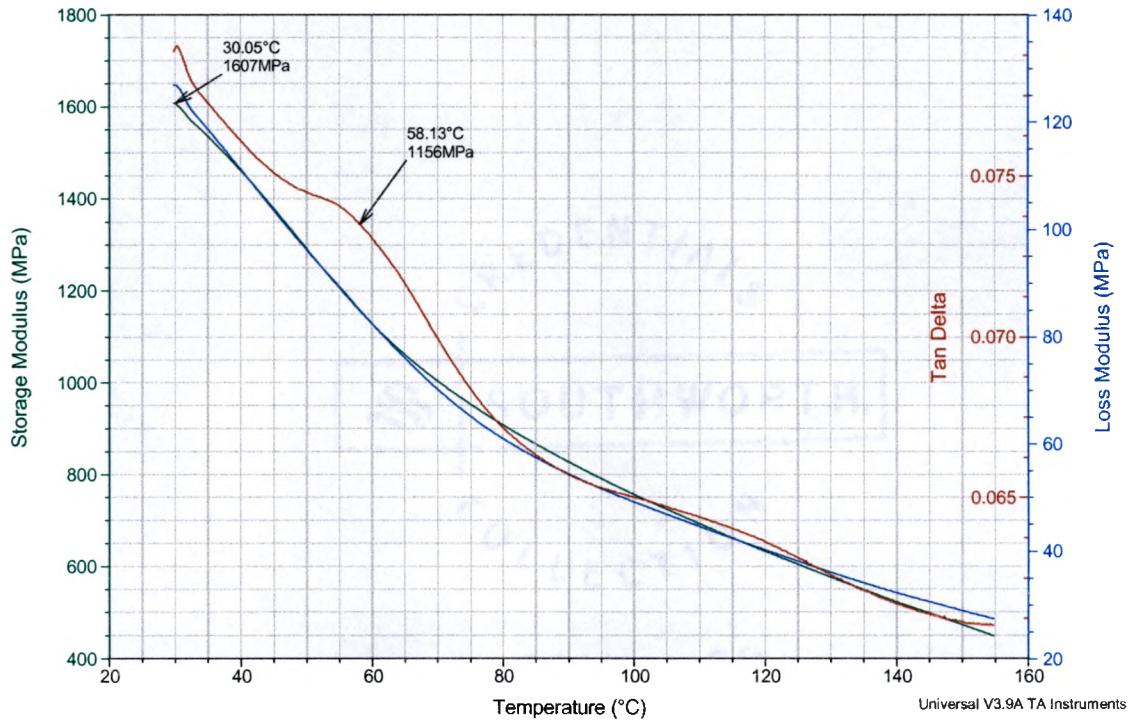


**Appendix C10-a – DMA of Surface Optimized – First Run**

Sample: Surface Optimized New  
 Size: 17.0600 x 13.4900 x 3.4300 mm  
 Method: Temperature Ramp

DMA

File: C:\...\Surface Optimized New.001  
 Operator: Stew  
 Run Date: 25-Jun-04 13:14  
 Instrument: DMA Q800 V5.1 Build 92

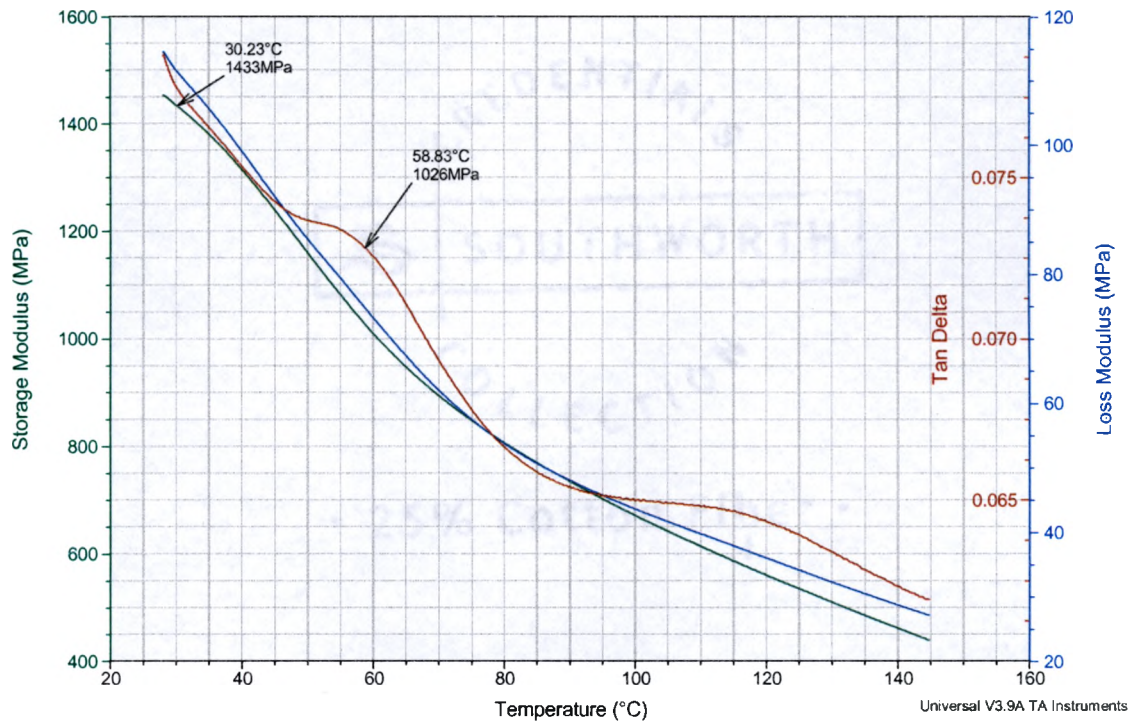


## Appendix C10-b – DMA of Surface Optimized – Second Run

Sample: Surface OptimizedNew #2  
Size: 17.2100 x 13.9700 x 3.5200 mm  
Method: Temperature Ramp

DMA

File: C:\...\Surface Optimized New #2.001  
Operator: Stew  
Run Date: 25-Jun-04 13:14  
Instrument: DMA Q800 V5.1 Build 92

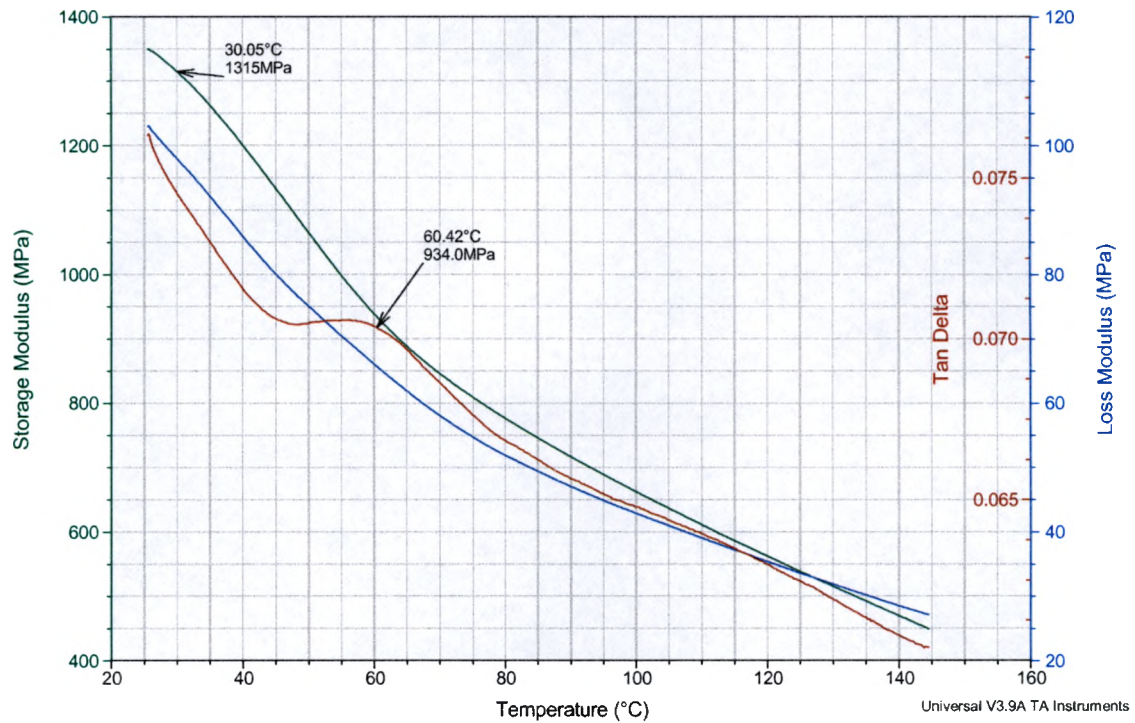


## Appendix C10-c – DMA of Surface Optimized – Third Run

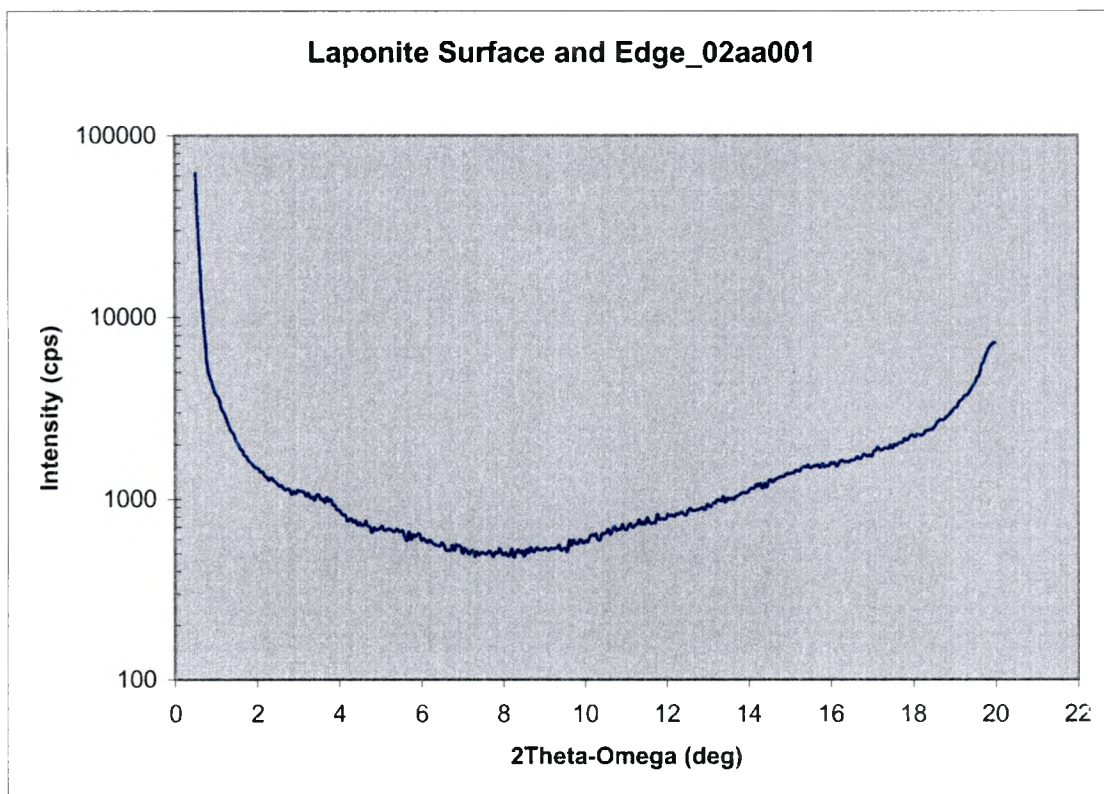
Sample: Surface Optimized New #3  
Size: 16.9800 x 13.7200 x 3.5400 mm  
Method: Temperature Ramp

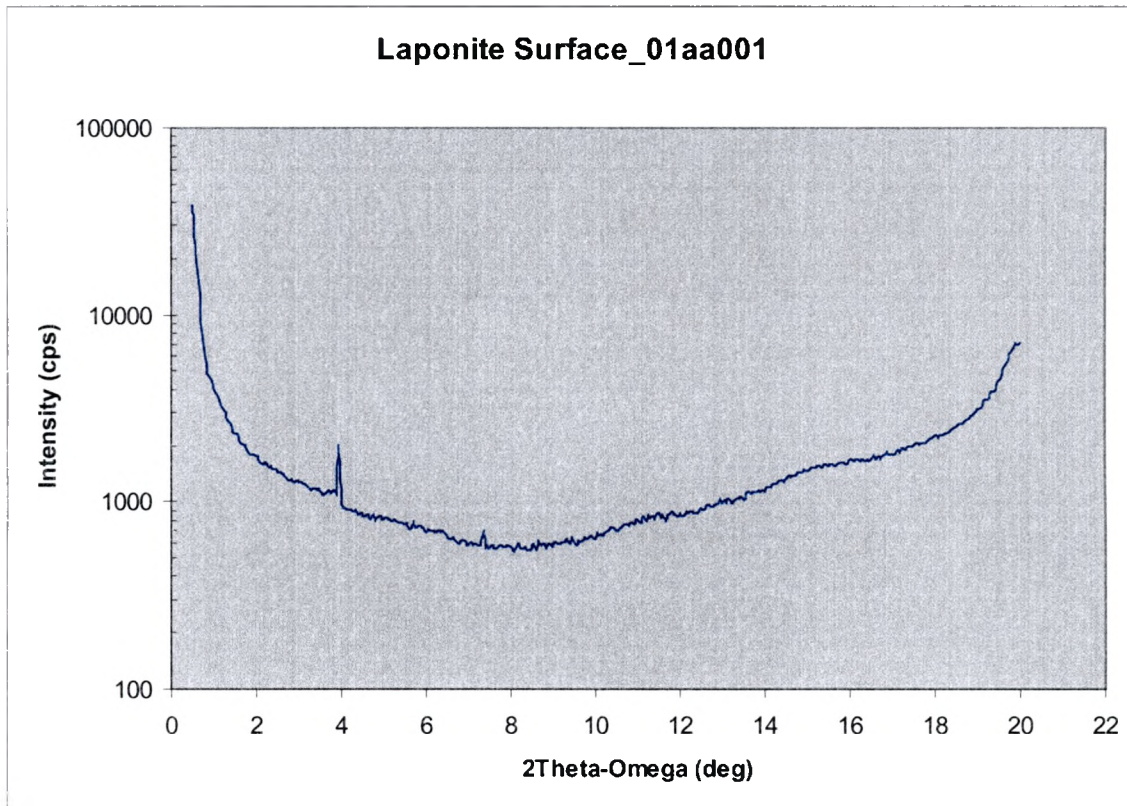
DMA

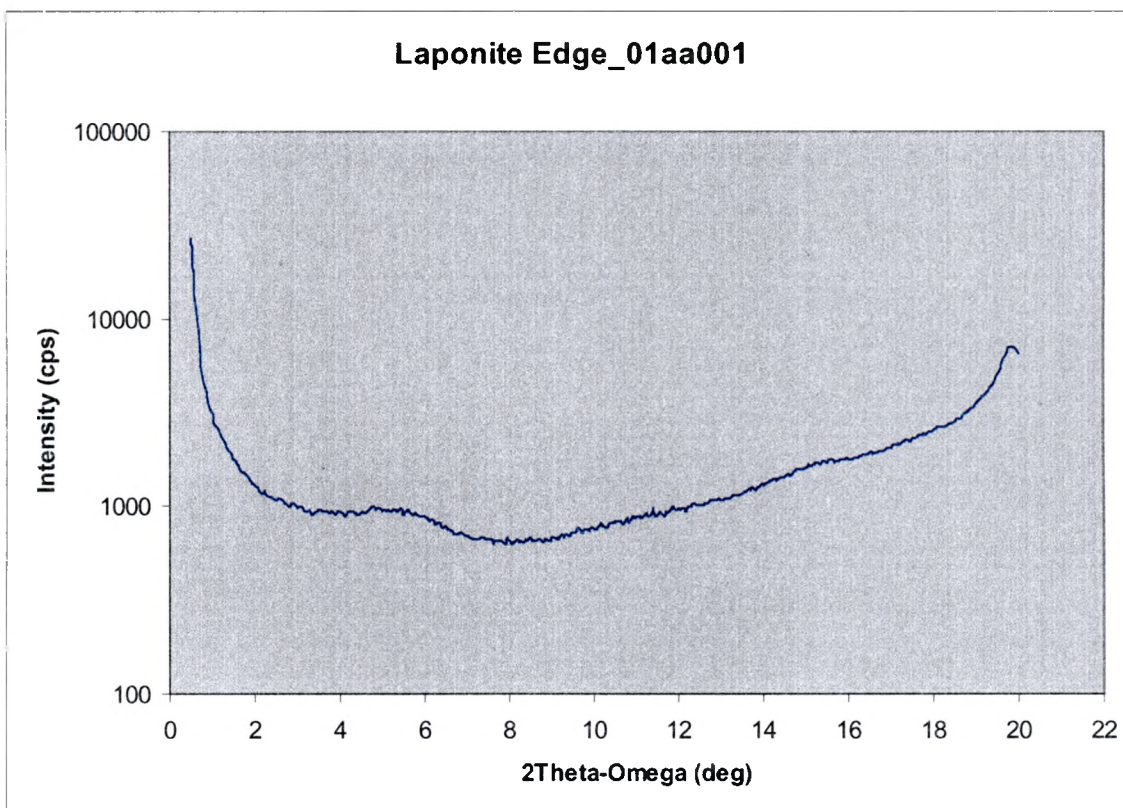
File: C:\...\Surface Optimized New #3.001  
Operator: Stew  
Run Date: 25-Jun-04 13:14  
Instrument: DMA Q800 V5.1 Build 92

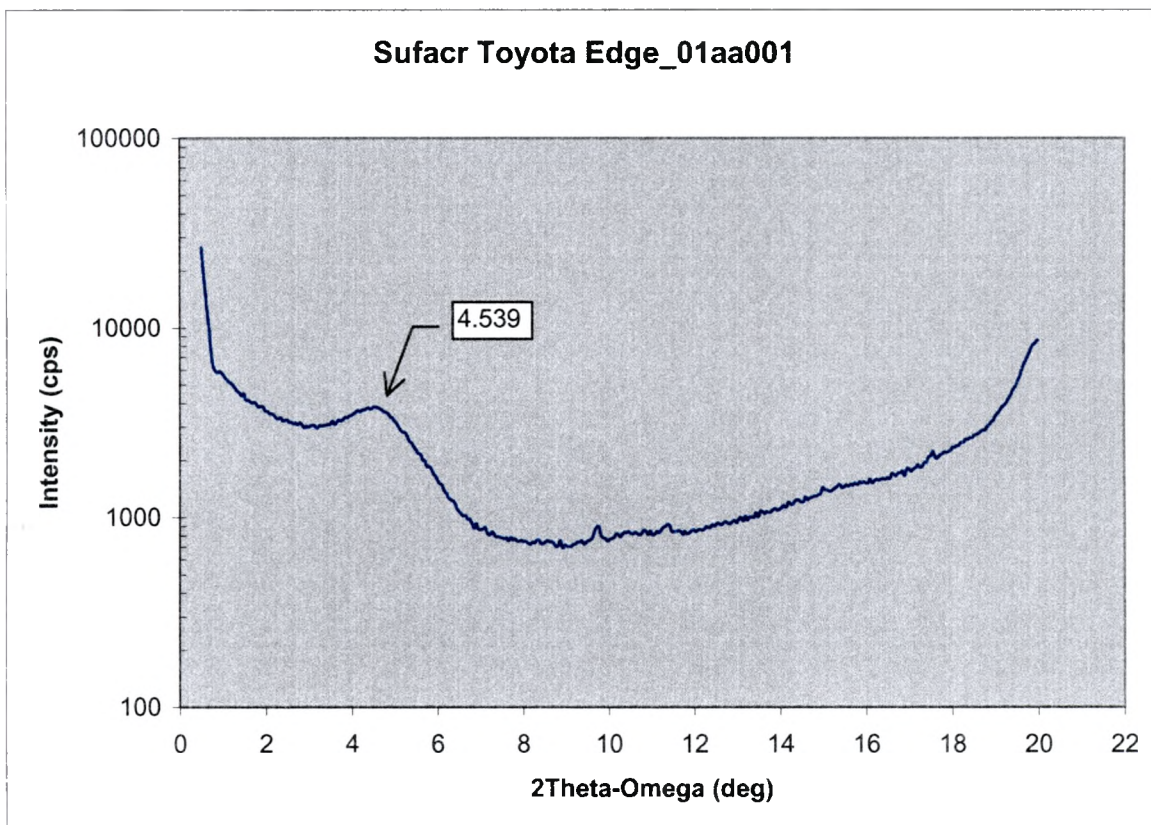


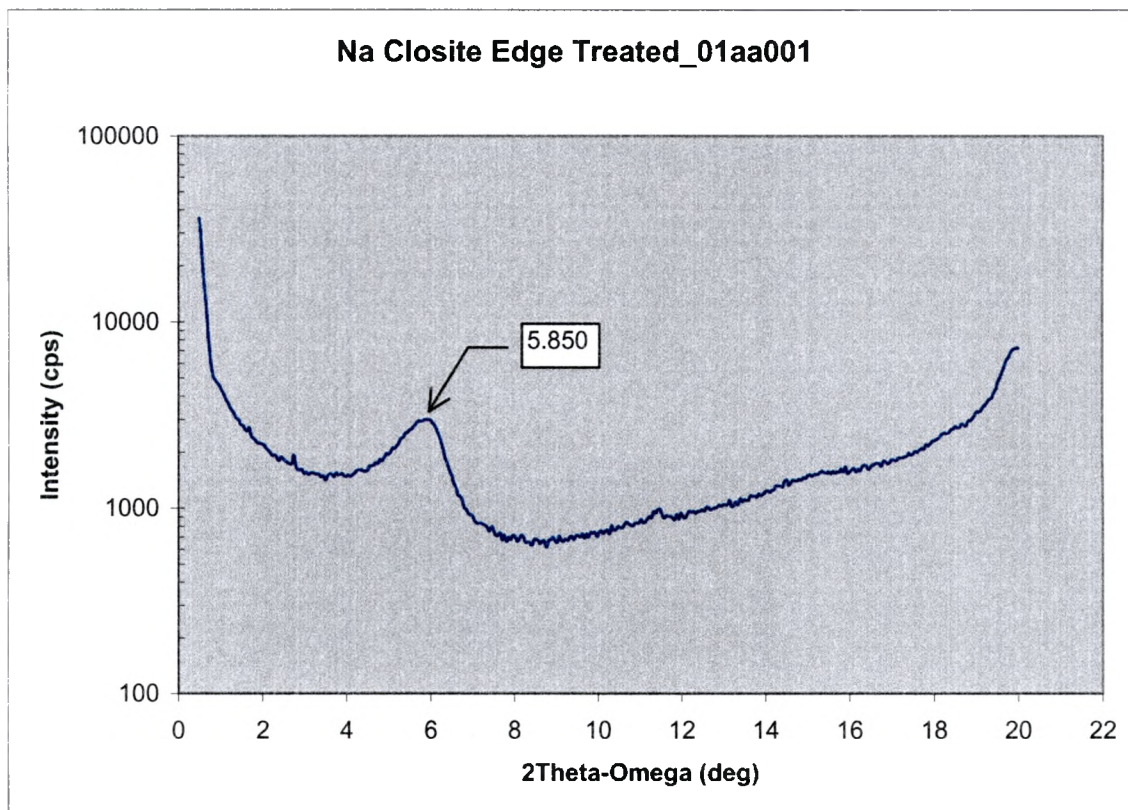
**APPENDIX D – X-RAYS OF NYLON 6 NANOCOMPOSITES**

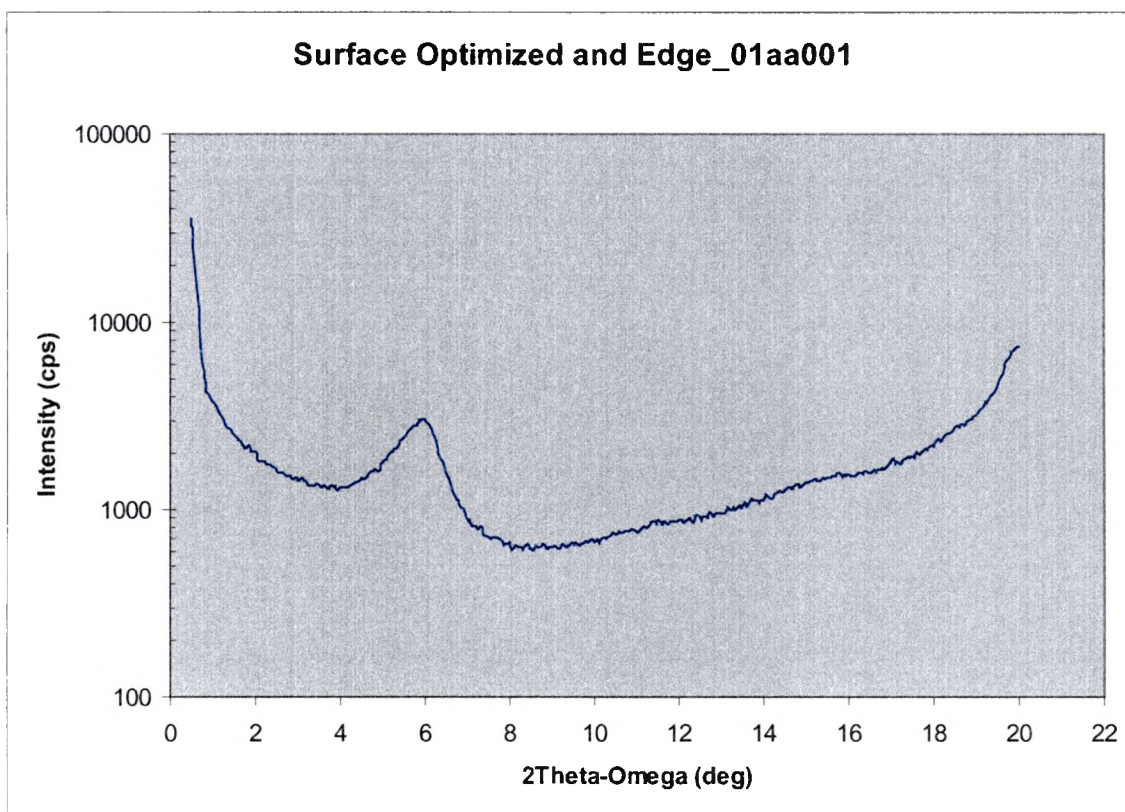
**Appendix D1 – X-ray of Laponite Surface & Edge**

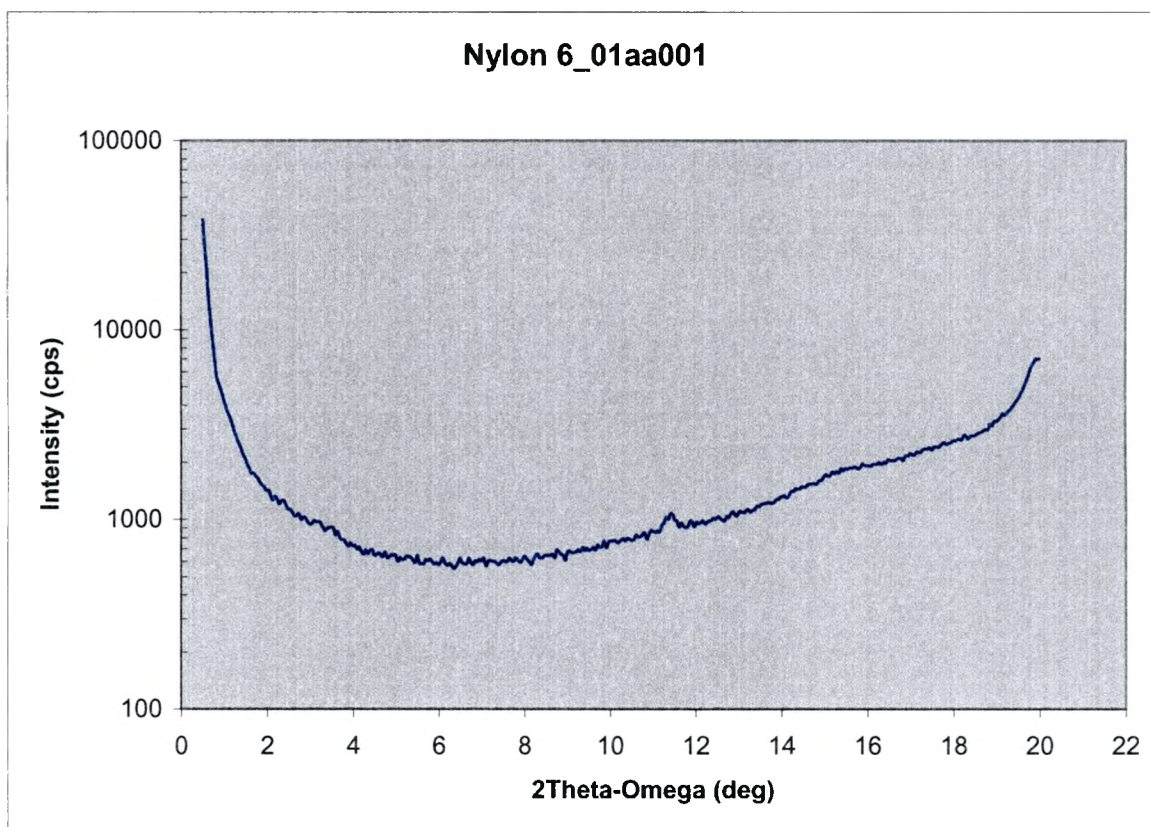
**Appendix D2 – X-ray of Laponite Surface**

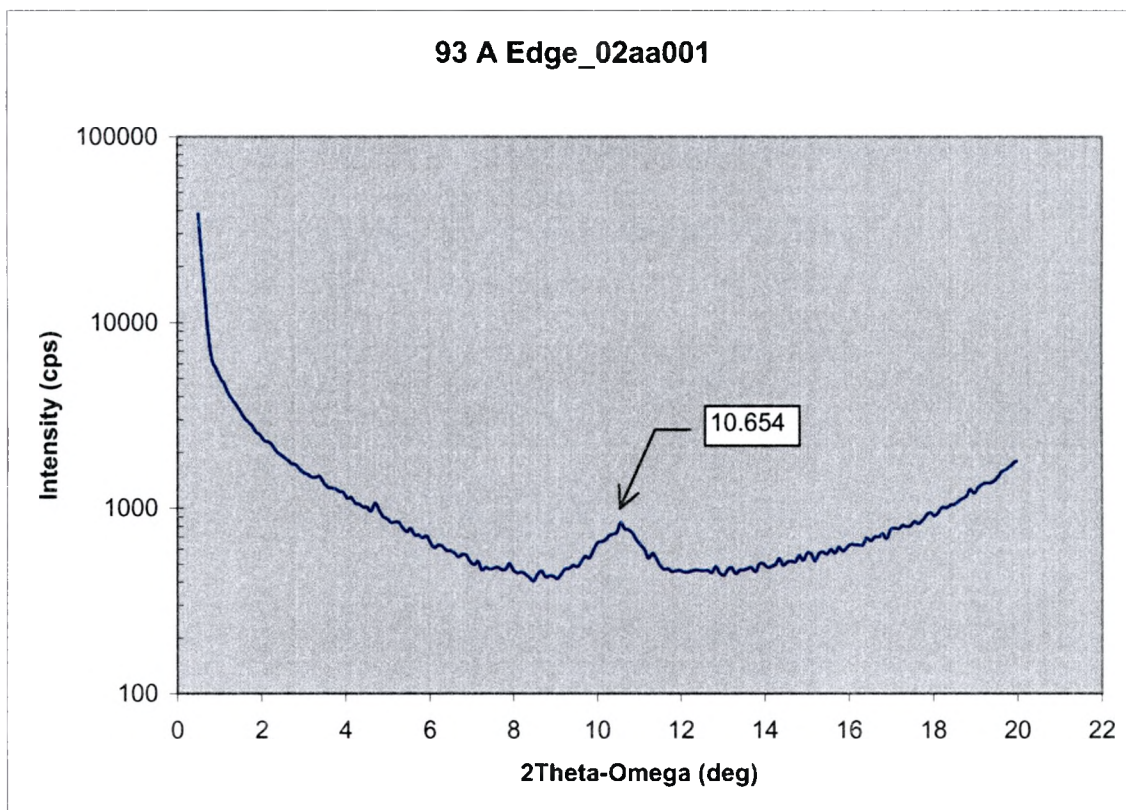
**Appendix D3 – X-ray of Laponite Edge**

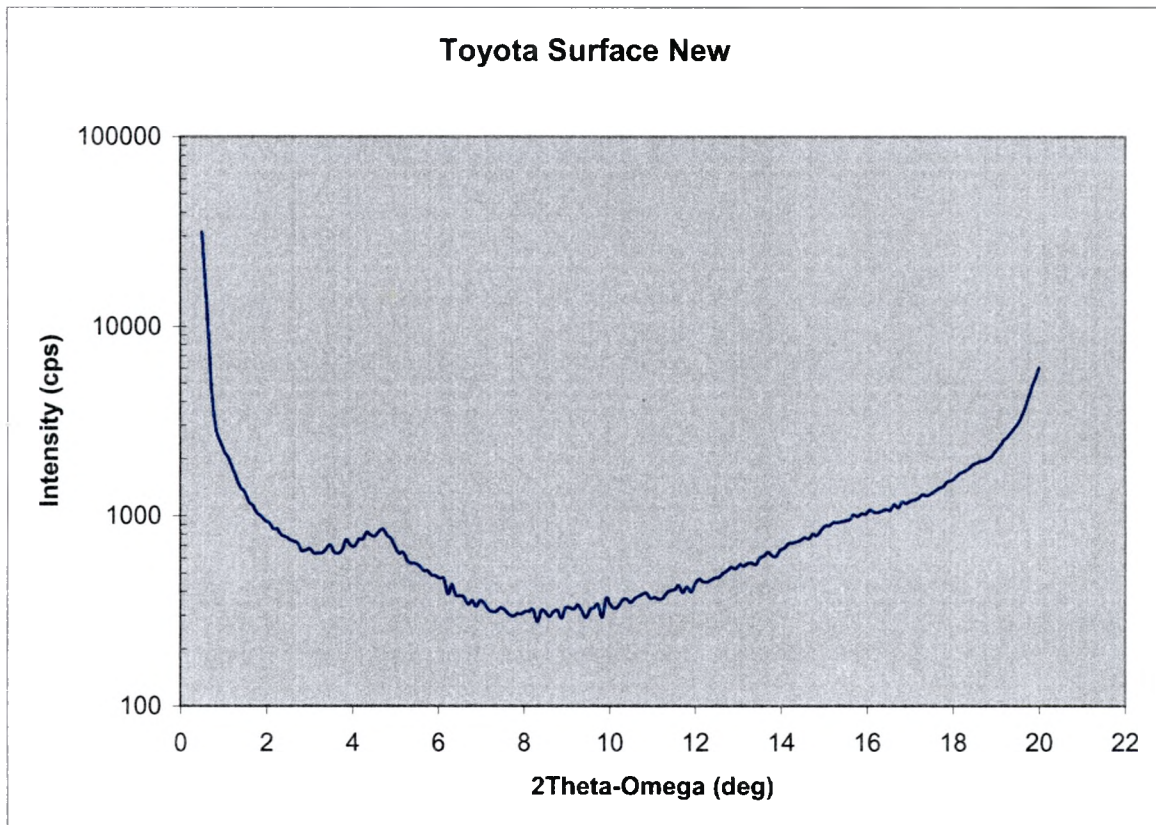
**Appendix D4 – X-ray of Surface Toyota & Edge**

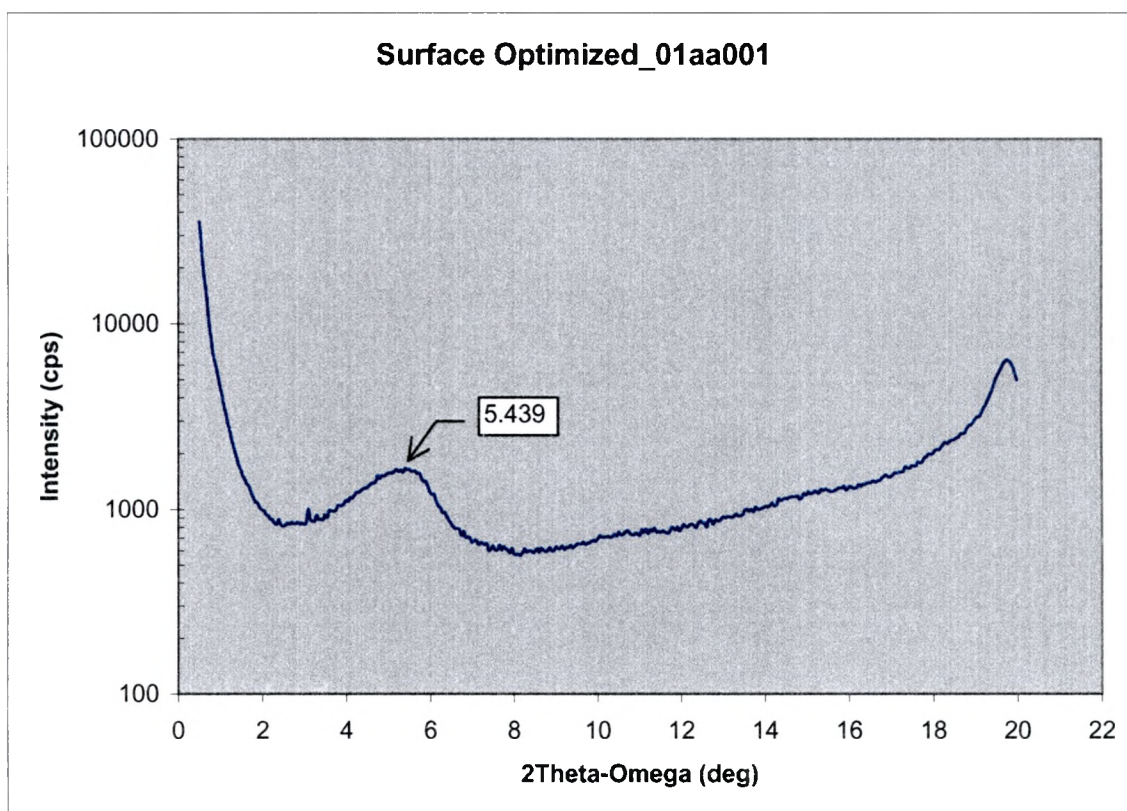
**Appendix D5 – X-ray of Na+ Closite Edge**

**Appendix D6 – X-ray of Surface Optimized & Edge**

**Appendix D7 – X-ray of Nylon 6**

**Appendix D8 – X-ray of 93 A Edge Treated**

**Appendix D9 – X-ray of Surface Toyota**

**Appendix D10 – X-ray of Surface Optimized**

## REFERENCES

1. Website – <http://www.nanocor.com>.
2. M.Motomatsu, T. Takahashi, H.-Y. Nie, W, H. Mizutani and H. Tokumoto, Microstructure study of acrylic polymer silica nanocomposite surface by scanning force microscopy, *Polymer*, 38,177-182 (1997).
3. B. K. G. Theng, Formation and properties of clay-polymer complexes, Elsevier, Amsterdam, p 133 (1979).
4. Dr. H.S. Jeon, <http://www.nmt.edu/~cheme/research/jeonr5.html>
5. E. P. Giannelis. *Adv. Mater.*8 (1996), pp. 29-35. Abstract-INSPEC Abstract-Compendex
6. T.Lan and T.J. Pinnavaia. *Chem.Mater.*6 (1994), pp. 2216-2219.
7. W. A. Deer and R. A. Howie, *Rock-Forming Minerals*, 3, p 240 (1962).
8. Website – <http://www.nanoclay.com>
9. Xavier Kornmann (Division of Polymer Engineering). Lulea University of Technology.
10. A.Okada, M. Kawasumi, A. Usuki, Y. Kojima, T. Kurauchi, and O. Kamigaito, Nylon 6- clay hybrid, *Mater. Res. Soc. Proc.*, 171, 45-50 (1990).
11. Kawasumi M, Kohzaki M, Kojima Y, Okada A, Kamigaito O. United States Patent Number 4810734; 1989 (assigned to Toyota Motor Co, Japan).
12. Usuki A, Kojima Y, Kawasumi M, Okada A, Fukushima Y, Kurauchi T, Kamigaito O. *J Mater Res* 1993;8(5):1179-84
13. Kojima Y, Usuki A, Kawasumi M, Okada A, Kurauchi T, Kamigaito O. *J Appl Polym Sci* 1993;49:1259-64.
14. Weimer MW. Chen H, Giannelis EP, Sogah DY. *J Am Chem Soc* 1999;121:1615-6
15. Lee DC, Jang LW. *J Appl Polym Sci* 1996;61:1117-22

16. Lee DC Jang LW. *J Appl Polym Sci* 1998; 68:1997-2005.
17. Gregar KC, Winans RE, Botto RE. US Patent 5308808, 1994 (assigned to US Department Energy).
18. Carrado KA, Xu L. *Chem Mater* 1998; 10:1440-5.
19. Liu L, Qi Z, Zhu X. *J Appl Polym Sci* 1999; 71:1133-8.
20. Vaia RA, Ishii H, Giannelis EP. *Chem Mater* 1993; 5:1694-6.
21. Christiani BR, Maxifield M. United States Patent Number 5747560.1998 (assignment to AlliedSignal Inc).
22. R. A. Vaia, H. Ishii, and E. P. Giannelis, Synthesis and properties of two-dimensional nanostructures by direct intercalation of polymer melts in layered silicates, *Chem. Mater.*, 1694-1696 (1993).
23. Polymer-Clay Nanocomposites T.J.Pinnavaia, G.W.Beall 2000.
24. Dennis HR, Hunter DL, Chang D, Kim S, White JL, Cho JW, Paul DR. *Polymer* 2001;42(23):9513-22.
25. Fornes TD, Yoon PJ, Keskkula H, Paul DR. *Polymer* 2001; 42(25):9929-40.
26. Fornes TD, Yoon PJ, Keskkula H, Paul DR. *Polymer* 2002; 43(7):2121-2.
27. Fornes TD, Yoon PJ, Hunter DL, Keskkula H, Paul DR. *Polymer* 2002;43(22):5915-33.
28. Fujiwara S, Sakamoto T, Japan , Patent No. JP-A-51-109998:1976 (assigned to Unitika Ltd. Japan).
29. A-Okada, Kawasumi; Masaya; et al US Patent # 4894411 January 16,1990
30. Arimitsu Usuki, Naoki Hasegawa, Hiroaki Kadoura, Tokuhiko Okamoto. *Nano letters* 2001; Vol.1, No. 5: 271-272.
31. Website – <http://www.laponite.com>
32. ASTM D256-04 “Standard Test Method for Determining the Izod Pendulum Impact Resistance of Plastics” ASTM International.

33. Vaia, R. A., Jandt, K. D., Karmer E. J and Giannelis, E. P. *Macromolecules*, **28**, 808 (1995).]
34. Aharoni SM n-Nylons, their synthesis, structure, and properties. Chichester; New York: Wiley; 1997
35. Wu T. M Lian C. S *Macromol Chem Phys* 2000: 201(18):2820-5] Wu.T M. Chen E.C Lian C.S *Polym Eng Sci* 2002;42(6):1141-50.
36. T.D, Fones, D.R Paul/ *Polymer* 44 (2003) 3945-3961.
37. Sperling LH. *Introduction to physical polymer sciencw*. 2<sup>nd</sup> ed. New York: Wiley,1992. p 198.] Fann DM, Huang SK, Lee JY. *Polym Engng Sci* 1998;38:265
38. Wunderlich B, *Macromolecular physics*,vol 2. New York: Acadmic Press; 1973
39. Davis R Gilman J. Vander Hart D. *Polym Degrd Stab* 2003;79:111-21
40. Gilman JW, Kashiwagi T,Lichtenhan JD. *Int SAMPE Symp* 1997;42:1078.

## VITA

Shagufta Shabbir was born in Karachi, Pakistan, on April 4, 1976, the daughter of Mushtaq and Fatima Ali. After graduating from St. Michael Convent School, Karachi, Pakistan, in 1992, she joined DHA Degree College for Women, Karachi, Pakistan, from where she received her Bachelor of Science degree in 1997. She then went on and joined the University of Karachi, Pakistan, and received her Master of Science degree in Chemistry in December of 1999. After her marriage in early 2000, she moved to United States. In August 2002, she joined Texas State University-San Marcos where she is expected to graduate in August 2004 with Master of Science degree in Chemistry.

Permanent Address: 3059 Hill Street,  
Round Rock, Texas 78664

This thesis was typed by Shagufta Shabbir.

